PHOTOEMISSION, PHOTOLUMINESCENCE AND PHOTOCONDUCTIVITY OF SOLIDS IN THE VACUUM ULTRAVIOLET REGION

By

William Pong

Final Report

May 1970

The research was supported by

NATIONAL AERONAUTICS AND SPACE ADMINISTRATION

Grant NsG-328 (NGR 12-001-002)

Department of Physics and Astronomy
University of Hawaii, Honolulu, Hawaii 96822

PHOTOEMISSION, PHOTOLUMINESCENCE AND PHOTOCONDUCTIVITY OF SOLIDS IN THE VACUUM ULTRAVIOLET REGION

By

William Pong

Final Report

May 1970

The research was supported by

NATIONAL AERONAUTICS AND SPACE ADMINISTRATION

Grant NsG-328 (NGR 12-001-002)

Department of Physics and Astronomy
University of Hawaii, Honolulu, Hawaii 96822

ABSTRACT

This report contains an account of several years of research on the interaction of photons with gases and solids in the spectral region of 2000 to 500 Å. While the principal aim was to investigate the photoelectric properties of solids, the study of gases was included to provide a convenient secondary standard for absolute yield measurements below 1000 Å. By comparing the ion current with the response of a calibrated thermocouple, the photo-ionization yield of xenon was found to be unity in the region 800-1000 Å.

The spectral quantum yields of a number of photoemissive films, e.g., alkali halides, MgF_2, CuI, Se, Te, Au, Al, ..., were measured. Some alkali-halide films have yields of approximately unity at photon energies slightly above twice the photoelectric threshold of the material. Photoemission from evaporated MgF_2 in the region of exciton absorption was measured; the results appear to be compatible with the viewpoint that exciton states may be present in the conduction band of MgF_2. In addition to the spectral-yield measurements, the escape length for photoelectrons in evaporated films such as CuBr, KBr, gold, and aluminum were estimated from the yield vs film-thickness data.

Exciton-induced photoemission from evaporated KCl films was observed. The effect of biasing radiation (visible light) on the interaction between excitons and F-centers was investigated. An application of this effect is suggested.

Preliminary studies of photoluminescence of sodium salicylate and photoconductivity of insulating crystals in the vacuum ultraviolet are discussed.

TABLE OF CONTENTS

ILLUSTRATIONS

ACKNOWLEDGMENT

This research was initiated in 1962 by the principal investigators, Professors K. Watanabe and W. Pong. The research would not have been possible without the initial effort and guidance of Professor K. Watanabe. His untimely death on August 15, 1969 was indeed a great loss to our program.

Special thanks are due to all those who have contributed much effort and time to the research: P. Metzger, F. Matsunaga, G. Yokotake, R. Tom, R. Norris, K. Fujita, R. Sumida, G. Moore, E. Cox, K. Shirakawa, D. Yogi, Jr., D. Lau, and D. Chan.

1. INTRODUCTION

This final report summarizes the important results of our efforts in studying the interaction of vacuum ultraviolet radiation with gases and solids. The research program was initiated in October 1962 with the support of NASA grant NsG-328. Our major objectives were to develop:

1) the technique of measuring the absolute intensity of vacuum ultraviolet radiation of wavelength below 2000 Å.
2) the technique of measuring the spectral photoionization yields of gases and quantum yields of photoemissive materials
3) the technique of measuring important parameters that are fundamental to the interpretation of photoelectric yield data.
4) the technique of measuring other photoeffects in solids for possible applications as ultraviolet photon detectors.

Attempts to accomplish these objectives have been motivated by the continuing need for suitable ultraviolet radiation detectors in the observational programs in space research.

Efforts in developing ultraviolet photodetectors have been reviewed by Dunkelman[1, 2]. In many applications, it is desirable to have photon detectors that

are spectrally selective. Ultraviolet detectors of current interest may be classified in two categories: (1) photo-ionization chambers which are sensitive in the spectral region 1050 - 1500 Å; (2) photomultiplier tubes which have photocathodes of relatively high threshold values for photoemission. In the first category, the spectral response of the detector depends on the ionization potential and the spectral photo-ionization yield of a gas. Although the quantum efficiency of this type of detector is high, its usefulness is limited by the transmission cutoff of the window material. In the second category, the spectral response depends on the photoemissive yield of a solid-state material. The advantage of this type of detector lies in the fact that it can operate in a vacuum without the window. It is therefore possible to extend the use of photoelectric detectors to the wavelength region below the LiF window cutoff of approximately 1050 Å. For applications above 1050 Å, LiF windowed multipliers have been developed. The desirable feature of being insensitive to long wavelength radiation can be incorporated in photoemissive detectors by using high work-function photocathodes. The work of Taft and Phillip[3] has shown that some alkali iodides and alkali halides have photoelectric thresholds in the vacuum u.v. region. Recently, Sommer[4] has summarized the published information on photocathode materials for applications below 2000 Å. However, our knowledge on

photoelectric properties of solids in the vacuum u.v. region is still somewhat limited and much can be learned from further research on photoemissive materials at higher photon energies.

While much attention has been given to the development of various types of ultraviolet detectors, relatively little effort has been directed towards improving the technique of absolute intensity measurements in the vacuum u.v. region. Earlier work on intensity measurements was done with calibrated thermocouple systems.[5, 6] Improvements in thermocouple technique were subsequently made in our laboratory. As a result of this effort, secondary standards for intensity measurements were obtained with the aid of a calibrated thermocouple. The results of this work led to the measurements of absolute photo-ionization yields of xenon and nitric oxide molecules.[7, 8] The yield value of unity in the spectral region of 860 - 1022 Å for xenon was verified.

In addition to the photo-ionization studies of gases, we performed measurements of absolute quantum yields of solids at photon energies between 6 and 23 eV. Particular attention was given to evaporated layers of alkali halides.[9] Some alkali halide films were found to have yield values of about unity at certain wavelengths below 1100 Å. Yield measurements were also made on semiconductors and evaporated metal films.[10-12]

In order to obtain a better understanding of the ultraviolet photoemission process, we focused our attention on the problem concerning the escape depth of the photoelectron. In this connection, we developed the technique of measuring the photoemission yield of evaporated films as a function of film thickness.[13-15] The results of these experiments are of practical and theoretical interest. For some materials, the yield is not optimized unless the film is sufficiently thick. The shape of the spectral yield curve can be affected by the film thickness. From the yield versus thickness data, we can obtain information on the attenuation length for the photoelectrons excited at a certain photon energy. The attenuation-length information can be related to important theoretical parameters such as mean free paths for electron-phonon and electron-electron collisions in solids.

In the following sections of this report, first we shall summarize briefly the work that we have published. Then we shall describe in detail the unpublished work that we have completed recently. Some of our experiments were exploratory studies and we hope to extend the work in more satisfactory detail before submitting the results for publication.

2. RECENT PUBLICATIONS OF THE PRINCIPAL INVESTIGATORS AND THOSE WHO PARTICIPATED IN THE RESEARCH SUPPORTED BY NASA GRANT NSG-328

1. "Photoionization Yield and Absoprtion Coefficient of Xenon in the Region of 860-1022 Å."
   F.M. Matsunaga, R.S. Jackson and K. Watanabe
   J. Quant. Spectros. Radiat. Transfer 5, 329 (1965).
2. "On the Quantum Efficiencies of Twenty Alkali Halides in the 12-21 eV region."
   P.H. Metzger, J. Phys. Chem. Solids 26, 1879 (1965).
3. "Photoemission from Amorphous and Metallic Selenium in the Vacuum Ultraviolet."
   W. Pong and R. Norris, J. Opt. Soc. Am. 55, 1189 (1965).
4. "Photoemission from SiC Crystals in the Vacuum Ultraviolet."
   W. Pong and K. Fujita, J. Appl. Phys. 37, 445 (1966).
5. "Attenuation Length Measurements of Photoexcited Electrons in CuBr Films."
   W. Pong, J. Appl. Phys. 37, 3033 (1966).
6. "Absorption Coefficient and Photoionization Yield of NO in the Region 580-1350 Å."
   K. Watanabe, F.M. Matsunaga and H. Sakai
   Applied Optics 6, 391 (1967).
7. "Escape Depth for Excited Photoelectrons in KBr Films."
   W. Pong, J. Appl. Phys. 38, 4103 (1967).
8. "Photoemission from AL-AL_2O_3 Films in the Vacuum Ultraviolet
   W. Pong, J. Appl. Phys. 40, 1733 (1969).
9. "Attenuation Length for Photoelectrons in Metal Films."
   W. Pong, R. Sumida and G. Moore, J. Appl. Phys. 41, 1869 (1970).

3. ABSTRACTS OF PUBLICATIONS

1. "Photoionization Yield and Absorption Coefficient of Xenon in the Region of 860-122 Å."

Abstract--Absorption coefficient and absolute photoionization yield of xenon gas have been measured by photoelectric methods with 0·2 Å bandwidth in the 860-1022 Å region. Ionization yields were obtained with a platinum detector calibrated against a calibrated thermocouple. A yield value of unity was obtained throughout this region which includes preionized Rydbery lines. The absorption coefficient at most wavelengths fell between the spread of previous values.

2. "On the Quantum Efficiencies of Twenty Alkali Halides in the 12-21 eV Region."

Abstract--Absolute photoelectric yields of twenty alkali halides have been measured, using a rare gas ion chamber to determine the flux distribution of the He_2 continuum between 12·4 and 21·2 eV. In addition, semiquantitative absorption coefficients were obtained by evaporating AX (alkali halide) films on 300 Å thick Al_2O_3 windows. For most of these materials the photoelectric yield rises to values as high as 0·8 electron/incident photon in the fundamental band beyond the stable exciton region. At photon energies near twice the threshold (or approximately 2 E_T) the yield often

reaches a distinct minimum of the order of 0·4 electron/incident photon. This region is likely characteristic of double exciton production. Beyond 2 E_T the yield generally rises to very large values, even over 1·0, strongly implying double excitation processes. Many broad diffuse bands, sometimes well correlated with the absorption coefficients, appear in the electron emission spectrum.

3. "Photoemission from Amorphous and Metallic Selenium in the Vacuum Ultraviolet."

Abstract--Photoelectric yields of amorphous and metallic selenium films were measured over the spectral range of 2000 to 1100 Å. No appreciable difference between the yields (number of electrons per incident photon) of the two forms was observed. However, the retarding potential data show that the emitted photoelectrons from metallic Se are distributed over a slightly higher energy range than those from the amorphous form. The results can be explained on the basis of the energy band model of Se.

4. "Photoemission from SiC Crystals in the Vacuum Ultraviolet."

Abstract--The results of quantum yield measurements on p and n type SiC crystals of hexagonal structure are in agreement with the theoretical expectation that p-

type samples should exhibit a higher quantum yield than n-type samples. The higher yield of the p-type crystal can be accounted for by assuming the existence of space-charge band bending at the surface.

5. "Attenuation Length Measurements of Photoexcited Electrons in CuBr Films."
Abstract--The attenuation length of photoexcited electrons in evaporated layers of CuBr was estimated by measuring the photoemission yield as a function of thickness. The attenuation length was found to be less than the optical absorption depth at photon energies between 8 and 11 eV. At hv=9.7 eV, the attenuation length is approximately 51 Å.

6. "Absorption Coefficient and Photoionization Yield of NO in the Region 580-1350 Å."
Abstract--Photoionization yield and absorption coefficient of nitric oxide were measured at many wavelengths in the region 580-1350 Å. H_2 emission and helium continuum sources were used with a 1-m monochromator. Absolute intensity measurements were based on a calibrated thermocouple.

7. "Escape Depth for Excited Photoelectrons in KBr Films."
Abstract--We have investigated the backward photoemission from KBr films as a function of film thickness.

The attenuation length for electrons excited by photons of 10.2 eV was found to be about 180 Å, which is slightly greater than the absorption length for photons in KBr. The mean free path for electron-phonon collisions at 300°K was estimated to be approximately 42 Å.

8. "Photoemission from AL-AL_2O_3 Films in the Vacuum Ultraviolet Region."

Abstract--Measurements of quantum yield of Al-Al_2O_3 films were made at photon energies between 7 and 22 eV. The photoelectric threshold for intrinsic photoemission from amorphous Al_2O_3 appeared to be about 8 eV. Approximately 1 eV was estimated for the electron affinity of Al_2O_3. The yield of anodic oxide film on aluminum at 10.2 eV decreased with increasing oxide thickness while the yield at 21.2 eV increased. The decrease in yield at 10.2 eV was attributed to photoelectrons originating from the aluminum film beneath the oxide layer. Attempts were made to study the escape probability function for electrons moving through the oxide into the vacuum. An attenuation length of about 130 Å for the photoelectrons in the oxide was obtained by using the exponential-function approximation. The maximum initial energy of the electrons was estimated to be 7.8 eV above the vacuum level. The electron mean free path for electron-phonon collisions in the oxide was estimated to be approximately

sixteen angstroms. In the analysis of the mean free path, the emission of one phonon of 0.1 eV was assumed in each energy-loss collision.

9. "Attenuation Length for Photoelectrons in Metal Films." **Abstract**--Photoelectric yields of evaporated gold and aluminum films of various thicknesses were measured in the photon-energy region of 7.7 to 11 eV. From the analysis of the yield data, the attenuation length for the excited photoelectrons was estimated. For electrons excited by photons of 10.2 eV, the attenuation length for photoelectrons in aluminum is about five times as large as that for electrons in gold. By using the Kane model for collision effect in photoemission, we were able to show that the attenuation length obtained from our yield data for aluminum is consistent with the photoelectron mean free path values reported by Stuart and Wooten [Phys. Rev. 156, 364 (1967)].

4. CALIBRATION OF THERMOCOUPLE AND SECONDARY DETECTORS FOR ABSOLUTE INTENSITY MEASUREMENTS IN THE VACUUM ULTRAVIOLET.

4.1 Introduction

For reliable measurements of photon flux, it is necessary to use a radiation detector whose calibrated quantum efficiency remains constant with time and changes in vacuum conditions. In vacuum ultraviolet work, it is convenient to measure the incident intensity by means of windowless photoelectric detectors. Certain metals such as tungsten, platinum, and gold have been used as photocathodes. These metals have been found to be suitable secondary standards for intensity measurements below 2000 Å. They appear to be stable inasmuch as their quantum efficiencies are reproducible.

The absolute quantum yield of a photocathode can be determined by measuring the photoemission current, provided the incident photon flux is known. We define the quantum yield Y by the ratio of the number of electrons emitted per second to the number of incident photons per second. Accordingly, we write

$$Y = \text{number of electrons/number of photons.} \quad (1)$$

Thus if the yield is known, the photoemission current can be related to the incident photon flux. If the

spectral quantum yield is used to determine the photoelectric threshold of a material, it is desirable to define the quantum yield Y_A by the ratio of the number of electrons emitted per second to the number of photons absorbed per second. If the photocathode material is sufficiently thick and the reflectance R is given, we can relate Y_A to Y by

$$Y_A = Y/(1 - R), \qquad (2)$$

4.2 Thermocouple Calibration

Previous work has shown that the intensity of incident photons in the vacuum ultraviolet region can be measured by the use of a thermocouple.[5, 16] As described in our 1964-report on intensity measurements, a windowless Reeder compensated thermocouple with a detector area of 1 mm x 3 mm was used. Similar thermocouples were employed in other experiments in our laboratory. Each thermocouple was calibrated in air against a standard lamp from the National Bureau of Standards according to the recommended procedure.[17] Since the thermocouple for our experiments must operate in a vacuum chamber, the vaccum-to-air ratio was measured in order to determine the actual sensitivity under operating conditions. The sensitivity values of the thermocouples calibrated in our laboratory varied from 2.04 to 6.73 microvolts per

microwatt. The output response was measured by a breaker amplifier (Beckman Model 14) and a chart paper recorder.

The possible sources of error in our thermocouple calibration have been discussed.[7] A more detailed study of the Reeder thermocouple characteristics has been reported by Johnston and Madden.[18] Figure 1 illustrates a typical application of our thermocouple in measuring photon flux passing through the exit slit of a vacuum ultraviolet monochromator.

4.3 Absolute Quantum Yield of Metal-Foil Photocathodes

In our earlier work, the absolute quantum yields of some metals and semiconductors were measured in the spectral region 900 - 2000 Å by means of a calibrated thermocouple.[19] Since these measurements were made with the samples in a vacuum of about 10^{-5} Torr, the results may not be the same as those obtained with a better vacuum. In our recent work, the yield measurements in the region 2000 - 1100 Å were performed with the sample in a vacuum of 10^{-7} - 10^{-8} Torr. The experimental chamber with a sealed LiF window was initially evacuated by a sorption pump and then continuously by an ion pump (80 L/s). All removable parts of the vacuum system were assembled with copper gaskets. In our high vacuum measurements, a gold foil was employed as a secondary standard. Figure 2 illustrates the spectral

quantum yield of the gold foil. The metal foil was purchased from the Jarrell-Ash Company.

In the spectral region between 537 and 1216 Å, we used a tungsten foil as a secondary standard to determine the absolute intensity of the incident radiation. The yield of the foil at wavelength 584 Å was initially determined at the Far UV Radiation Laboratory-National Bureau of Standards.[20] The yield of the same tungsten foil was also measured with the calibrated thermocouple used in our laboratory. The yield values at wavelength 584 Å agree within the estimated experimental error of ± 5%. The calibrated yield at 584 Å is believed to be most reliable because the effect of scattered light is negligible in this spectral region. The yield values at other wavelengths were determined by comparing the photoemission currents with the photoluminescent response of sodium salicylate.[21, 22] Figure 3 illustrates the spectral quantum yield of the tungsten foil.

5. PHOTOEMISSION FROM METALLIC FILMS

Although the photoelectric effect was discovered many years ago, the detailed consideration of the photoemission process is still an area of basic research in contemporary physics. Since a photon contributes only negligible momentum in the optical excitation of electrons in a crystal, the excited electron must obtain momentum from the surface potential barrier or from the periodic potential inside the crystal. Consequently the question arises as to whether the surface or volume effect is the predominant mechanism. This problem has been discussed in the literature.[23-25] According to recent experimental evidence, photoemission from solids is primarily a volume effect.[26]

5.1 Quantitative Theory (One-Dimensional Model)

If we consider photoemission as a volume effect, it is useful to consider the mechanism in three steps: 1) absorption of a photon by an electron in the solid; 2) motion of the photoexcited electron to the solid-vacuum interface; 3) escape of the photoelectron over the surface barrier into the vacuum. This model appears to be adequate in explaining the quantum yields of metals. However, it has been suggested that it might be more appropriate to treat optical excitation, scattering, and the escape across the surface as a one-step process.[27, 28] For simplicity, we will employ the three-step model to

explain the results of our experiments.

In order to calculate the quantum yield of a photoemissive material, we need to know the escape probability function for the electron optically excited at some distance x beneath the surface. A model has been developed to determine the probability of escape.[29] In this model, we introduce a mean free path ℓ_p for electron-phonon scattering; a mean free path ℓ_e for electron-electron scattering; and a probability r that the photoelectron is reflected from the solid-vacuum interfact at x = 0. We will assume that the scattered photoelectron and the secondary electron produced in the electron-electron collision are not sufficiently energetic to escape into the vacuum. That is to say, both electrons are scattered into states below the vacuum level. This assumption is probably valid unless the surface work function or the electron affinity of the solid is greatly reduced by a thin surface layer of low work-function material such as cesium. We will also assume that the mean free paths are independent of the phonon energy loss. The phonon energy loss per collision is considered to be negligible.

If scattering is primarily due to electron-phonon and electron-electron collisions, we can derive an expression for the escape length in terms of the mean free paths for collisions. First of all, we specify

that the probability that the electron will make an electron-phonon collision after traveling through a distance Δx is $\Delta x/\ell_p$. The probability that the electron will make an electron-electron collision after traveling through the distance Δx is $\Delta x/\ell_e$. If $x = N\,\Delta x$, the probability that the electron will not make any collision in traveling a distance x is

$$g(x) = (1 - \frac{\Delta x}{\ell_p})^N\,(1 - \frac{\Delta x}{\ell_e})^N \quad . \tag{1}$$

We can simplify this expression by letting N become large and Δx become small. Accordingly, we can write

$$g(x) = e^{-cx}, \tag{2}$$

where $c = \ell_p^{-1} + \ell_e^{-1}$. With this relationship established, we specify the probability that an electron excited at x travels to the surface and escapes from the surface is

$$p_o(x) = (1 - R)\frac{1}{2}e^{-cx} \quad . \tag{3}$$

The factor ½ accounts for the fact that it is equally likely for the electron to move towards the surface or away from it.

Now suppose an electron is optically excited at x beneath the surface and arrives at position s without making any collision, where s = 0 is the surface. The probability that it will interact with a phonon at s is ds/ℓ_p. After the first collision, the probability that the electron at s will escape after (n-1) electron-

phonon collisions is $p_{n-1}(s)$. As shown in Fig. 4, there are three ways of getting to position s before the first collision. Letting $p_n(x)$ be the probability that an electron will escape from the surface after making n electron-phonon collisions, we write

$$p_n(x) = \frac{1}{2\ell_p}\left[\int_o^x p_{n-1}(s)\, e^{-c(x-s)}ds + r\int_o^\infty p_{n-1}(s)\, e^{-c(x+s)}ds + \right.$$

$$\left. + \int_x^\infty p_{n-1}(s)\, e^{-c(s-x)}ds\right]. \qquad (4)$$

The total probability of escape is

$$g(x) = p_o(x) + \sum_{n=1}^{\infty} p_n(x). \qquad (5)$$

Since

$$q(s) = \sum_{n=1}^{\infty} p_{n-1}(s),$$

we find

$$q(x) = \frac{1}{2\ell_p}\left[\int_o^x q(s)\, e^{-c(x-s)}ds + r\int_o^\infty q(s)\, e^{-c(x+s)}ds + \right.$$

$$\left. + \int_x^\infty q(s)\, e^{-c(s-x)}ds\right] + p_o(x) \quad . \qquad (6)$$

Differentiation with respect to x results in

$$q''(x) = (c^2 - c\ell_p^{-1})\, q(x) \quad . \tag{7}$$

For a semi-infinite medium, the solution is

$$q(x) = B\, e^{-x/L} , \tag{8}$$

where $L^{-1} = (c^2 - c\ell_p^{-1})^{\frac{1}{2}}$. The constant B can be evaluated by substitution in Eq. (6). The parameter L is called the escape length or attenuation length for the photoelectron.

Equation (8) appears to be a good approximation for the probability of escape. It has been used successfully in explaining the essential features of photoemission yields.[30] Furthermore, the escape probability function of the form similar to Eq. (8) has been found to be satisfactory in the theoretical treatment of secondary emission.[31]

Since the escape length or attenuation length L is related to the mean free paths for collisions, it should be of interest to see how the mean free paths can be calculated from the fundamental theory of electron scattering in solids. A brief discussion of the important scattering processes is given in the following sections.

Electron-phonon Scattering

The mean free path ℓ_p can be related to the energy band structure of the photoemissive material. According to Kane[32], ℓ_p can be calculated from the expression

$$\ell_p = v_g/w_p \ , \tag{9}$$

where v_g is the group velocity of the photoelectron, and w_p is the transition probability per unit time for electron-phonon interaction. Applying the Golden Rule of time-dependent perturbation theory,[33] we can write

$$w_p = (2\pi/\hbar)\ M^2\ \rho(E), \tag{10}$$

where w_p represents the phonon scattering rate, and $\rho(E)$ is the density of final unperturbed states. The quantity M^2 is assumed to be approximately constant. The group velocity v_g can be calculated for a given energy band structure E(k), i.e.,

$$v = (1/\hbar)\nabla_k E \ . \tag{11}$$

Electron-electron Scattering

The mean free path for electron-electron collisions can be calculated from

$$\ell_e = v_g/w_e \ , \tag{12}$$

where w_e denotes the scattering rate due to electron-electron interaction. Using the Golden Rule, we write

$$w_e = (2\pi/\hbar)\, M^2\, \rho(E), \qquad (13)$$

where the matrix element M can be calculated from the screened Coulomb interaction including exchange.

The inelastic scattering mechanism due to electron-electron collisions has been studied also by Berglund and Spicer[34]. Following the approach used by Motizuki and Sparks[35], they considered the situation in which the photoelectron in state (E', k') is scattered to state (E, k) while the interacting electron is scattered from state (E_o, k_o) to state (E_1, k_1). The probability per unit time for this to occur is given by

$$P = (2\pi/\hbar)\,|\langle k', k_o|H_{ee}|k, k_1\rangle|^2\, \delta[(E'-E)-(E_1-E_o)], \qquad (14)$$

where H_{ee} is the perturbation Hamiltonian for electron-electron interaction. In the work of Motizuki and Sparks, a phenomenological Yukawa potential of the form

$$V(r) = e^2\, e^{-k_c r}/r$$

was assumed for the interaction potential function. In order to find the total probability per unit time of an electron of energy E' being scattered to any energy E, Eq. (14) must be summed over all possible states corresponding to k', k_o, k, k_1, E, E_1, and E_o. This can be done if the wave functions are known.

Since accurate information on wave functions may not be available, it is worthwhile to note that approximations can be made in evaluating the total probability per unit time of an electron with energy E' being scattered to any energy E. In the study of photoemission from metals, Berglund and Spicer[34] have demonstrated that it is a good first order approximation to assume that the matrix element in Eq. (14) is independent of the k vectors of the electrons involved. By using the appropriate densities of states and Fermi functions, they pointed out that the total probability per unit time can be written as

$$P_t(E') = \frac{2\pi}{\hbar} \int_{E_o=0}^{\infty} \int_{E=0}^{\infty} M_{ee}^2 \, \rho(E_o) \, \rho(E_o + E' - E) \times F(E_o) \times [1-F(E_o + E' - E)] dE_o \times \rho(E) \times [1-F(E)] \, dE \, . \quad (15)$$

It should be noted that $P_t(E')$ is the reciprocal of the lifetime for electron-electron scattering of the photoelectron with energy E'. Therefore the mean free path ℓ_e can be expressed by

$$\ell_e = v(E')/(P_t(E') \, . \quad (16)$$

It should be mentioned that the mean free path ℓ_e for electrons in a metal has been calculated by Quinn[36]. He used the dielectric constant approach in which the

conduction electrons were assumed to be a degenerate electron gas. For low energies, the mean free path ℓ_e is given by

$$\ell_e \simeq \frac{24(\alpha r_s/\pi)^{\frac{1}{2}}[E_o^2(1/\xi_f^2 - 1/\xi_i^2) + 2E(1/\xi_f - 1/\xi_i)]a_o}{[\tan^{-1}(\pi/\alpha r_s)^{\frac{1}{2}} + (\alpha r_s/\pi)^{\frac{1}{2}}/(1 + \alpha r_s/\pi)]}, \quad (17)$$

where E_o is the Fermi energy; $\alpha \equiv (4/9\pi)^{1/3}$, and r_s is the radius (measured in units of the Bohr radius a_o) of a sphere equal in volume to the volume per electron. Eq. (17) represents the distance that an excited electron travels in going from an initial excitation energy ξ_i to a final excitation energy ξ_f. To satisfy our definition of ℓ_e, we make ξ_f equal to the work function of the metal. This distance is measured along the path of the excited electron. No random-walk situation is assumed in the calculations. Quinn has pointed out that the average energy lost by an excited electron in a typical electron-electron collision is not small compared to its initial excitation energy.

In order to obtain a theoretical estimate of the scattering lengths for electrons in metals, we used Eq. (17) to find ℓ_e for aluminum and gold. The following examples illustrate the theoretical estimates of the electron-electron scattering lengths for the same initial excitation energy.

Examples:

For excited electrons in aluminum ($r_s \approx 2$, $E_o \approx 12$ eV, $\xi_i \approx 10$ eV, $\xi_f \approx 4.2$ eV), we have $\ell_e \approx 50$ Å. For electrons in gold, ($r_s \approx 3$, $E_o \approx 5.5$ eV, $\xi_i \approx 10$ eV, $\xi_f \approx 4.7$ eV), we find $\ell_e \approx 7$ Å.

Improvements in calculating the electron-electron mean free path were subsequently made by considering the effect of virtual transitions, band structure, and exchange processes.[37-39] If these corrections are taken into account, the calculated mean free path is somewhat larger than that predicted by the free electron gas model.

Electron-Plasmon Scattering

In some metals, the excited photoelectron may be sufficiently energetic to interact with the plasma oscillations of the electrons in the metal. It is well known that the energy loss due to plasmon creation depends on the concentration of free electrons in the metal.[40] It is possible to generate both volume and surface plasmons. This type of inelastic scattering should be considered if high-energy photoelectrons are involved. Examples of volume plasmon energies are 5.7 eV for sodium, and 15.3 eV for aluminum. The surface plasmons have lower energies.

Auger Process

If an electron is optically excited from a low-energy state of energy E_1, another electron from an upper state of energy E_2 may occupy the state of energy E_1. The energy released from this transition may be absorbed by a third electron situated at some energy level E_3 above E_1. The third electron excited to a state E (above the Fermi level), where $E-E_3=E_2-E_1$, is called an Auger electron.[34] If the Auger electron is sufficiently energetic, it may escape into the vacuum. Thus the onset of the Auger process can give rise to a higher quantum yield.

5.2 Experimental Study of Photoemission from Metal Films.

As shown in Fig. 5, photocathodes may be fabricated for applications with radiation incident from the vacuum interface from which photoelectrons are emitted or from the substrate interface. The "front" illumination refers to the situation indicated in Fig. 5a; the "back" illumination is the situation indicated by Fig. 5b. The case of "back" illumination is of practical interest.[4] It is obvious that "back" illumination requires semitransparent photocathodes, in which case the optimum quantum yield depends on the thickness of the photoemissive film.

The principal aim of our experimental study on metal films has been to measure the quantum yields for "back" illumination as a function of film thickness in the spectral region above 1100 Å. Polished LiF crystals were used as substrates for the evaporated metal films. The experimental information should be of considerable interest to those who are directly concerned with the development of photoelectric detectors with LiF windows. In addition to the practical value of the results, the yield versus thickness data can be used to determine the attenuation length for photoelectrons.

5.3 Attenuation Length for Photoelectrons in Metal Films. Photoemission from Gold and Aluminum Films

Scattering of electrons in metal films is of current interest because the hot-electron transport process in thin-film devices does not appear to be well understood.[41] Some experimental studies[42-45] have been made to determine the mean free path for excited electrons in metals, but very little work has been done to extend the investigation to electrons excited by vacuum ultraviolet radiation. The purpose of our experiments has been to investigate the attenuation of vacuum uv photoexcited electrons in evaporated metal films.

The important scattering mechanisms in a solid film are assumed to be electron-electron and electron-phonon collisions. The combined effect of these collisions on the excited electrons can be expressed in terms of the attenuation length. As shown in a simple model for collision effects in photoelectron emission,[29, 46] the attenuation length L is related to the escape probability by

$$q(x) = B\, e^{-x/L} , \qquad (1)$$

where x is the distance between the surface and the point at which the electron is excited; B is the escape probability for the electron excited at the surface. The escape probability function is useful in calculating the photoelectric yield of a photo-emissive material. The photoelectric yield described in the present work is defined as the number of electrons emitted per incident photon.

As described in our previous studies,[13, 14] the electrons in a thin film can be excited by photons which pass through the LiF substrate. In the present study, the metal films were deposited on polished LiF crystals of 25 mm diameter and 2 mm thick. The crystal was mounted near the exit slit of a vacuum uv monochromator. For electrical contact with the evaporated film, a gold film was previously deposited on the LiF surface adjacent to the substrate areas for

the evaporated films. It was possible to deposit three films on the crystal, each on a different section of the crystal surface. As shown in Fig. 6, the position of the crystal could be changed by means of a linear-motion feedthrough. Photoemission measurements were made immediately after evaporation at a pressure of approximately 10^{-7} Torr. Sorption and ion pumps were used to evacuate the photocell and evaporator chamber.

The thickness of the evaporated film was determined by comparing the measured transmittance with the transmittance calculated as a function of film thickness for photons of 10.2 eV. The effect of interference due to multiple reflections was taken into account in computing the transmittance of the metal film. Figures 7 and 8 illustrate the calculated transmittance and reflectance as a function of film thickness for gold and aluminum at 10.2 eV. Particular attention was given to gold and aluminum because the values of the optical constants of these metal films in the vacuum uv region can be found in the literature.[47-49] The photon flux which passed through the LiF substrate was measured by a calibrated gold-foil photoelectric detector. The typical value of the photon flux of 10.2 eV was approximately 4×10^9 photons per second. The size of the incident light beam at the crystal surface was 1 mm x 3 mm.

The photoemission currents at a number of wavelengths between 1608 Å and 1117 Å were measured as a function of time after the film was deposited on the substrate. A noticeable change of photoelectric yield with time immediately after evaporation was observed. It was particularly noticeable for aluminum. The yield at photon energies below 9 eV decreased while the yield above 9.7 eV increased with time. The maximum change of yield over a period of 60 minutes after evaporation was about 33 percent for aluminum at 11 eV. The change of yield with time may be attributed to absorbed atoms or molecules on the metal-vacuum surface. With the assumption that the change of yield with time was due to surface contamination or oxidation,[50] the yield of the clean metal film was obtained by extrapolating the yield versus time curve to zero time. Figures 9 and 10 illustrate the extrapolated yields of several films of different thicknesses for evaporated gold and aluminum. It should be mentioned that the change of yield with time after evaporation of aluminum in a vacuum of 5×10^{-10} Torr has been observed.[51] This suggests that the coverage of the surface by atoms of the residual gas may not be the only cause of the observed change of photoemission yield.

In order to find the attenuation length for the photoelectrons from the experimental data, we compared

the measured yield with the calculated yield. If we use the escape probability function described by Eq. (1), we can express the yield for photoemission from the backside of a film of thickness t as

$$Y = [B\,(1 - R)\,I_o \int_o^t \alpha e^{-\alpha s}\, e^{-(t-s)/L}\, ds]/I_o, \quad (2)$$

where α is the absorption coefficient; R, the reflectance; I_o, the number of incident photons per second. Upon evaluating the integral in Eq. (2), we get

$$Y = B\alpha L\,(1 - R)\,(e^{-\alpha t} - e^{-t/L})/(1 - \alpha L). \quad (3)$$

It is assumed that the value of L in Eq. (3) is characteristic of the average energy of the electrons initially excited by the photons. A smaller L value is expected for a higher average energy. We can estimate the value of L by comparing the measured yield as a function of film thickness with the yield calculated from Eq. (3). An example of this comparison is shown in Fig. 11. The values of B and L were selected to fit the yield data. The L values for the photoelectrons excited at different photon energies are shown in Fig. 12. The results indicate that the attenuation length for electrons in aluminum is about five times as large as that for electrons in gold at 10.2 eV. The lack of strong dependence on the photon energy in this region suggests that a relatively large fraction of low-energy photoelectrons can still be

excited initially by photons of higher energies.

In order to compare the attenuation-length value obtained from our experiments with the scattering lengths reported by Stuart and Wooten[52], we used the expression derived by Kane[29], which relates the attenuation length to the mean free path ℓ_e for electron-electron collisions and the mean free path ℓ_p for electron-phonon collisions. This expression is given by

$$L = \ell_e / (1 + \ell_e/\ell_p)^{\frac{1}{2}}. \qquad (4)$$

The values of the mean free paths obtained by Stuart and Wooten were $\ell_p \sim 130$ Å and $\ell_e \sim 500$ Å for electrons excited by photons of 9.2 eV in aluminum. If these values are used in Eq. (4), the attenuation length would be approximately 230 Å, which is in good agreement with the value obtained from our yield data.

Scattering-length measurements based on electron-beam attenuation were reported recently by Kanter[53]. For electrons in gold, the values ($\ell_e \sim 45$ Å and $\ell_p \sim 250$ Å) are in agreement with our data. However, for electrons in aluminum, the values ($\ell_e \sim 50$ Å and $\ell_p \sim 250$ Å near 5 eV above the Fermi level) are in disagreement with the results of Stuart and Wooten[52]. From our point of view, the values from Kanter's measurements do not give the same attenuation-length value obtained from our data for electrons in aluminum.

It should be noted that Kanter's definition of attenuation length is different from the one used in photoemission studies. In Kanter's work, the relationship between attenuation length and the mean free path is given by

$$L^{-1} = \ell_e^{-1} + \ell_p^{-1} .$$

In our work, the attenuation length or escape length is defined in terms of the escape probability $q(x) = B \exp(-x/L)$, where L is related to the mean free paths described in Kane's model. The two L values agree only if ℓ_p is much larger than ℓ_e.

Photoemission from Nickel Films

Previous measurements of photoemission from evaporated nickel films have stimulated much interest concerning the density of states of nickel. Energy distribution measurements[54] of the emitted electrons from nickel indicated a strong peak in the optical density of states at approximately 4.5 eV below the Fermi level. In disagreement with this result were soft x-ray studies[55] and ion neutralization spectroscopy work[56] which showed a dominant peak in the density of states within 2 eV of the Fermi level. Furthermore, the anomalous peak was not in agreement with the results of one-electron band calculations for nickel. Recently, the question was resolved by

further photoemission studies[57] which showed that the anomalous peak was sensitive to the surface condition of nickel. The surface contamination of nickel films at 3×10^{-8} Torr was also reported by Vehse and Arakawa[58].

It appears that energy distribution measurements are extremely sensitive to the surface conditions of some metals. Eastman and Krolikowski[57] pointed out that the surface conditions of nickel are important because the electron escape depths are very short. They concluded that the scattering lengths for electrons in nickel are about 5 to 15 Å for energies greater than 7 eV above the Fermi level.

If the escape depth is about 15 Å, a very thin film of nickel should have optimum yield. In an effort to get a better understanding of the photoelectric properties of very thin films, we prepared nickel films on polished LiF crystals and measured the yield immediately after evaporation. The film thickness was estimated from transmission measurements at wavelength 1216 Å. The calculated transmittance of a nickel film on a LiF substrate as a function of film thickness is shown in Fig. 13. The spectral quantum yields of nickel films of different thicknesses under "back" illumination are illustrated in Fig. 14. The fact that photoemission from a very thin nickel film can be measured indicates that the evaporated film is sufficiently continuous to provide electrical contact

with the metallic film electrode around the substrate area. The spectral quantum yield of nickel under "front" illumination by photons of energies between 10 and 23 eV is shown in Fig. 15. In our measurements, we observed a gradual change of yield with time immediately after evaporation at 10^{-7} Torr. The yield values shown in Fig. 15 are extrapolated yield data at zero time for films of different thicknesses. The gradual change of yield may be attributed to surface contamination or a gradual change in film structure immediately after deposition.[51] The experimental chamber for measuring photoemission in the spectral region of 10 to 23 eV is shown in Fig. 16. The helium-continuum light source and a one-meter normal incidence monochromator were used to provide the dispersed radiation.

A few remarks in regard to the quantum yield of nickel films should be made. No significant change in yield with increasing film thickness larger than 20 Å under "front" illumination was observed. The yield of very thin films (less than 20 Å according to transmittance measurements) is somewhat higher than the yield of thicker films. The lack of increase in yield with increasing film thickness greater than 20 Å under "front" illumination suggests that the electron escape length is less than 20 Å. This estimate is in agreement with the results of Eastman and Krolikowski[57].

The slightly higher yield of the thin films might be due to backscattering from the substrate interface.

The yield in the region 10 to 23 eV can be calculated for a sufficiently thick film of nickel. Since the escape length is small in comparison with the absorption depth, the expression for the quantum yield should be proportional to $(1-R)\alpha$, where α is the absorption coefficient and R is the reflectance. Figure 17 illustrates $(1-R)\alpha$ as a function of photon energy. Comparing the shape of the yield curve with the spectral values of $(1-R)\alpha$, we find they are in qualitative agreement.

Photoemission from Beryllium Films

While optical studies on beryllium films in the far ultraviolet region have been reported,[59] not much work has been done to determine the photoelectric yield of pure beryllium. For this reason, we performed yield measurements on evaporated Be films in the spectral region 10 to 23 eV.

Pure beryllium flakes purchased from the Johnson, Matthey & Company were evaporated from a tantalum boat to form a film on a polished LiF substrate. The thickness of the film was estimated from transmittance measurements at 10.2 eV. The transmittance and reflectance as a function of film thickness at wavelength 1216 Å

are shown in Fig. 18. A gradual change of yield with time immediately after evaporation was observed at 10^{-7} Torr. The yield versus time curves were plotted and the extrapolated yield at zero time was determined for various photon energies.

Figure 19 illustrates the spectral quantum yield of evaporated beryllium. Comparing the spectral yield curve with the $(1-R)\alpha$ curve for Be, we see that the spectral yield does not decrease as rapidly as $(1-R)\alpha$ for photon energies above 13 eV. The $(1-R)\alpha$ values shown in Fig. 20 were calculated from the optical data published in reference (59).

6. PHOTOEMISSION FROM SEMICONDUCTORS

When electrons are optically excited from the valence band of a semiconductor, the excited electron may move to the surface and escape into the vacuum. In the absence of band bending, the surface energy barrier for the photoelectron is called the electron affinity of the semiconductor. The electron affinity E_A represents the energy between the vacuum level and the bottom of the conduction band.

The escape condition for the photoelectron is

$$mv_x^2/2 > E_A \ ,$$

where v_x is the component of the electron velocity along the direction normal to the surface. The probability of escape at the surface can be estimated by considering the angle of incidence of the excited electron upon arrival at the surface. If a photoelectron of kinetic energy E relative to the bottom of the conduction band approaches the surface at angle θ with respect to the normal, the escape condition requires that

$$\cos^2 \theta > E_A/E \ .$$

Hence the "escape" cone is limited by the angle

$$\theta_m = \cos^{-1}(E_A/E)^{\frac{1}{2}}, \qquad (1)$$

If the angle of incidence is greater than θ_m, the photoelectron should be reflected back into the solid.

Assuming the probability that the excited electron of energy E moves in any direction is the same, we can express the probability that it will approach the surface at some angle between θ and $\theta + d\theta$ by

$$d\Omega/4\pi = \tfrac{1}{2} \sin \theta \, d\theta \, . \qquad (2)$$

$d\Omega$ is the element of solid angle. By integrating Eq. (2) over the angle of the escape cone, we see that the probability of escape at the surface is given by

$$P_s(E) = \int_0^{\theta_m} d\Omega/4\pi = \tfrac{1}{2}[1 - (E_A/E)^{\frac{1}{2}}] \, . \qquad (3)$$

Equation (3) is useful in electron-emission studies.[60,61]

For most semiconductors, the value of E_A is not larger than 5 eV. For most metals, the surface barrier is about 10 eV, i.e., the Fermi energy plus the work function. According to Eq. (3), the electrons excited to states of energy E in most metals would have a lower probability of escape at the surface than the excited electrons of the same energy in semiconductors. However, photoemission is predominantly a volume process; so the quantum yield depends on electron scattering processes beneath the surface in addition to the escape situation at the surface.

In a semiconductor, the photoelectron may lose energy by making collisions with phonons, defects, and electrons in the valence band. The inelastic collisions which create additional free electrons and holes are of particular interest in photoemission studies.[62, 63] Impact ionization (across the band gap) is also an important mechanism of electrical conduction in semiconductors.[64-66] Sommer and Spicer[67] have summarized the published information concerning the threshold energy for electron-hole pair production in various semiconductors. For most materials, the threshold energy appears to be greater than $2E_g$, where E_g is the band-gap energy. This is an important relationship as far as photoemission is concerned. If the electron affinity is not small and the band gap is not sufficiently large, inelastic scattering involving impact ionization would reduce the total probability of escape for the excited electron in the semiconductor. This type of interaction leads to small quantum yield. On the other hand, if the electron affinity is small and impact ionization occurs, the scattered photoelectrons and the secondary electrons may escape into the vacuum and thereby give rise to high quantum yield.

The theoretical consideration of photoemission from semiconductors near the threshold for a general band structure has been discussed by Kane[68]. He showed that the yield vs energy relation near the threshold can be

related to a number of possible optical excitation and escape mechanisms involving volume and surface states in semiconductors. In the presence of surface states, band bending in semiconductors occurs. The dominant effect of band bending is to raise or lower the effective photoelectric threshold for the photoelectrons originating from increasing depths below the surface.[69, 70]

6.1 Photoemission from Silicon

Silicon is a well known semiconductor. The electrical properties of silicon are fairly well understood. The optical constants of Si in the region 1 to 10 eV were measured by Philipp and Taft[71]. Further measurements of the optical constants in the region 10 to 19.2 eV were reported by Sasaki and Ishiguro[72]. The optical data showed evidence that plasma oscillation can be excited by photons of approximately 17 eV. Photoemission studies[73-75] on silicon crystals in the region below 6 eV have been performed. Recently, Callcott[76] reported some work on Si in the region 6 to 9.6 eV. While photoemission studies have contributed important knowledge on the band structure of silicon, information on the photoelectric yield above 6 eV does not appear to have been published. The principal aim of our work on

silicon has been to determine how much effect the oxide layer has on the spectral quantum yield.

The silicon samples used in our experiments were p-type silicon slices (14 mm diameter and 0.25 mm thick) with (111) surfaces. The resistivity of the crystals was approximately 15 ohm-cm. In our experiments, a thin silicon crystal was heated to a temperature of approximately 1200 ^{o}C in a tantalum foil holder. The duration of the heat treatment was about 3 minutes in a vacuum of about 1 x 10^{-7} Torr. The quantum yield was measured before and after heating. The results are illustrated in Fig. 21. It is interesting to note that the effect of heating is the reduction of quantum yield above 10 eV. The spectral quantum yield of a heat-treated Si crystal from 7.5 to 23 eV is shown in Fig. 22.

Our tentative explanation of the change of yield after heat treatment is that the untreated Si crystal has a thin layer of silicon oxide on its surface. Photoemission from the oxide layer under optical excitation above 10 eV would contribute to a higher yield of the crystal before heating. At 1200 ^{o}C, the oxide layer could be removed from the surface. Consequently, the yield of the heat treated silicon crystal should be lower for photon energies above the photoelectric threshold of silicon oxide. The results shown in Fig. 21 suggest that the photoelectric threshold

of silicon oxide is approximately 10 eV. It would be desirable to measure the spectral quantum yield of pure silicon oxide to substantiate our conclusion.

The decrease in yield of silicon above 17 eV may be an indication that the photoelectrons are scattered by plasmons in the crystal. A lower quantum yield would be expected if a large fraction of the excited electrons are scattered to states below the vacuum level.

6.2 Photoemission from SiC

Low-temperature optical absorption and luminescence of pure SiC crystals have been investigated extensively in recent years.[77] The breaks observed in the transmission curve near the absorption edge have been attributed to excitations of acoustic and optic phonons. The luminescence at low temperature can be explained on the basis of recombination of an exciton bound to an unknown impurity (possibly nitrogen).

It has been demonstrated that silicon carbide crystals can be made p or n-type by doping the crystal with aluminum or nitrogen atoms.[78] The black crystals are p-type; the green crystals are n-type.

Previous investigations of photoemission from SiC crystals were made in the spectral region below 11 eV.[11,79] Our measurements showed that p-type SiC has

a higher yield than the n-type crystal. The difference is probably due to space-charge band bending near the surface of the crystal.

We have performed further yield measurements on the p-type SiC crystal in the spectral region above 11 eV. Heat treatment at approximately 950 °C for 5 minutes in a vacuum of about 1×10^{-7} Torr can change the quantum yield appreciably at higher photon energies. The spectral yields measured before and after heating are shown in Fig. 23.

6.3 Photoemission from Se and Te.

The electrical and optical properties of selenium and tellurium are of current interest. It has been discovered that selenium and tellurium approach a metallic state under high-pressure conditions.[80] There are various forms of selenium. Amorphous selenium is selenium in a glassy state with no well defined freezing point. This form of Se consists of Se_8 rings, along with a few atoms (5%) in a weak nearest-neighbor trigonal symmetry.[81] The amorphous form of Se can be obtained by vacuum evaporation. The metallic form can be produced easily by heating the amorphous form to about 75 °C.[82] Similar to the structure of crystalline Se, tellurium exists in a hexagonal chain structure.[83]

Results of optical studies on selenium and tellurium in the vacuum ultraviolet region have been reported.[84-86] The energy-loss function $-\mathrm{Im}(\varepsilon)^{-1}$, which can be calculated from the optical data, shows peaks at 5.3 and 19 eV for amorphous Se; at 5.6 and 17 eV for Te. The peaks at 19 eV for Se and 17 eV for Te have been attributed to creation of volume plasmons[87].

If the volume plasmons are indeed excited at 19 and 17 eV in Se and Te, inelastic scattering of photoelectrons by plasmons would occur above a certain photon energy. If this occurs, the spectral quantum yield should decrease at photon energies above the plasmon energy. In order to see this, we measured the quantum yield of evaporated selenium and tellurium in the spectral region 10 to 23 eV, using the helium-continuum light source. Figures 24 and 25 illustrate the results. The decrease of yield appears at the expected range of photon energy. While the spectral yield curves are in agreement with the occurrence of electron-plasmon scattering, the spectral absorption curves illustrated in Figs. 26 and 27 could also be used to explain the decrease in yield with increasing photon energy. That is to say, the absorption length could be longer than the escape length for the photoelectron.

In the spectral region below 10 eV, we used the hydrogen-discharge tube as a light source for the monochromator. When hydrogen is used, the sample chamber should have a LiF window because hydrogen can react with Se and form hydrogen selenide. Previous yield measurements on Se agree with our present data over the overlapping region 10 to 11 eV.[10]

The spectral yield of evaporated Te for photon energies below 11 eV is shown in Fig. 28. The measurements were performed with a LiF windowed experimental chamber.

6.4 Photoemission from Cuprous Halides

Cuprous halides are semiconductors whose energy band gaps are approximately 3 eV. The crystals have a zincblende structure below 643 ^{o}K. Results of optical studies on cuprous halides in the spectral region 3 to 10 eV have been reported by Cardona[88]. According to luminescence studies,[89] the exciton-band structure of CuI at low temperature was found to be sensitive to the film thickness. The Stoke shift was attributed to exciton diffusion.

Photoemission from copper iodide has been reported.[90-92] CuI photocathode is of particular interest in photon-detector development because CuI has the desirable spectral yield for vacuum u.v.

applications. LiF-windowed photomultiplier tubes with CuI photocathode are now commercially available.[93]

In order to develop a better understanding of the photoelectric properties of cuprous halides, photoemission experiments were performed to determine the density of states and electron attenuation length in these compounds.[94,13] In our experiments on evaporated CuBr under "back" illumination, the yield of the photoemissive layer on a LiF substrate was measured as a function of film thickness. As shown in Fig. 29, the spectral yield of CuBr was found to be sensitive to the film thickness. It is interesting to note that the spectral response can be adjusted by varying the film thickness. Figure 30 illustrates the yield of CuI as a function of film thickness under "back" illumination of 10.2 eV. The film thickness was estimated from transmittance measurements. The results show that the optimum quantum yield of CuI at 10.2 eV is obtained for a film of approximately 50 Å thick.

Previous yield measurements[95] on cuprous halides were limited to the wavelength region above the LiF cut-off. In order to determine the yield above 11 eV, a windowless experimental chamber was used to perform the measurements. The sample chamber and evaporator were evacuated by a LN baffled 4-in oil diffusion pump. The sample powders were purified by distillations in vacuum before being placed in a quartz boat

for evaporation in the experimental chamber. The film was deposited on a polished LiF substrate. The cuprous halide film made electrical contact with a gold or silver film electrode which was previously deposited on the LiF surface adjacent to the substrate area. The purpose of the LiF substrate was to provide sufficient transmittance of u.v. radiation for estimating the thickness of the film. The helium-continuum light source was used with the monochromator to provide radiation of wavelengths between 1216 and 537 Å. Hydrogen-discharge was employed for the longer wavelength region.

Figure 31 illustrates the spectral yield of evaporated cuprous iodide under "front" illumination. A broad peak with its maximum near 12 eV may be related to the optical excitations from the d band of copper[94]. The yield over the spectral region 11 to 21 eV appears to be relatively uniform.

6.5 Photoemission from Evaporated CdTe.

CdTe is a semiconductor whose band gap is 1.45 eV. The electron affinity is approximately 4.5 eV. CdTe has received a great deal of attention in recent years because CdTe films deposited obliquely exhibit a large photovoltaic effect.[96] The technique of preparing good CdTe films has been discussed by a number of workers[97,98].

It has been shown that pure CdTe films can be produced by vacuum deposition if the substrate temperature is kept slightly above 300°C.

Photoemission from CdTe crystals has been investigated by Scheer and van Laar[99], and by Shay and Spicer[100]. In the Shay and Spicer experiments, the photoemission measurements were made on cleaved CdTe single crystals in ultrahigh vacuum. From the energy-distribution measurements of the photoemitted electrons, they were able to determine the absolute energies of the initial and final states for the observed optical transitions. Their estimate of the width of the valence band is about 3.7 eV. Furthermore, their yield measurements below 11 eV showed a gradual rise in yield in the region above 9 eV. The rise in yield was attributed to the escape of secondary electrons.

In order to determine whether electron-hole pair production contributes to a higher yield with increasing photon energy, we extended the yield measurements to energies above 11 eV. In our experiment, the pure CdTe film was prepared by evaporating CdTe powder from a resistance-heated tantalum boat onto a hot tantalum foil. The yield of the evaporated film was measured at room temperature.

As shown in Fig. 32, the spectral yield of CdTe

appears to be similar to that of evaporated tellurium in the photon-energy region above 10 eV.

6.6 Photoemission from Evaporated GaAs

The photoelectric properties of GaAs crystals have been investigated recently.[101-103] The band-gap energy is 1.4 eV. The photoelectric threshold is approximately 5.5 eV. The quantum yield for photon energies between 5.5 and 11 eV has been measured. Similar to CdTe, the ratio of the band gap to the electron affinity is low. Therefore, low quantum yield would be expected.

In previous work, a clean surface of GaAs was obtained by cleaving a single crystal in ultrahigh vacuum. While single crystals are suitable for photoemission studies of band structure and electron-transport properties of the material,[104,105] they are not as useful as the thin films which are required for photoelectric applications. Unfortunately, it is difficult to produce a pure GaAs film by conventional vacuum evaporation. GaAs will decompose when the sample is heated slowly. However, it has been reported that an epitaxial film of GaAs can be deposited on a hot germanium-crystal surface by flash evaporation.[106,107] The substrate temperature should be in the range of 400 to 600°C.

In our experiment, the GaAs film was prepared by the flash-evaporation method. The GaAs powder was purchased from Semi-Elements, Inc., Saxonburg, Pa. The substrate was a thin Ge crystal with surface (111). The crystal was mounted in a tantalum-foil holder, which also served as the substrate heater. The spectral yield of a GaAs film on a Ge substrate is shown in Fig. 33. A broad peak appears near 14 eV. Since the film thickness was not measured, we are not certain that the observed yield is optimum for GaAs.

There is another technique of preparing GaAs films. It involves separate gallium and arsenic evaporation sources. Steinberg [Appl. Phys. Letters 12, 63 (1968)] has shown that cesiated GaAs films can be prepared in this manner for photoelectric applications.

7. PHOTOEMISSION FROM LARGE BAND-GAP SOLIDS

Large band-gap materials with low electron affinity have photoelectric properties which are desirable for vacuum u.v. applications. The useful characteristics are high photoelectric threshold and high quantum yield. Large band-gap materials are suitable for use as photocathodes of "solar blind" photon detectors.

The high yield of a large band-gap solid with low electron affinity can be understood readily by considering the scattering processes for the excited electrons in the solid. If the band gap is large, inelastic scattering by the valence-band electrons should not occur in the vacuum u.v. region. Therefore, the scattering of the photoelectron is limited to electron-phonon and electron-defect collisions. Since the energy loss associated with these collisions is small, most of the excited electrons arriving at the solid-vacuum interface would still be sufficiently energetic to escape into the vacuum.

The motivation for further photoelectric studies of large band-gap solids is that optical excitations and electron-transport properties of insulating solids are not fully understood. It has been suggested that exciton states of alkali halides are likely to be present above the band-gap energy.[108] Some photoemission

data appear to be compatible with this viewpoint. If the continuum-state exciton can move through some distance before dissociating into a free electron-hole pair, the attenuation length for a photoelectron could be longer than the free-electron attenuation length of the same energy. Evidence of relatively long escape length for photoelectrons in alkali halide films has been reported.[14]

7.1 Photoemission from Alkali Halides

Results of experiments on photoemission and optical absorption of alkali halides have been reported.[109,110] In previous work, the yield measurements of alkali halides were limited to the spectral region below 11 eV. The recent yield measurements performed in our laboratory covered the spectral range 12 to 21 eV.[9] From these measurements, the yield values were found to be approximately 100% at certain photon energies. Duckett and Metzger[111] proposed a random-walk model of electron scattering to explain the high yield of alkali halides. According to this model, the electron makes many electron-phonon collisions while diffusing to the surface. The random-walk assumption leads to a high probability of escape if the electron escape length is longer than the absorption length for the incident photon.

There is no doubt that multiple scattering involving electrons and phonons occurs in the photoelectric process.

More important, we should recognize that impact ionization caused by the energetic photoelectron is likely to occur if photoemission is initiated by high-energy photons. Thus the rise in yield due to emission of the secondary electrons may appear in photoemission from solids in the extreme u.v. and soft x-ray region.

An important aspect of photoemission studies is the relationship between the quantum yield and film thickness. It has been pointed out that optimum yield is not obtained unless the photoemissive film is sufficiently thick.[112] We refer to the situation under "front" illumination. Perhaps it is useful to show how the escape length is related to the yield. For the case defined by "front" illumination, the yield vs thickness relation is given by

$$Y = Y_o T(t)\, e^{-t/L_o} + B(1-R)\alpha L[1-e^{-(\alpha+\frac{1}{L})t}]/(1+\alpha L), \quad (1)$$

where $T(t)$ is the fraction of the incident light intensity transmitted into the substrate; Y_o, the yield of photoemission from the substrate into the photoemissive film of thickness t; L_o, the attenuation length for the excited electrons (from the substrate) moving through the film into the vacuum; L, the escape length for the photoelectron excited in the film; α, the absorption coefficient. It should be noted that $T(t)$ approaches zero as t becomes sufficiently large. Equation (1)

reduces to

$$Y = B(1 - R)\alpha L/(1 + \alpha L) \qquad (2)$$

for large values of t. The essential character of yield vs film thickness data can be explained in terms of Eq. (1). If the yield saturates rapidly with respect to thickness, a small escape length compared to the absorption length is expected.

In order to substantiate the description given by Eq. (1), we measured the quantum yield of evaporated KBr films as a function of film thickness in the spectral region between 10 and 23 eV. The yield was measured immediately after the KBr film was prepared by vacuum evaporation in situ at approximately 1×10^{-7} Torr from a resistance-heated quartz crucible. Each KBr film was deposited on a polished LiF crystal whose surface was pre-coated with a thin film of silver (approximately 50% transmission at 1216 Å). The silver film served as a conductive substrate for the insulating KBr film. The thickness of the KBr film was estimated from the transmittance data at 10.2 eV. Results of yield measurements for three different film thicknesses are shown in Fig. 34. It is interesting to note that the yield does not change appreciably beyond 200 Å in the low yield region. This is illustrated in greater detail in Fig. 35. However, the optimum yield does not appear unless the thickness is about 900 Å in the high-

yield region. An example of this is shown in Fig. 36. The results are in qualitative agreement with Eq. (1).

7.2 Exciton-Induced Photoemission from KCl Films

Exciton-induced photoemission is a process in which the excitons produced by the incident radiation transfer their energy to F-center electrons, thereby causing electron emission into the vacuum. Previous work on exciton-induced photoemission from F-centers in alkali iodide films was reported some years ago by Apker and Taft[113]. The results of their experiments showed structure in the yield curve at the spectral region of the exciton band. An attempt to explain the spectral yield was made by assuming a thin surface layer in which no exciton-induced emission could arise.[114] However, in later experiments on single crystals of KI, it was found that an inversion in the exciton-induced emission yield could be attributed to the sharply peaked surface reflectivity.[115]

Evidence for exciton-induced emission has been found also in the photoelectric studies of other materials. In the measurement of photoemission from BaO containing donor atoms, sharp structure in the spectral yield curve showed up clearly at 80 ^{o}K, and this was believed to be due to ionization of donor centers by excitons.[116] In the study of CdS, Shuba[117] observed

that the velocity distribution of the emitted photoelectrons was not sensitive to the change of photon energy from 5 to 6.5 eV. His results were interpreted as an indication of exciton effect. However, Spicer[118] pointed out that a velocity distribution which is insensitive to photon energy was not sufficient evidence for exciton-induced emission, and the results could be explained by assuming direct excitation from the defect levels.

The mechanism of exciton-induced emission from F-centers is still a subject of vigorous discussion. In the analysis of energy distribution of photoelectrons from F-centers, Apker et al. explained the appearance of the low-energy electron emission in terms of energy loss of the excited electron before escape.[113] Recently, Spicer[119] suggested that the velocity distribution observed in their experiment can also be explained by assuming the exciton relaxes before giving its energy up to the F-center electron. While the interpretation of previous measurements needs to be clarified, there is no doubt that useful information concerning excitons can be obtained from experiments on exciton induced photoemission.

KCl was selected for our experiments because luminescence and ultraviolet absorption studies on this material have been reported.[120,121] There is an exciton band at approximately 8 eV for KCl.

Although photoemission from the valence band of KCl has been measured,[109] the electron emission from F-centers in KCl films in the presence of exciton absorption does not appear to have received much attention. The principal aim of this paper is to describe some new experimental results on photo-emission from evaporated KCl films in the spectral region of exciton absorption. A gradual rise of photoelectric emission with time was observed under steady ultraviolet excitation of approximately 8 eV. In the presence of strong biasing radiation (visible light), the gradual enhancement of emission did not appear. An attempt is made to explain the transient enhancement in terms of electron emission from new F-centers formed by excitons.

Experimental Method

Photoelectron emission was measured immediately after the KCl film was prepared by vacuum evaporation in situ at approximately 10^{-7} Torr from a resistance-heated quartz crucible. The KCl films were deposited on polished LiF crystals (25 mm diameter and 2 mm thick) which were pre-coated with a thin film of nickel or silver. The transmission of the metal film was approximately 60% at wavelength of 1216 Å. The pur-pose of the thin metal film was to provide a conductive

substrate for the KCl film and to allow sufficient transmission of radiation for estimating the thickness of the KCl film. The absorption coefficient of KCl at 1215 Å is about 4.2×10^5 cm^{-1}.[108]

The experimental chamber was mounted directly on the exit-slit housing of a one-meter normal incidence vacuum u.v. monochromator. The chamber was evacuated continuously with a liquid nitrogen baffled 4-inch diffusion pump. A LN cold trap was also used near the exit slit of the monochromator. As shown in Fig. 37, a tungsten foil of known spectral yield was employed to determine the incident photon flux. Since the tungsten foil was attached to a linear-motion feed-through, it was possible to adjust its position to permit the biasing radiation (visible light) from a tungsten filament lamp to come through the LiF-metal film substrate and strike the KCl film.

Results and Discussion

Figure 38 illustrates the photoelectric yield of a KCl film before and after ultraviolet irradiation for 45 minutes in the exciton band. The increase of yield near 8 eV depends on the duration of pre-irradiation at wavelengths of about 1600 Å. There is a noticeable decrease of yield at photon energies above 9 eV immediately after the irradiation

period at the exciton band. The slight decrease of yield may be attributed to inelastic collisions of the photoelectrons from the valence band with the new defects created by excitons during pre-irradiation. The enhancement of yield near 8 eV can be interpreted as exciton-induced photoemission from new F-centers formed by excitons.

Figure 39 shows the gradual rise of photoemission currents under steady ultraviolet excitation of wavelength 1577 Å for two different excitation intensities. The rate of enhancement appears to be somewhat greater for higher excitation intensity. The effect of biasing radiation (visible light) is illustrated in Fig. 40. In the presence of exciton absorption, the growth of emission current appears. If the biasing radiation is switched on, an abrupt increase of electron emission current is observed. While the visible light is on, the current decays rapidly to the level slightly above the initial emission current. In the presence of the biasing radiation, the exciton-induced emission current is quenched.

The photoemission yield of KCl in the spectral region between 7.5 and 8.5 eV is probably due to direct ionization of impurities and to exciton-induced emission. It is assumed that some initial concentration of negative-ion vacancies exists in the KCl film. When excitons are produced in the film, they may interact

with the vacancies to form F-centers. An F-center is an electron which has been trapped at a negative ion vacancy. Assuming that the photoemission yield is proportional to the F-center concentration, we may describe the gradual rise in photoemission current i as a function of time t in the presence of exciton absorption by

$$i(t) = K\,[F_o + F(t)], \tag{1}$$

where K is a constant which depends on the incident light intensity; F_o is the initial concentration of impurities, and F(t) is the concentration of F-centers formed by excitons. Thus the gradual rise of photoemission may be related to the change of F-center concentration F(t).

In order to see how the concentration F(t) varies with time, we must consider the processes which lead to the generation and decay of F-centers. For simplicity, we write

$$\frac{dF}{dt} = AVX - BXF - CF, \tag{2}$$

where V is the vacancy concentration; X, the exciton concentration; A, a parameter characterizing the vacancy-exciton interaction; B, a parameter characterizing exciton-F-center interaction; C, a parameter characterizing direct ionization of the F-centers. The vacancy concentration V can be written as $(V_o - F)$,

where V_o is the initial vacancy concentration.[122] If the lifetime of the exciton is τ, the exciton concentration X is given by

$$X = \tau I_o \ , \tag{3}$$

where I_o is the rate at which excitons are produced per unit volume, and this rate should be proportional to the incident light intensity. Accordingly, Eq. (2) becomes

$$\frac{dF}{dt} = AV_o\, I_o - [(A+B)\tau I_o + C]F. \tag{4}$$

Solving this equation for F = o at t = o, we have

$$F = \frac{AV_o\, I_o}{[(A+B)\tau I_o + C]} \left(1 - e^{-[(A+B)\tau I_o + C]t}\right), \tag{5}$$

The exponential saturation indicated by Eq. (5) appears to be in qualitative agreement with experimental observation. The effect of the biasing radiation can be understood readily in view of Eq. (5). In the presence of strong biasing radiation (visible light), the value of parameter C must be large because the F-centers created are rapidly ionized by the visible light. Consequently, the ultimate concentration of F-centers is greatly reduced. Furthermore, this reduced concentration would be established rapidly in the presence of strong biasing radiation because the exponent of the time dependent term increases with C. Hence the gradual growth of F(t) does not appear.

An attempt was made to check the rate of rise of the photoemission current for different excitation intensities of wavelength 1577 Å. Equations (1) and (5) were used to describe the emission current as a function of time. As shown in Eq. (5), the factor $[(A+B)\tau I_o + C]$ should be greater for higher light intensity. When the intensity was slightly more than doubled, a factor of about 1.3 times as large was sufficient to match the experimental data. This suggests that the factor is not a linear function of the light intensity. A possible explanation for this is that the dominant term of the expression is $(A+B)\tau I_o$, and the lifetime τ of the exciton becomes smaller for larger I_o.

It should be mentioned that for higher light intensity the gradual growth of emission current with time does not follow accurately the exponential saturation specified by Eq. (5). The deviation at large values of time is consistent with the suggestion that new vacancies can be produced by excitons.[123]

Applications

It might be of interest to suggest a possible application of the exciton-induced effect in KCl films. Since the production of F-centers by excitons in KCl occurs only in the spectral region 1500

to 1700 Å, a photoelectric detector with a KCl-film photocathode can be used as a spectrally selective device for measuring radiation of approximately 1600 Å. If the device is exposed to the u.v. radiation, the intensity information can be stored in the photocathode. Upon exposing the photocathode to visible light, the intensity information will appear as a current pulse. The pulse height can be related to the u.v. intensity and exposure time.

7.3 Photoemission from MgF_2 Films

Magnesium fluoride has optical properties which are desirable for vacuum ultraviolet applications. The transmission quality is almost as good as LiF in the vacuum u.v. region. The cutoff wavelength is about 1100 Å. It is well known that MgF_2 is widely used as a protective coating for mirrors and gratings.[124] A MgF_2 layer can preserve the reflecting quality of a metallized surface by preventing rapid oxidation of the metal.

The optical properties of MgF_2 have been studied extensively in the vacuum u.v. region.[125-127] As shown in Fig. 41, the absorption curve shows a sharp peak at 11.8 eV. It has been suggested that this peak is due to an exciton transition, and the absorption beginning at about 13 eV is due to band-to-band transitions.[127]

According to this interpretation, the threshold for photoemission from the valence band of MgF_2 should be higher than 13 eV.

In order to see whether this conclusion is valid, we measured the photoemission yield of evaporated MgF_2 in the spectral region between 7 and 23 eV. The film was prepared by evaporating optical-grade MgF_2 in situ at approximately 1×10^{-7} Torr from a tantalum boat onto a polished LiF crystal. The LiF substrate was pre-coated with a thin film of nickel. The purpose of the thin nickel film was to provide a conductive substrate for the MgF_2 film. Sufficient transmission at wavelength 1117 Å was obtained through the (LiF + Ni) substrate to estimate the film thickness of MgF_2 from the transmittance data.

The spectral yield was measured for different film thicknesses. If the film is not sufficiently thick, the electrons optically excited in the metallized substrate can diffuse through the MgF_2 layer and escape into the vacuum. Figure 42 illustrates this type of photoemission at wavelength of 1608 Å for which optical absorption in MgF_2 is very low. A similar effect has been observed in the photoemission study of $Al-Al_2O_3$ films.[15] The true yield of MgF_2 is obtained from measurements on a sufficiently thick layer of the material. The spectral yield of a MgF_2 film (approximately 2700 Å thick) is shown in Fig. 43. It is obvious that the

photoelectric threshold is not above 13 eV.

The yield curve shown in Fig. 43 has two noticeable shoulders which can be related to the optical properties of MgF_2. The rise in yield at 10.3 eV may be attributed to optical absorption beginning at approximately 10.3 eV.[126] The additional rise in yield at 11.2 eV may be associated with a sharp decrease in reflectance near 11 eV.[127] In Fig. 44, we express the yield in terms of number of electrons per absorbed photon by dividing our yield data by (1-R), where R is the reflectance value reported in reference 27. The increase in yield at 10.3 eV is clearly shown.

If we accept the absorption edge at 1300 Å (9.5 eV) reported by Schneider and O'Bryan[128] as the band gap and the threshold for photoemission from the valence band as 10.3 eV, we would obtain an electron affinity of approximately 0.8 eV. According to this model, the photoemission from MgF_2 at photon energies below 10.3 eV must be interpreted as emission from impurity centers. This model is not necessarily in disagreement with the suggestion that the absorption peak at 11.8 eV is associated with an exciton transition. As suggested by Philipp and Ehrenreich[108], exciton states are likely to be present at energies higher than the band gap in solids such as MgF_2 and alkali halides with relatively small dielectric constants and large lattice parameters. The exciton of energy greater than the band gap can

decay by dissociating into a free electron-hole pair. The electron from this process may escape into the vacuum.

7.4 Photoemission from KBr-KCl Mixture.

Optical absorption in mixed system such as KBr-KCl has been studied extensively by Mahr[129]. It was found that a halogen site in the mixture can be occupied either by a Cl^- or a Br^- ion. As a result, two series of absorption bands were observed. The heights of the absorption peaks depend on the relative concentrations of the two ions. With the exception of the high energy band of KBr between 8 and 9 eV, the energy values of the bands generally shift to higher energy as KBr concentration increases.

In view of the observed change in the absorption peak with composition, it was considered worthwhile to measure the photoelectric yield of the mixture KBr-KCl. From previous work,[109] we know that the photoelectric thresholds of KBr and KCl are approximately 7.8 and 8.7 eV, respectively. The principal aim of the experiment was to see whether the threshold for photoemission from the mixture can be shifted by adjusting the composition.

A 50-50% mixture of KBr-KCl was first fused in a quartz boat. Then the mixture was placed in the experimental chamber for evaporation and yield measurements.

The experimental chamber with a sealed LiF window was evacuated continuously by an ion pump. As a check on the composition, a film of the mixture was evaporated on a thin LiF substrate, and the optical density was measured immediately after evaporation. As shown in Fig. 45, the optical-density data of the 50-50% mixture agree with the results of previous work[129]. Using the same mixture, a film was formed on a gold-foil substrate for the quantum yield measurements. The spectral yield of the film is shown in Fig. 46. Comparing the yield of the mixture to that of pure KBr, we find that there is a significant difference in yield in the region between 7.8 and 9 eV. The effective photoemission threshold of the 50-50% mixture appears to be about 0.4 eV higher than that of pure KBr. A further study of yield vs composition would be desirable.

8. PHOTOLUMINESCENCE AND PHOTOCONDUCTIVITY

Although the luminescent properties of molecular crystals have been studied extensively, the redistribution of the absorbed optical energy and the process of emission are still not fully understood. For example, the fluorescence efficiency of sodium salicylate is high and uniform over a wide range of the vacuum u.v. spectrum. Whether the emission is characteristic of the molecule or the crystal is still a problem for further study.

In regard to photoconductivity of solids in the vacuum u.v. region, we must be aware of the photoemission effect which can contribute to the measured response associated with photoconductivity. Because of the experimental difficulties, it is difficult to give a reliable interpretation of the photoconductive response that may appear in this spectral region.

8.1 Temperature Dependence of Photoluminescence of Sodium Salicylate.

Sodium salicylate is a material which is widely used as a detector for vacuum ultraviolet radiation. It has two useful photoluminescent properties. The peak of the fluorescent intensity lies in the spectral region in which an ordinary photomultiplier tube (S-11) has the maximum-response sensitivity. It is particularly

useful in radiation-intensity measurements because the relative luminescence efficiency of this material is essentially constant over a wide spectral range in the vacuum ultraviolet.[21,22]

Although sodium salicylate has been used in radiation detection work for many years, only recently attempts were made to measure its absolute quantum efficiency. Unfortunately, there appear to be discrepancies in the published results. Kristianpoller[130] reported a quantum efficiency of 64% for incident radiation of 2537 Å at room temperature. The results of Allison, Burns, and Tuzzolino[131] indicate a quantum efficiency of almost 100%. Previous estimate[121] was only 10%.

An attempt[132] was made to explain the discrepancies by pointing out that the sensitivity of the phototube commonly used in the measurements is not independent of the angle of incidence. If the instrumental problems are taken into account, the absolute efficiency value of 99% at room temperature is believed to be the most reliable one. However, the question concerning the 99% efficiency arises when the effect of temperature change is considered. Kristianpoller and Knapp[133] reported some measurements of fluorescent yield of sodium salicylate at 80 °K. The fluorescence intensity was found to be 25% higher than that at room temperature. In an effort to obtain more information on the temperature

effect, we made measurements of the relative luminescence efficiency at high and low temperatures. An attempt is also made to provide a theoretical explanation of the temperature dependence.

Dependence on Temperature

When a molecular crystal is excited by incident radiation, it can dissipate some of its absorbed energy by internal quenching before making a fluorescent transition from the lowest excited singlet state.[134] The excess energy of the excited molecule in a crystal can be transferred to the crystal lattice inasmuch as the period of the individual molecular vibration is much smaller than that of a crystal vibration. Furthermore if the temperature is sufficiently high, the transition from the lowest excited state to the normal state may occur without emission of radiation.[135]

For organic molecules, it has been suggested that the lowest triplet state[136] can account for the temperature dependence of fluorescence and phosphorescence. If the triplet state intersects the excited singlet state at a high vibrational level, the quenching of the fluorescent state becomes more probable with temperature rise. This model assumes that the lowest vibrational level of the triplet state is lower than that of the excited singlet state. It is clear that phosphorescence originates from the triplet state because

the low probability of transition from the triplet state to the normal singlet state implies long-lived emission.

If we consider a film of sodium salicylate as a layer of molecular crystals, it may be more convenient to describe the fluorescence in terms of molecular excitons.[137] It is assumed that absorption of light produces excitons, which may disappear by luminescence and transformation into heat or triplet excitons. Thus a relationship between luminescence and temperature can be established by assuming that the photoluminescence efficiency is proportional to the ratio of the number of excitons converted to radiation to the number of excitons formed by the incident ultraviolet radiation. The ratio[138] is given by

$$r = \frac{P_L}{P_L + P_T} , \qquad (1)$$

where P_L is the probability per unit time that the exciton emits energy in the form of radiation, and P_T is the probability per unit time that the exciton transfers its energy to lattice vibrations. There is no reason why P_L should be dependent on the temperature. P_T is described by $A\ e^{-E/kT}$, where E is the activation energy of the radiationless transition, and A is a constant which depends on the frequency of lattice vibration.[139] If ε_o is the low temperature luminescence

efficiency, the higher temperature efficiency may be expressed as

$$\varepsilon = \varepsilon_o \, P_L/(P_L + A \, e^{-E/kT}) \quad . \qquad (2)$$

Equation (2) shows that the luminescence efficiency decreases with increasing temperature.

It may be of interest to see how the activation energy E can be estimated if experimental data on relative luminescence efficiency as a function of temperature are available. If the efficiency at high temperature is normalized to that at a low reference temperature T_o, Eq. (2) can be written as

$$\varepsilon/\varepsilon_o = \frac{1 + s \, e^{-K/kT_o}}{1 + s \, e^{-K/kT}} \quad , \qquad (3)$$

where s is A/P_L. Suppose we select two temperatures T_1 and T_2 such that

$$(1/T_o - 1/T_2) = 2(1/T_o - 1/T_1) \quad . \qquad (4)$$

With these two specified temperature values, we may eliminate the unknown quantity s and obtain

$$(1-R_1)R_2 \, y^2 - (1-R_2)R_1 \, y + (R_1-R_2) = 0 \, , \qquad (5)$$

where $R_1 = \varepsilon_1/\varepsilon_o$, $R_2 = \varepsilon_2/\varepsilon_o$, and $y = e^{(\frac{1}{T_o} - \frac{1}{T_1})E/k}$. The relative luminescence efficiencies at T_1 and T_2 can be determined by experiment. Hence E can be calculated by solving Eq. (5) for the given values of R_1 and R_2.

Experimental Method

The monochromatic radiation for the photoluminescence experiment was obtained from a 40-cm normal incidence, vacuum monochromator. A windowless hydrogen discharge tube (Hanovia 906-A32) was used as a light source. As shown in Fig. 47 a thin LiF window was placed in front of the exit slit to isolate the sample chamber from the vacuum chamber of the monochromator. The purpose of the sealed window was to eliminate the possible contamination [140] of the sodium salicylate film by diffusion-pump oil vapor and the hydrogen gas from the light source. The removable parts of the sample chamber were sealed with copper gaskets. The stainless steel chamber was evacuated initially by a sorption pump and then continuously by an ion-pump.

The sodium salicylate film was deposited on a thin (1 mm) quartz plate by the spray method. The effects of cooling and heating were studied on the same sample without breaking the vacuum. The higher temperature condition was established by placing an electric heater in the external cavity of the copper block on which the quartz plate was mounted. The photoluminescent response was detected by a photomultiplier tube. The current from the photomultiplier tube was measured by a micro-volt ammeter (Hewlett-Packard 425A) and a Sanborn-320 recorder. The spectral

fluorescent response from 1200 to 1650 Å was measured when a steady-state temperature was observed.

Results and Discussion

The photoluminescent response over the whole wavelength range decreased with temperature rise. The average normalized response as a function of temperature is shown in Fig. 48. The emission intensity at approximately 130 °K is approximately 14% higher than that at room temperature. This is in satisfactory agreement with the increase of 25% at 80 °K reported by Kristianpoller and Knapp[133]. Our data show that the luminescence intensity decreases gradually to about 400 °K. The luminescent response of the films which were heated to temperatures below 400 °K appeared to recover upon cooling in the vacuum. It should be mentioned that if the sodium salicylate film is heated to temperatures above 450 °K, the luminescence efficiency may be permanently reduced. Other factors besides temperature quenching may have to be considered to explain the abrupt decrease at the higher temperatures.

The activation energy E for sodium salicylate can be estimated from the normalized response data shown in Fig. 48. Since the normalized response represents the relative luminescence efficiency, the values of

R_1 and R_2 can be obtained directly from the graph. From the solution of Eq. (5), we find E = 0.07 eV. A comparison of the relative efficiency described by Eq. (3) with the experimental data is also shown in Fig. 48. The relative efficiency curve for s ~ 3 gives a good fit over a major portion of the data.

The relatively small value of E for sodium salicylate seems to be consistent with the situation in which the triplet state intersects the excited singlet state at a vibrational level of energy E above the minimum energy of the excited singlet state. As the temperature increases above T_o, the fluorescent state is quenched by the excited singlet-triplet radiationless transition. If the minimum energy of the vibrational levels of the triplet state is appreciably lower than that of the excited singlet state, phosphorescence may arise, and it may be more pronounced for higher temperatures. This is an interesting point which deserves further theoretical and experimental investigation.

8.2 Photoconductivity

The search for intrinsic photoconductivity of alkali-halide crystals in the vacuum ultraviolet has been discussed by several authors.[141-144] The experimental problems encountered in their work were

photoemission from the crystal and polarization of the crystal in the presence of the external electric field. The recommended technique for reducing photoemission was vacuum evaporation of a LiF film on the crystal surface. Low light intensities were used to avoid polarization and the build-up of color centers. Although the electrical response to the incident light was weak ($\sim 10^{-15}$ Amp.), some workers[142,143] believed they have detected photoconductivity in the spectral range of the fundamental absorption bands. The results of the more recent work indicate that the band-gap energies of some alkali halides can be obtained from the photoconduction data.[144]

Since polarization phenomena contribute a disturbing effect to photoconductivity measurements, we thought it might be useful to see how the state of polarization is affected by the photoexcited carriers. A change of polarization should occur as a result of neutralization of trapped charges by the optically excited carriers.[145] The method of observation involves the following procedure: 1) Establishment of an internal electric field by polarization; 2) The rate of decay of the internal field can be taken as a measure of the rate of excitation of free electrons and holes in the crystal. Thus the photoresponse should be characteristic of the volume process. Consequently, the observable effect would be evidence for photoconductivity in the solid.

We have investigated the photoeffect in the presence of the internal electric field of a pure KBr crystal. The dimensions of the crystal were 2 x 12 x 12 mm. Both surfaces (12 x 12 mm) were coated with gold films for electrical connection to the electrometer. The crystal was clamped on a teflon holder in a vacuum chamber. The surface of 2 x 12 mm was exposed to the incident beam of light from the exit slit of the vacuum u.v. monochromator. In order to minimize the contribution from photoemission, we performed the experiment in the spectral region near the photoelectric threshold of the crystal. Figure 49 illustrates a typical response at wavelength of 1608 Å. In the presence of the external electric field, the photoresponse was observed. The decay of current is an indication of the space-charge build-up. Upon removing the applied voltage, i.e., electrode N was grounded, a displacement current was observed. When the dark current became sufficiently small, the crystal was exposed to the u.v. light. A photocurrent appeared. Since the current was in the direction opposite of that obtained when the external voltage was applied, the excited carriers were assumed to be accelerated by the internal electric field due to the residual space charge.

We have not completed our study of the decay characteristic of polarization as a function of the incident

light intensity. A more detailed investigation would be desirable.

Another interesting aspect of photoconductivity study which deserves further attention is the surface effect due to exciton dissociation. Evidence of this effect has been presented by Sydor [Phys. Rev. 183, 846 (1969)].

EQUIPMENT FOR FURTHER RESEARCH

We recognize that important information on the photoelectric properties of thin films can be obtained from the electron-energy-distribution measurements. For further study, we plan to use a hemispherical analyzer shown in Fig. 51 to determine the energy distribution of the emitted photoelectrons as a function of film thickness.

9. CONCLUSIONS

The most significant feature of our work on secondary standards for intensity measurements is the experiment in which we showed that the photoionization yield of xenon in the spectral region of 860 to 1022 Å is unity. The result supports the suggestion that a rare-gas ion chamber is the most convenient device to use for absolute intensity measurements below 1000 Å. Thus other devices, including thermocouples, can be calibrated in the 800-1000 Å region with a xenon ion chamber. The calibration procedure is simpler than the technique involving the use of a thermocouple.

In the study of alkali halide films in the spectral region below 1000 Å, we found the yields of some alkali halide films to be almost unity at photon energies above $2E_T$, where E_T is the photoelectric threshold of the material. A noticeable dip in the yield curves was observed at photon energies of approximately $2E_T$. The optimum yield was not observed unless the photoemissive layer was sufficiently thick. For example, the optimum yield of KBr was obtained for a thickness of about 900 Å.

The explanation for high quantum yield can be given in terms of low surface barrier and the ratio of escape length for the photoelectron to the absorption

length for the incident photon. For high yield materials such as KBr, we have some evidence that the escape length is slightly longer than the absorption length.

The most disturbing effect observed in our photoemission experiments on evaporated metals was the gradual change of yield with time immediately after evaporation. This can be attributed to: 1) contamination of the metal surface by residual gases in the vacuum system; 2) a gradual change in film structure immediately after deposition. In spite of these difficulties, we were able to estimate the attenuation lengths for the photoelectrons excited at certain photon energies. The results of our work can serve as an independent check on the predicted values of the electron mean free path in metals. However, we note that a comparison of the theoretical value of the mean free path with that obtained from photoemission data is difficult because we have no reliable information on the initial energy of the photoelectron. While we have the results suggesting long attenuation length for the photoelectrons excited at $h\nu$ in aluminum, we have no assurance that the initial energy of the electron is always equal to energy $h\nu$ above the Fermi level. If the initial energy is considerably less than $h\nu$, the long attenuation length would be in qualitative agreement with the theory.

In our study of semiconducting crystals, we suggested that the difference in yields of n and p-type SiC is an indication of band bending at the surface of the crystal. Our experimental results are in agreement with the conclusion that the p-type crystal of semiconductors has the higher yield.

According to our results on photoemission from Si crystals, the yield due to photoemission from the silicon oxide layer appears to be quite significant in the spectral region below 1100 Å. In order to see if this conclusion is correct, attempts are being made to determine the quantum yield of pure silicon monoxide.

The spectral-yield curve of MgF_2 indicates a noticeable rise in yield at photon energies associated with an exciton transition. The result is best explained by assuming the presence of exciton states at energies higher than the band gap of MgF_2. In this study, we also pointed out that the true yield of evaporated MgF_2 is not obtained unless the film is sufficiently thick. We demonstrated how the photoemission yield at wavelength of 1608 Å decreased with increasing MgF_2 thickness. The photoemission was due to photoelectrons excited in the metallic substrate. Since these electrons must diffuse through the MgF_2 layer in order to escape into the vacuum, the emission can be attenuated by increasing thickness of

MgF_2. This situation suggests a method by which one can determine experimentally how low-energy electrons can be attenuated in a medium which has low photoelectric yield. For example, films of organic materials can be evaporated on the metallized substrate to attenuate the emission of photoelectrons. From the analysis of the data, we should be able to determine the electron mean free path in the material.[15]

Evidence of exciton-induced photoemission was found in our study of photoemission from evaporated KCl films. The exciton effect appeared as a gradual enhancement of photoemission with time under steady u.v. excitation in the exciton band. The transient effect was attributed to the creation of new F-centers by excitons. The fact that the gradual rise is not observed in the presence of strong biasing radiation (visible light) indicates that the F-centers can be ionized rapidly by the visible light and hence the rate of exciton-F center interaction can be greatly reduced.

10. REFERENCES

1. L. Dunkelmann, J. Quant. Spectrosc. Radiat. Transfer. 2, 533 (1962).
2. L. Dunkelman, J.P. Hennes, and W.B. Fowler, Space Research III, p. 1174, W. Priester, ed., North-Holland Publishing Company, Amsterdam (1963).
3. E. Taft and H.R. Phillip, J. Phys. Chem. Solids 1, 159 (1956); 3, 1 (1957).
4. A.H. Sommer, "Photoemissive Materials", pp. 186-221, John Wiley and Sons, Inc., New York (1968).
5. D.M. Packer and C. Lock, J. Opt. Soc. Am. 41, 699 (1951).
6. H.E. Hintereger, J. Quant. Spectrosc. Radiat. Transfer. 2, 561 (1962).
7. F.M. Matsunaga, R.S. Jackson, and K. Watanabe, J. Quant. Spectrosc. Radiat. Transfer 5, 329 (1965).
8. K. Watanabe, F.M. Matsunaga, and H. Sakai, Appl. Optics 6, 391 (1967).
9. P.H. Metzger, J. Phys. Chem. Solids 26, 1879 (1965).
10. W. Pong and R. Norris, J. Opt. Soc. Am. 55, 1189 (1965).
11. W. Pong and K. Fujita, J. Appl. Phys. 37, 445 (1966).
12. W. Pong, R. Sumida, and G. Moore, J. Appl. Phys. 41, 1869 (1970).
13. W. Pong, J. Appl. Phys. 37, 3033 (1966).
14. W. Pong, J. Appl. Phys. 38, 4103 (1967).

15. W. Pong, J. Appl. Phys. 40, 1733 (1969).

16. K. Watanabe and E.C.Y. Inn, J. Opt. Soc. Am. 43, 32 (1953); N. Wainfan, W.C. Walker, and G.L. Weissler, J. Appl. Phys. 24, 1318 (1953).

17. NBS standard lamp C-980.

18. R.G. Johnston and R.P. Madden, Appl. Optics 4, 1574 (1965).

19. K. Watanabe, F.M. Matsunaga, and R.S. Jackson "Some Intensity Measurements in the Vacuum Ultraviolet" (June, 1964) NASA-Report.

20. Measured at NBS according to procedure described in ref. 18.

21. J.A.R. Samson, J. Opt. Soc. Am. 54, 6 (1964).

22. K. Watanabe and C.Y. Inn, J. Opt. Soc. Am. 43, 32 (1953).

23. H.Y. Fan, Phys. Rev. 68, 43 (1945).

24. M.J. Buckingham, Phys. Rev. 80, 704 (1950).

25. F. Wooten and T. Huen, J. Opt. Soc. Am. 57, 102 (1967).

26. F.J. Piepenbring - "Optical Properties and Electronic Structure of Metals and Alloys" (North-Holland Publishing Co., Amsterdam, 1966) pp. 316-323.

27. L. Sutton, Phys. Rev. Letters 24, 386 (1970).

28. N.V. Smith and W.E. Spicer, Phys. Rev. 188, 593 (1969).

29. E.O. Kane, Phys. Rev. 147, 335 (1966).

30. W.E. Spicer, J. Appl. Phys. 31, 2077 (1960).

31. A.J. Dekker, Stolid State Physics, edited by F. Seitz and D. Turnbull, Vol. 6, Academic Press, Inc., New York, 1958, p. 251.

32. E.O. Kane, J. Phys. Soc. of Japan 21, Supplement p. 37 (1966).

33. E. Merzbacher, "Quantum Mechanics" p. 470, John Wiley & Sons, Inc. (1961).

34. C.N. Berglund and W.E. Spicer, Phys. Rev. 136, A 1030 (1964).

35. K. Motizuki and M. Sparks, J. Phys. Soc. of Japan 19, 486 (1964).

36. J.J. Quinn, Phys. Rev. 126, 1453 (1962).

37. J.J. Quinn, Appl. Phys. Letters 2, 167 (1963).

38. S.L. Adler, Phys. Rev. 130, 1654 (1963).

39. R.H. Ritchie and J.C. Ashley, J. Phys. Chem. Solids 26, 1689 (1965).

40. S. Raimes, Repts. Progr. Phys. 20, 1 (1957).

41. R.W. Davies, Phys. Rev. 181, 1118 (1969).

42. C.R. Crowell, W.G. Spitzer, L.E. Howarth, and E.E. LaBate, Phys. Rev. 127, 2006 (1962).

43. C.R. Crowell and S.M. Sze, "Physics of Thin Films" vol. 4, pp. 325-371 (1967), Academic Press, New York.

44. G.A. Katrich and O.G. Sarbei, Soviet Phys.-Solid State 3, 1181 (1961).

45. S.M. Sze, J.L. Moll, and T. Sugano, Solid-State Electronics 7, 509 (1964).

46. R. Stuart, F. Wooten, W.E. Spicer, Phys. Rev. 135, A 495 (1964).

47. L. R. Canfield, G. Hass, and W. R. Hunter, Le Journal De Physique 25, 124 (1964).

48. L.R. Canfield, G. Hass, and J. E. Waylonis, Appl. Optics 5, 45 (1966).

49. W.R. Hunter, Le Journal De Physique 25, 154 (1964).

50. R.P. Madden, L.R. Canfield, and G. Hass, J. Opt. Soc. Am. 53, 620 (1963).

51. B.P. Feuerbacher and W. Steinmann, Optics Communications 1, 81 (1969).

52. R.N. Stuart and F. Wooten, Phys. Rev. 156, 364 (1967).

53. H. Kanter, Phys. Rev. B, 1, 522 (1970).

54. A.J. Blodgett, Jr. and W.E. Spicer, Phys. Rev. 146, 390 (1966).

55. J.R. Cuthill, A.J. McAlister, M.L. Williams, and R.E. Watson, Phys. Rev. 164, 1006 (1967).

56. H.D. Hagstrum and G.E. Becker, Phys. Rev. 159, 572 (1967).

57. D.E. Eastman and W.F. Krolikowski, Phys. Rev. Letters 21, 623 (1968); D.E. Eastman, J. Appl. Phys. 40, 1387 (1969).

58. R.C. Vehse and E.T. Arakawa, Phys. Rev. 180, 695 (1969).

59. J. Toots, H.A. Fowler, and L. Marton, Phys. Rev. 172, 670 (1968).

60. P.A. Wolff, Phys. Rev. 95, 56 (1954).

61. F. Wooten and R.N. Stuart, Phys. Rev. 186, 592 (1969).

62. W.E. Spicer, J. Phys. Chem. Solids 22, 365 (1961).

63. E.O. Kane, Phys. Rev. 159, 624 (1967).

64. P.A. Wolff, Phys. 95, 1415 (1954).

65. F. Seitz, Phys. Rev. 76, 1376 (1949).

66. J. Appel, Phys. Rev. 125, 1815 (1962).

67. A.H. Sommer and W.E. Spicer, "Photoelectric Materials and Devices", Edited by S. Larach, D. Van Nostrand Co., Inc., New York, 1965, p. 181.

68. E.O. Kane, Phys. Rev. 127, 131 (1962).

69. D. Redfield, Phys. Rev. 124, 1809 (1961).

70. N.B. Kindig, J. Appl. Phys. 38, 3285 (1967).

71. H.R. Philipp and E.A. Taft, Phys. Rev. 120, 37 (1960).

72. T. Sasaki and K. Ishiguro, Phys. Rev. 127, 1091 (1962).

73. W.E. Spicer and R.E. Simon, Phys. Rev. Letters 9, 385 (1962).

74. W.E. Spicer and R.E. Simon, J. Phys. Chem. Solids 23, 1817 (1962).

75. G.W. Gobeli and F.G. Allen, Phys. Rev. 127, 150 (1962).

76. T.A. Callcott, Phys. Rev. 161, 746 (1967).

77. L. Patrick, D.R. Hamilton, W.J. Choyke, Phys. Rev. 143, 526 (1966).

78. R.N. Ghoshtagore and R.L. Coble, Phys. Rev. 143, 623 (1966).

79. H.R. Philipp and E.A. Taft, Proc. Conf. Silicon Carbide, J.R. O'Connor and J. Smiltens (Eds.), Pergamon, New York, 1960.

80. B.C. Deaton and F.A. Blum, Jr., Phys. Rev. 137, A1131 (1965).

81. R. Kaplow, T.A. Rowe, and B.L. Averbach, Phys. Rev. 168, 1068 (1968).

82. M.P. Givens, Rev. Sci. Instr. 25, 1130 (1954).

83. A. von Hippel, J. Chem. Phys. 16, 372 (1948).

84. H. Merdy, S. Robin-Kandare, and J. Robin, C.R. Acad. Sci. (France) 257, 1526 (1963).

85. A.G. Leiga, J. Opt. Soc. Am. 58, 1441 (1968).

86. J.D. Hayes, E.T. Arakawa, and M.W. Williams, J. Appl. Phys. 39, 5527 (1968).

87. D. Pines, Rev. Mod. Phys. 28, 184 (1956).

88. M. Cardona, Phys. Rev. 129, 69 (1963).

89. T. Goto, T. Yashiro, and M. Ueta, J. Phys. Soc. Japan 20, 2185 (1965).

90. J. Mattler, Compt. rend. 217, 447 (1943).

91. D.W. Turner, Nature 179, 1022 (1957).

92. A.H. Sommer, RCA Rev. 28, 75 (1967).

93. M. Rome, IEEE Transactions on Nuclear Science, pp. 93-99, June, 1964.

94. W.F. Krolikowski and W.E. Spicer, Bull. Amer. Phys. Soc. 9, 735 (1964); Technical Report No. 5218-1, May 1967.

95. J.A.R. Samson, "Techniques of Vacuum Ultraviolet Spectroscopy", p. 243, John Wiley & Sons, Inc., New York, 1967.

96. B. Goldstein and L. Pensak, J. Appl. Phys. 30, 155 (1959).

97. J. Matsuno and M. Inoue, Japanese J. Appl. Phys. 6, 297 (1967).

98. K.V. Shalimova and E.N. Voronkov, Soviet Physics-Solid State 9, 1169 (1967).

99. J.J. Scheer and J. van Laar, Philips Res. Repts. 16, 323 (1961).

100. J.L. Shay and W.E. Spicer, Phys. Rev. 161, 789 (1967).

101. G.W. Gobeli and F.G. Allen, Phys. Rev. 137, A 245 (1965).

102. L.W. James, R.C. Eden, J.L. Moll, and W.E. Spicer, Phys. Rev. 174, 909 (1968).

103. M.L. Cohen and J.C. Phillips, Phys. Rev. 139, A 912 (1965).

104. L.W. James and J.L. Moll, Phys. Rev. 183, 740 (1969).

105. F. Herman and W.E. Spicer, Phys. Rev. 174, 906 (1968).

106. M.H. Francombe and J.E. Johnson, "Physics of Thin Films" Edited by G. Hass and R.E. Thun, Vol. 5, pp. 176-179, 1969, Academic Press, New York.

107. J.L. Richards, P.B. Hart, and L.M. Gallone, J. Appl. Phys. 34, 3418 (1963).

108. H.R. Philipp and H. Ehrenreich, Phys. Rev. 131, 2016 (1963).

109. E.A. Taft and H.R. Philipp, J. Phys. Chem. Solids 3, 1 (1957).

110. J.E. Eby, K.J. Teegarden, and D.B. Dutton, Phys. Rev. 116, 1099 (1959).

111. S.W. Duckett and P.H. Metzger, Phys. Rev. 137, A 953 (1965).

112. L. Heroux, W.J. McMahon, and H.E. Hinteregger, Appl. Optics 5, 1338 (1966).

113. L. Apker and E. Taft, Phys. 79, 964 (1950); Phys. Rev. 81, 698 (1951); Phys. Rev. 82, 814 (1951).

114. M.H. Hebb, Phys. Rev. 81, 702 (1951).

115. H.R. Philipp and E.A. Taft, Phys. Rev. 106, 671 (1957).

116. E.A. Taft, H. Philipp, and L. Apker, Phys. Rev. 113, 156 (1959).

117. J.A. Shuba, Soviet Phys. Tech. Phys. 1, 1104 (1956).

118. W.E. Spicer, J. Phys. Chem. Solids 20, 134 (1961).

119. W.E. Spicer, Phys. Rev. 154, 385 (1967).

120. P.L. Hartman, J.R. Nelson, and J.G. Siegried, Phys. Rev. 105, 123 (1957).

121. T. Timusk and W. Martienssen, Phys. Rev. 128, 1656 (1962).

122. J.H. Parker, Jr., Phys. Rev. 124, 703 (1961).

123. P.V. Mitchell, D.A. Wiegand, and R. Smoluchowski, Phys. Rev. 121, 484 (1961).

124. G. Hass and R. Tousey, J. Opt. Soc. Am. 49, 593 (1959).

125. A. Duncanson and R.W.H. Stevenson, Proc. Phys. Soc. London 72, 1001 (1958).

126. B. Vodar, J. Quant. Spectry. and Radiative Transfer 2, 393 (1962).

127. M.W. Williams, R.A. MacRae, and E.T. Arakawa, J. Appl. Phys. 38, 1701 (1967).

128. E.G. Schneider and H.M. O'Bryan, Phys. Rev. 51, 293 (1937).

129. H. Mahr, Phys. Rev. 122, 1464 (1961).

130. N. Kristianpoller, J. Opt. Soc. Am. 54, 1285 (1964).

131. R. Allison, J. Burns, and A.J. Tuzzolino, J. Opt. Soc. Am. 54, 747 (1964).

132. K.J. Nygaard, J. Opt. Soc. Am. 55, 944 (1965).

133. N. Kristianpoller and R.A. Knapp, Appl. Optics 3, 915 (1964).

134. F.D. Brooks, "Progress in Nuclear Physics", Vol. 5, edited by O.R. Frisch (Pergamon Press, London and New York, 1956), p. 252.

135. N.F. Mott, Proc. Roy. Soc. (A), 167, 384 (1938).

136. M. Kasha, Chem. Revs. 41, 401 (1947).

137. R.M. Hochstrasser, Revs. Mod. Phys. 34, 531 (1963).

138. A.S. Davydov, "Theory of Molecular Excitons", translated by M. Kasha and M. Oppenheimer, Jr. (McGraw-Hill Book Co., Inc., New York, 1962). p. 117.

139. F.A. Kroger, "Some Aspects of the Luminescence of Solids" (Elsevier Publishing Co., Inc., New York, 1948), p. 213.

140. R.A. Knapp and A.M. Smith, Appl. Optics 3, 637 (1964).

141. J.W. Taylor and P.L. Hartman, Phys. Rev. 113, 1421 (1959).

142. Y. Nakai and K. Teegarden, J. Phys. Chem. Solids 22, 327 (1961).

143. G. Kuwabara and K. Aoyagi, J. Phys. Chem. Solids 22, 333 (1961).

144. G.R. Huggett and K. Teegarden, Phys. Rev. 141, 797 (1966).

145. J.A. Elmgren and D.E. Hudson, Phys. Rev. 128, 1044 (1962).

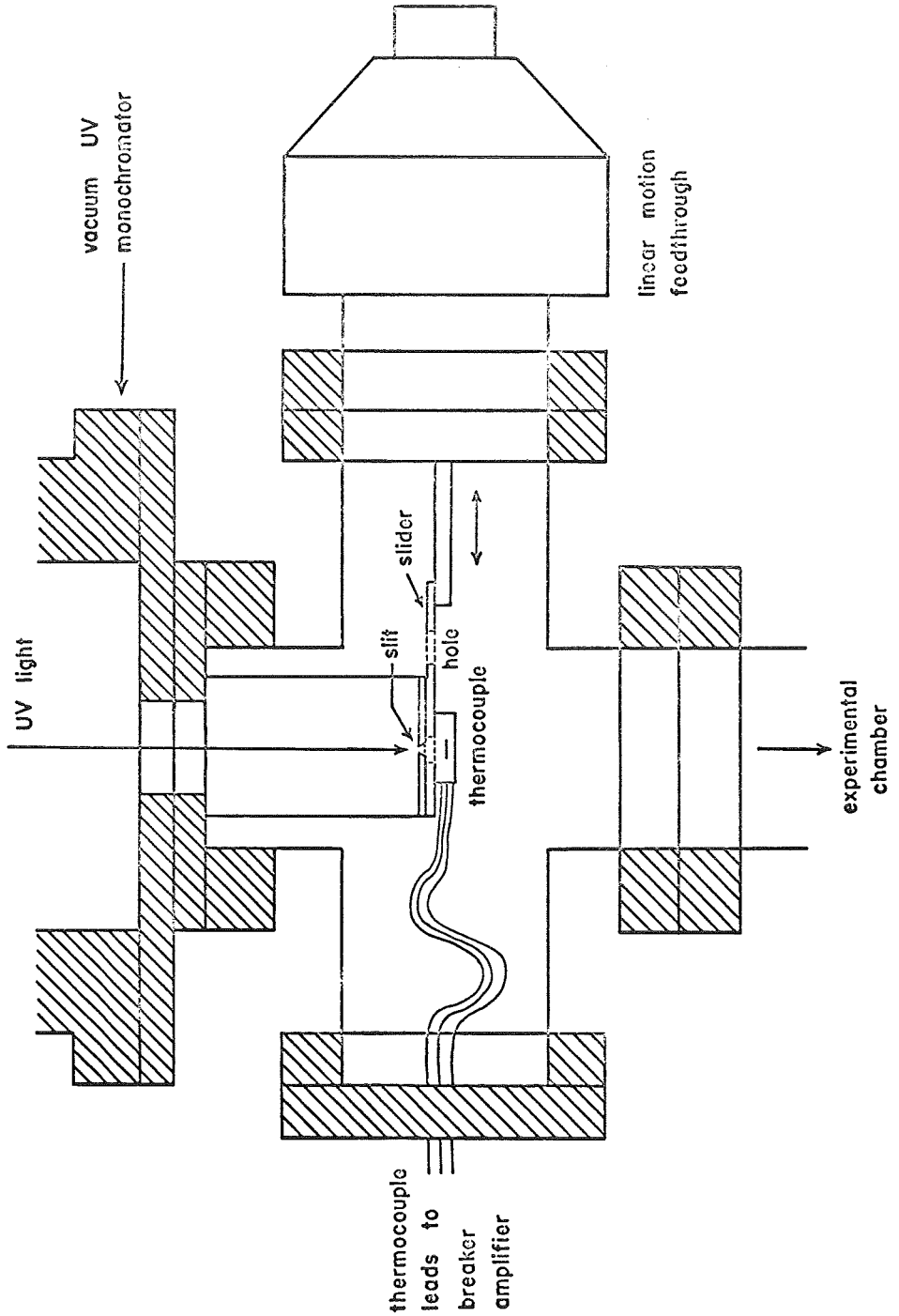

Fig. 1 Calibrated thermocouple for absolute intensity measurements.

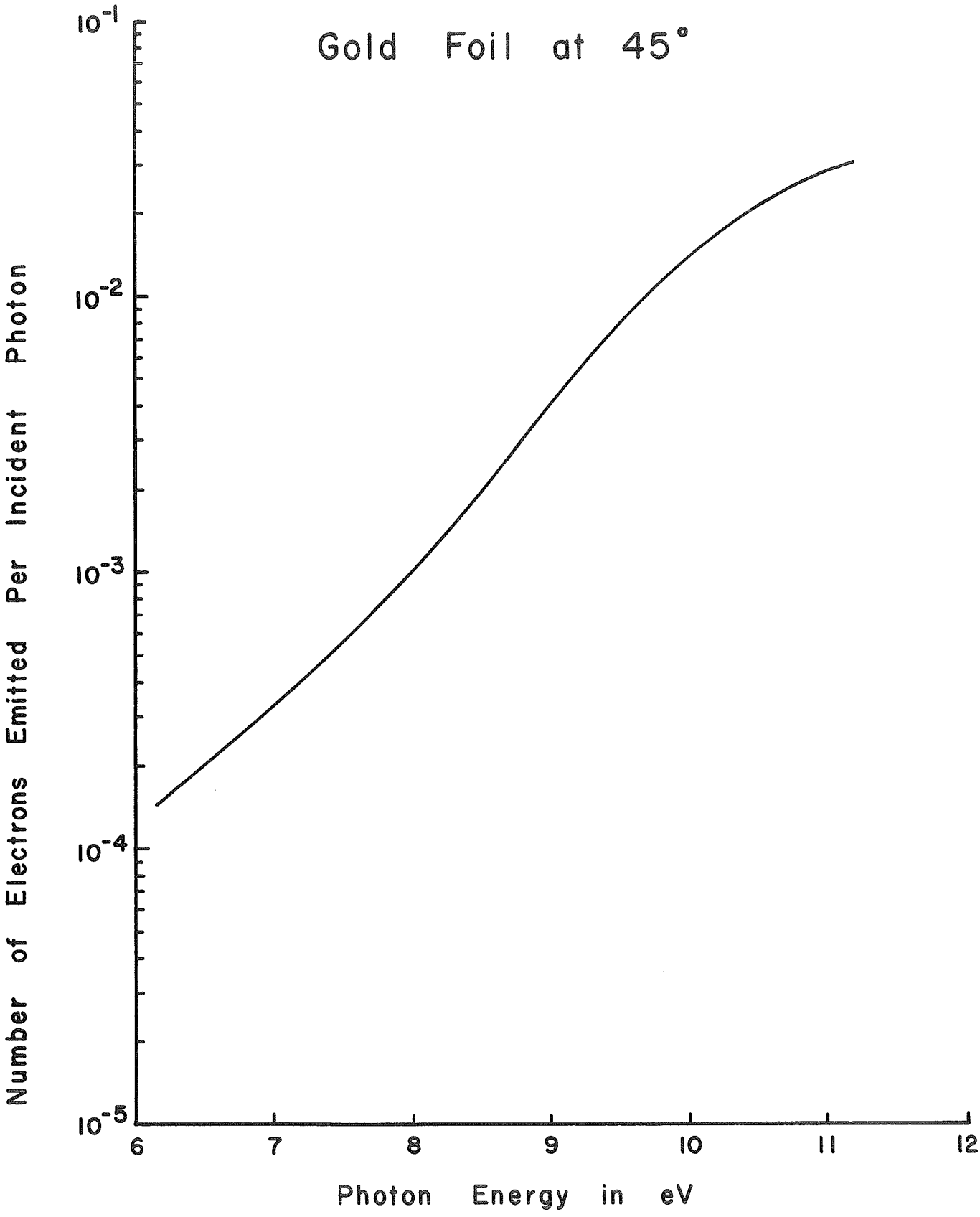
Gold Foil at 45°
Number of Electrons Emitted Per Incident Photon
10⁻¹
10⁻²
10⁻³
10⁻⁴
10⁻⁵
6
7
8
9
10
11
12
Photon Energy in eV

Fig. 2

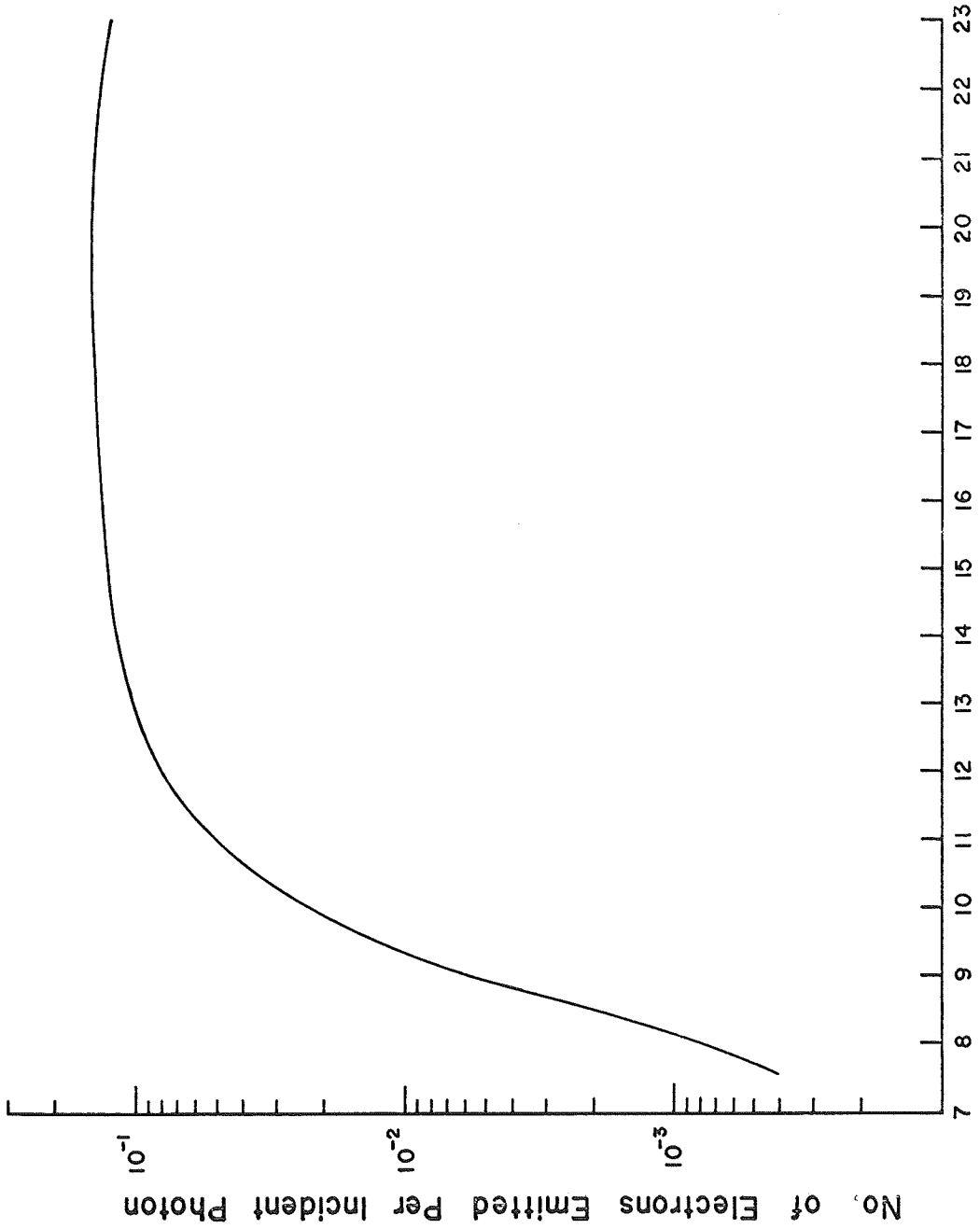

Fig. 3 Spectral quantum yield of a tungsten foil .

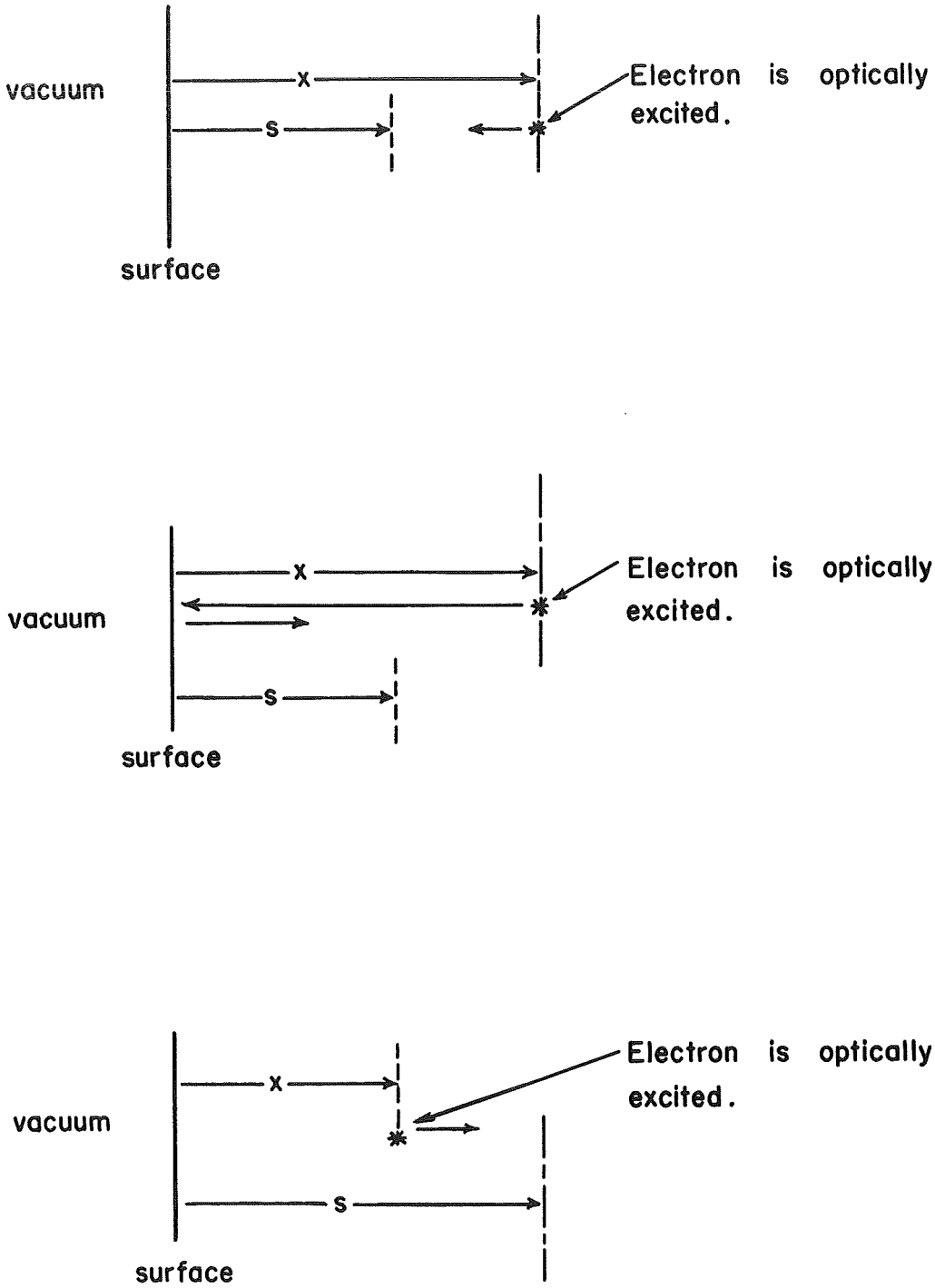
vacuum
x
s
Electron is optically excited.
surface
vacuum
x
s
Electron is optically excited.
surface
vacuum
x
s
Electron is optically excited.
surface

Fig. 4

Fig. 5a "Front" illumination

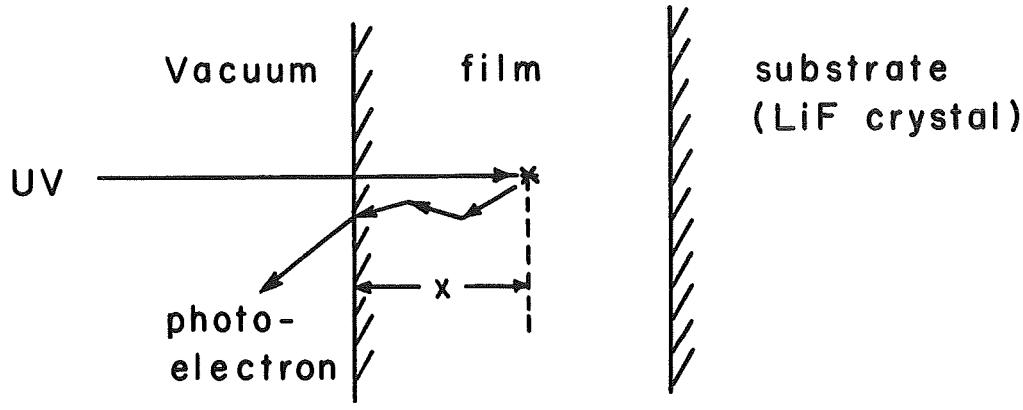

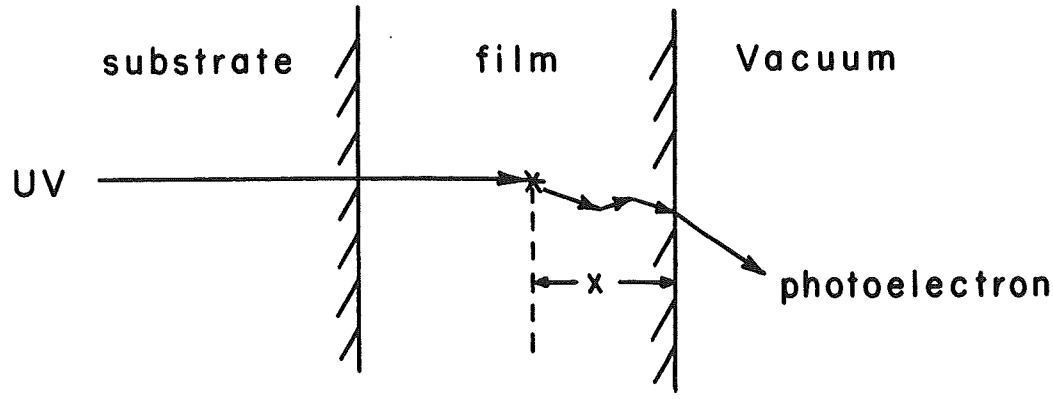

Fig. 5b "Back" illumination

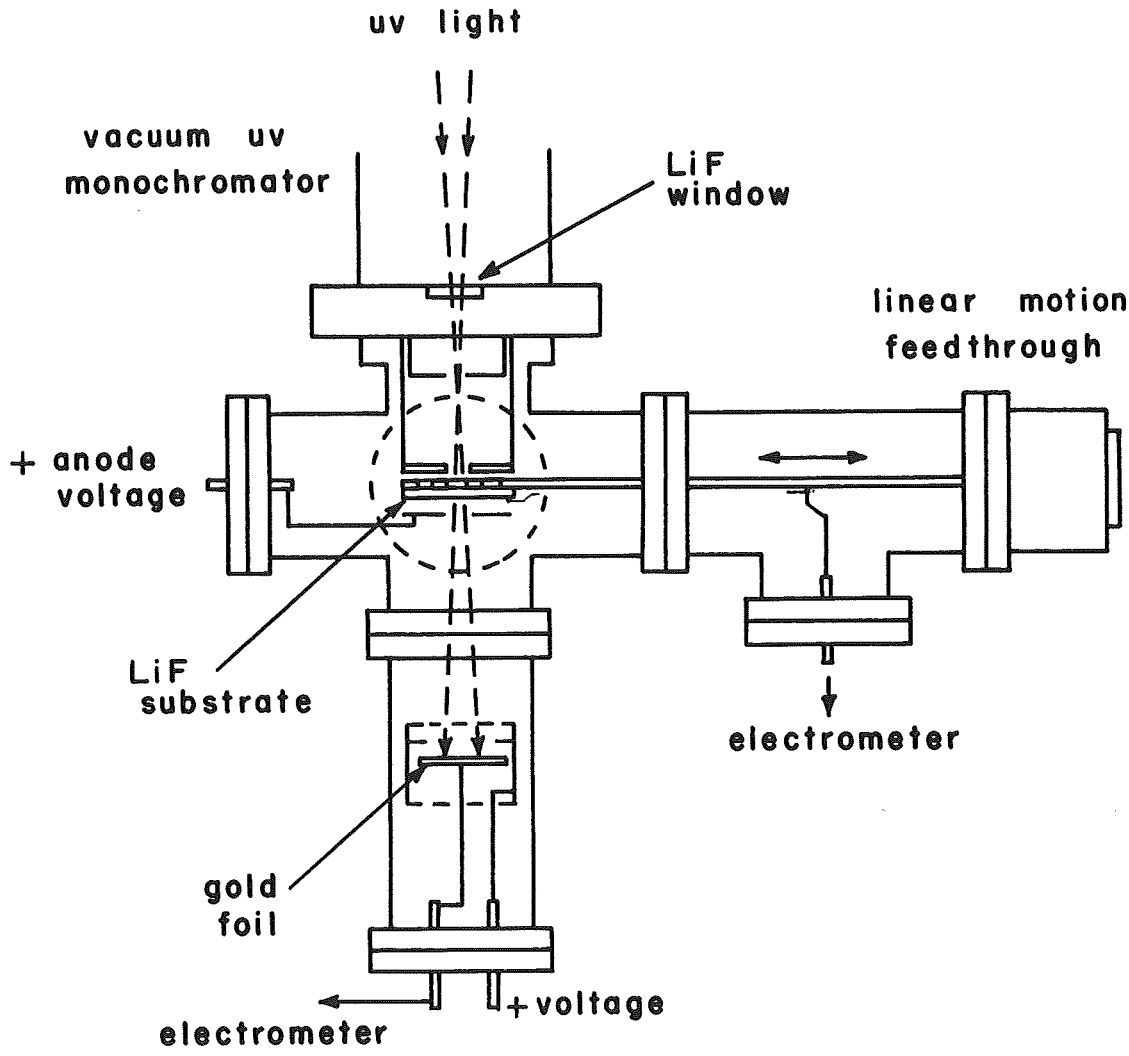

Photoemission Chamber

Fig. 6 Top-view of experimental chamber for measuring photoemission from evaporated films under "back" illumination.

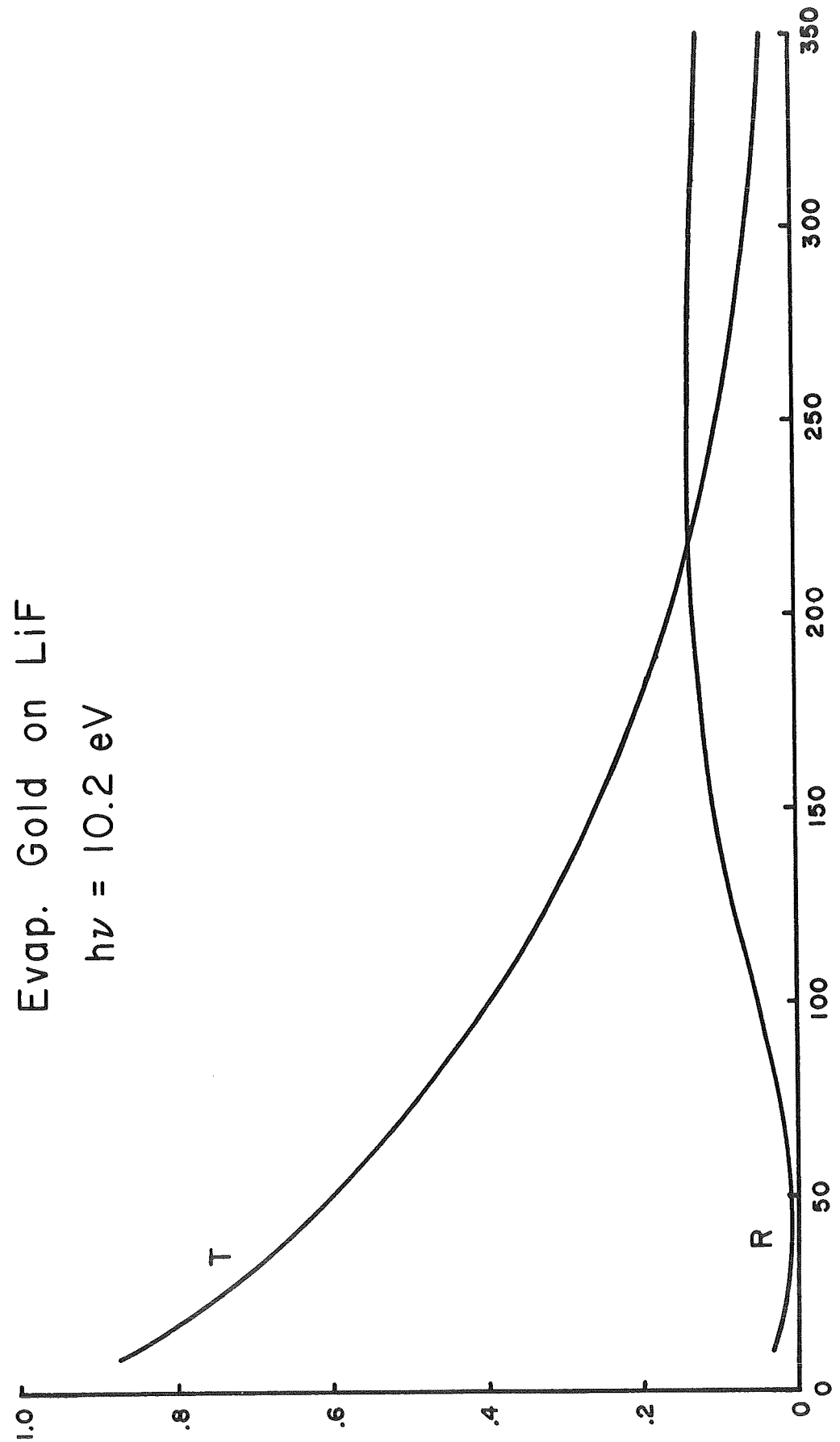

Fig. 7 Transmittance and Reflectance vs film thickness.

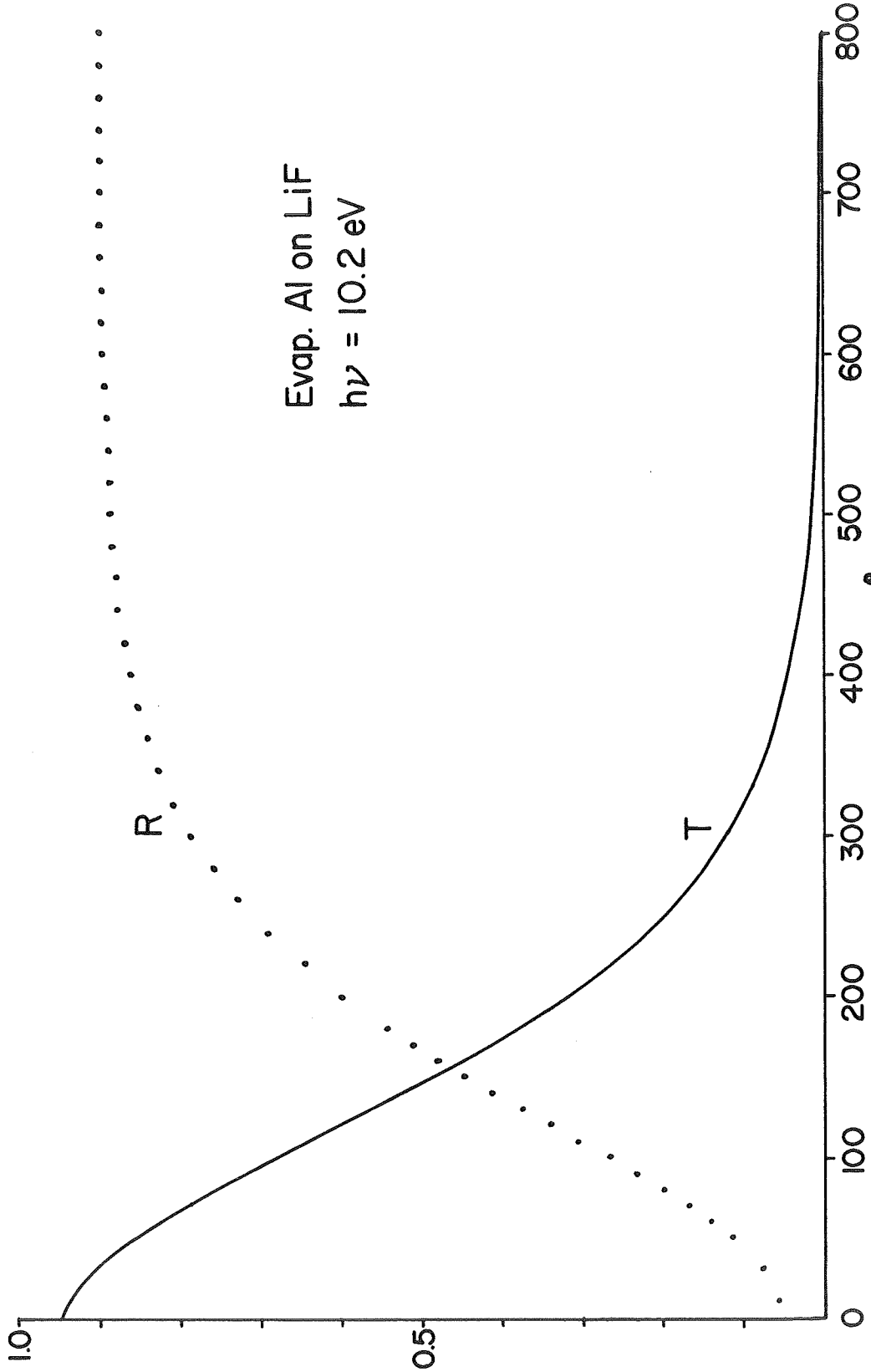

Fig. 8 Transmittance and Reflectance vs film thickness.

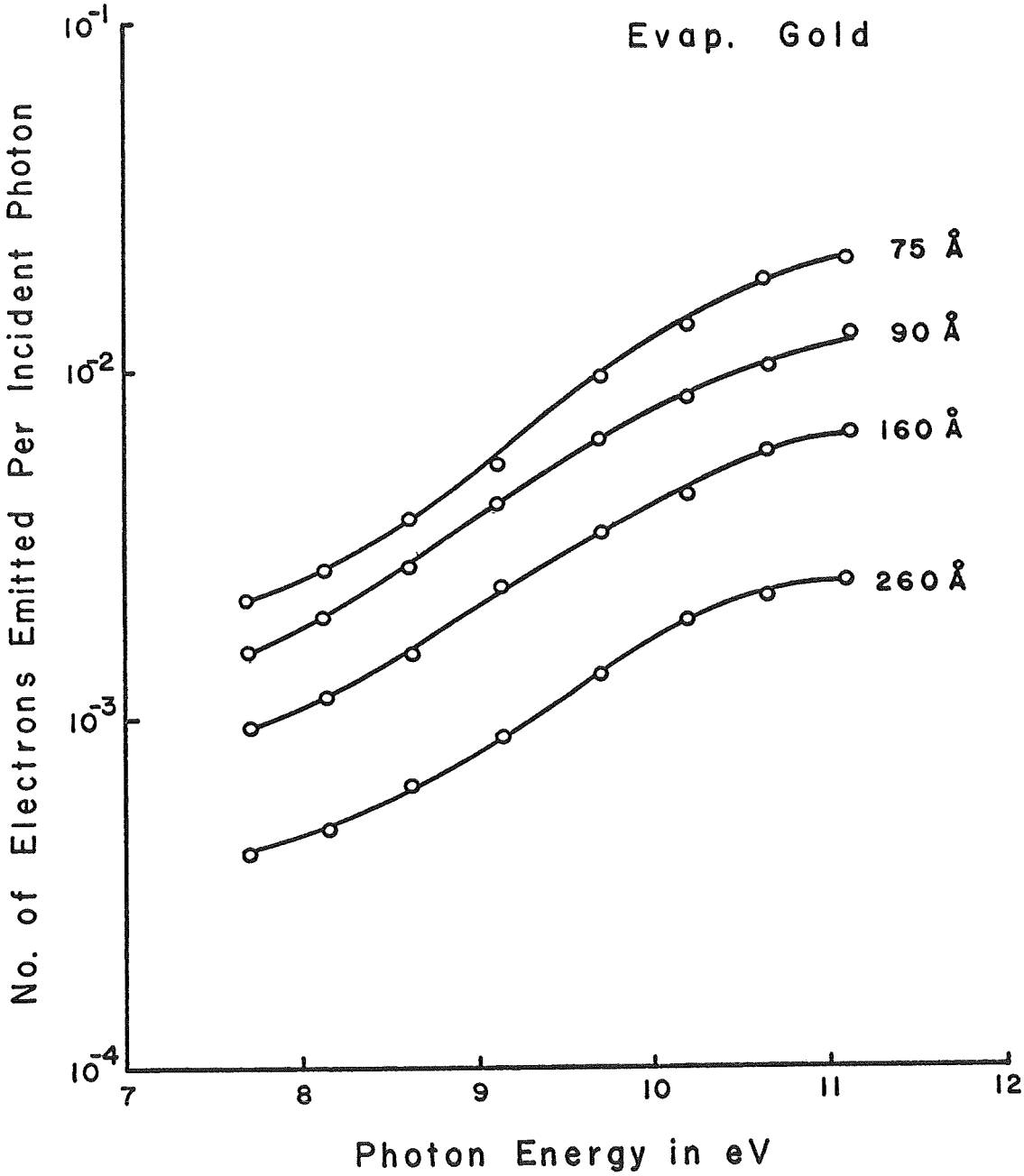

Fig. 9 Photoemission from gold films under "back" illumination.

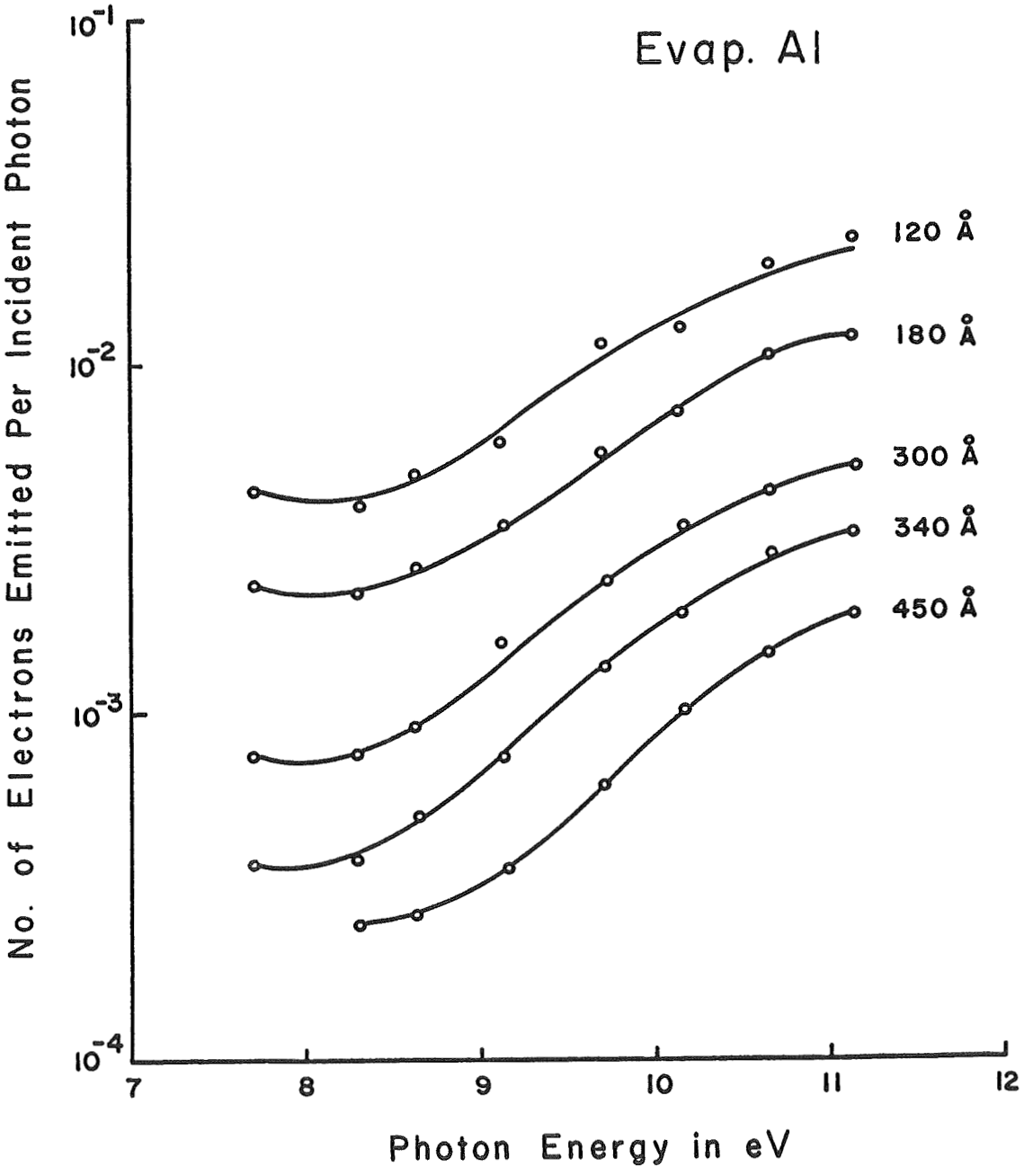

Fig. 10 Photoemission from aluminum films under "back" illumination.

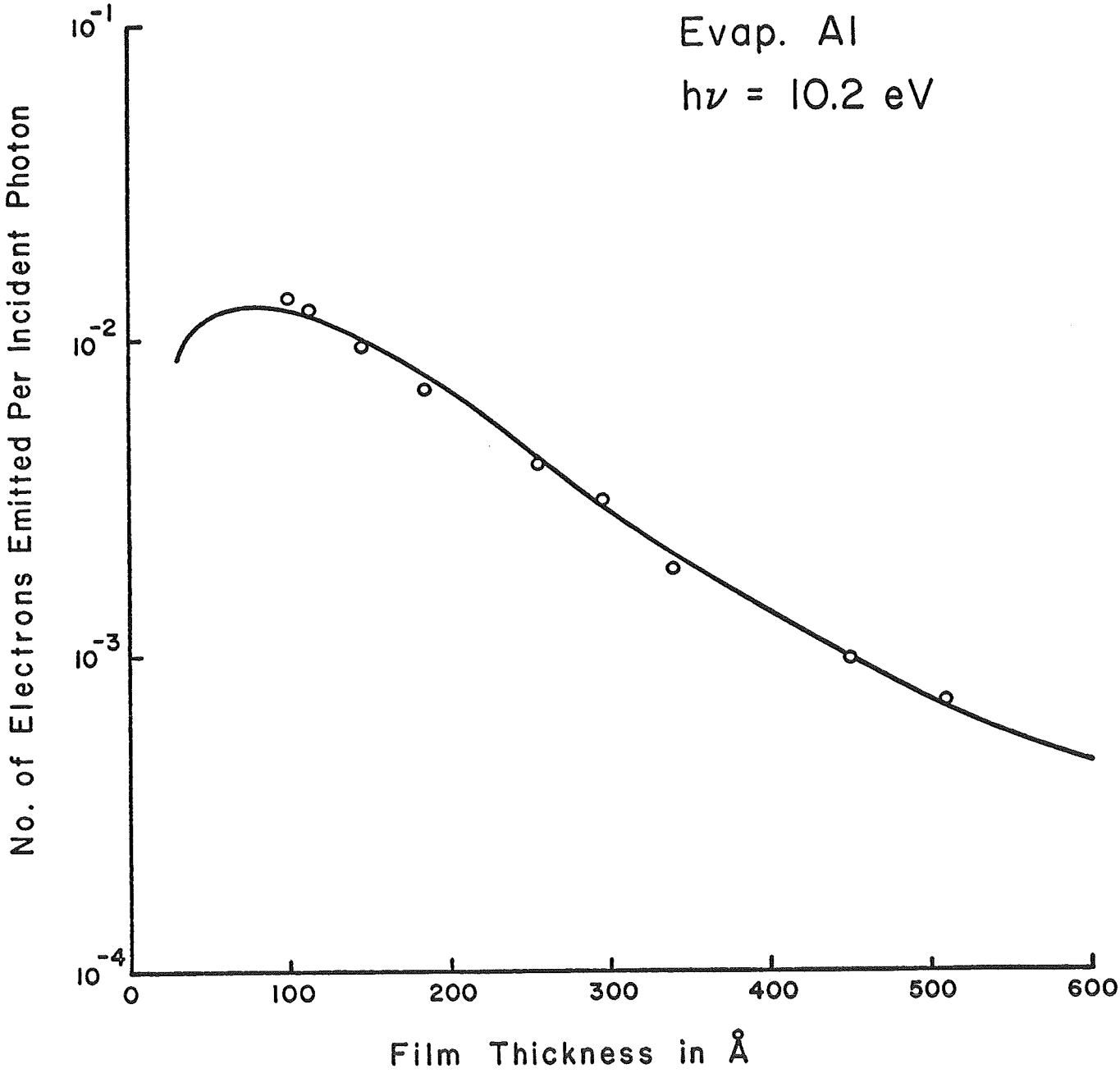

Fig. 11 o Experimental data ; _____ Calculated curve for L= 238 Å.

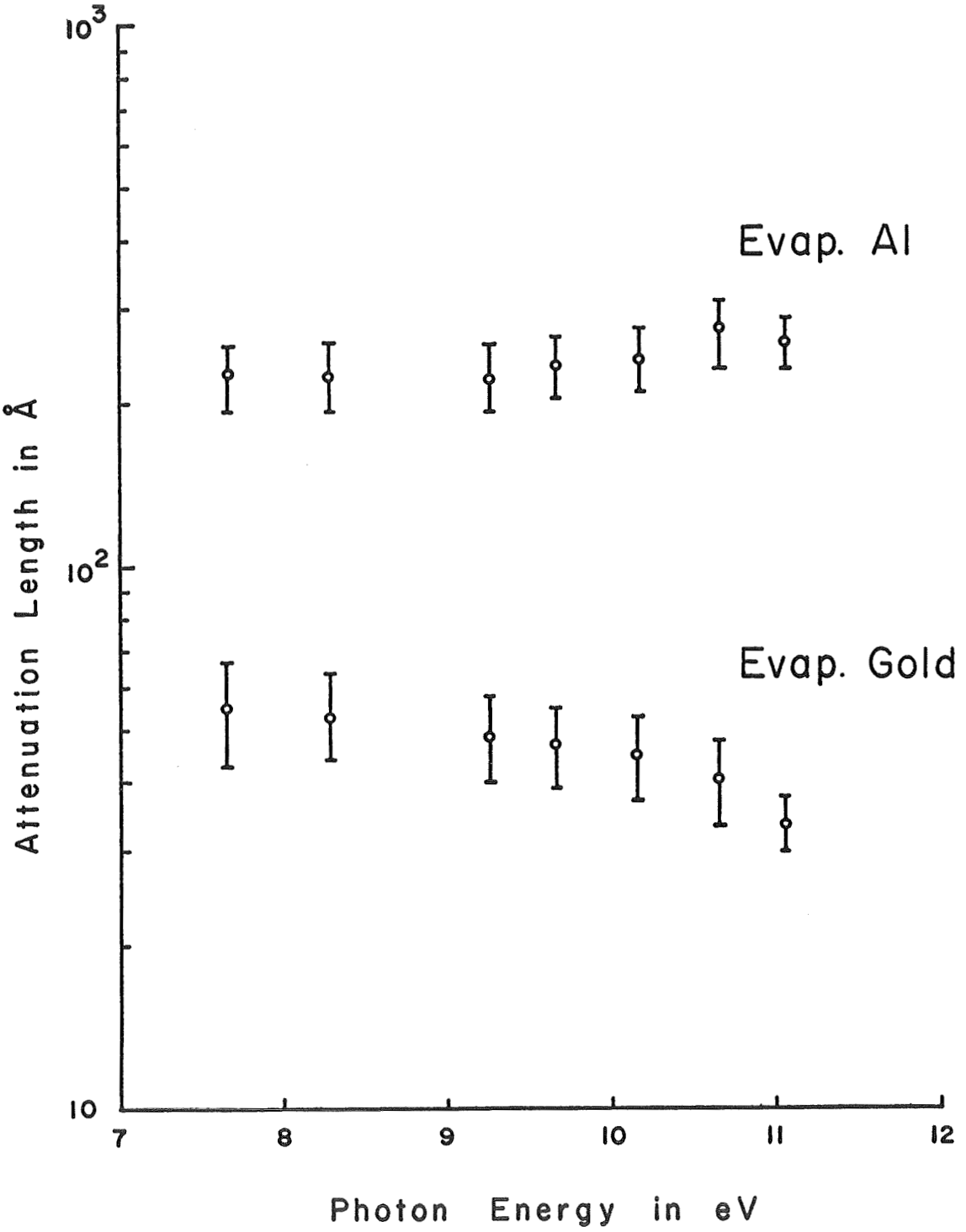

Fig. 12 Attenuation length values for photoelectrons in aluminum and gold films.

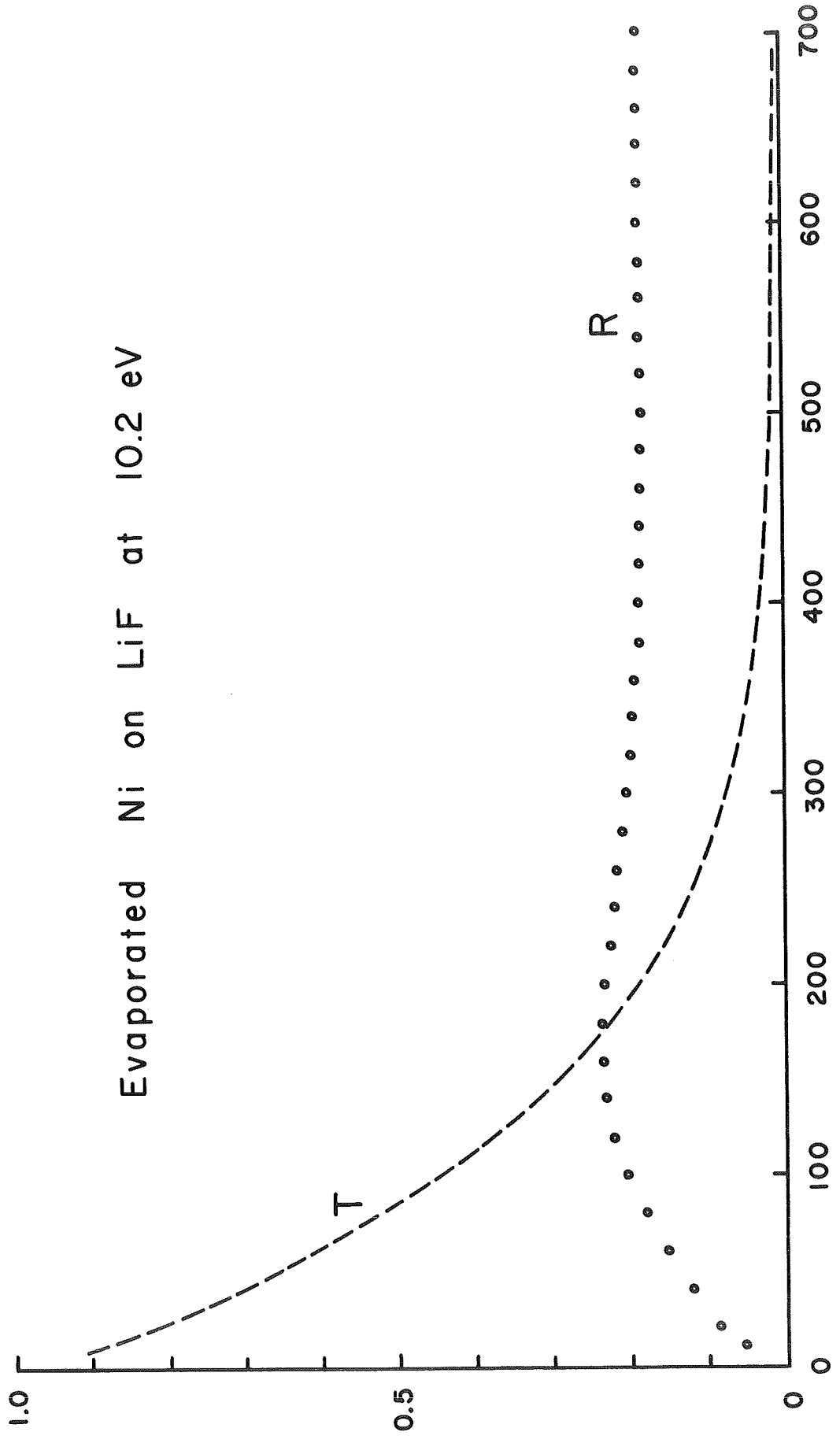

Fig. 13 Transmittance and Reflectance vs film thickness.

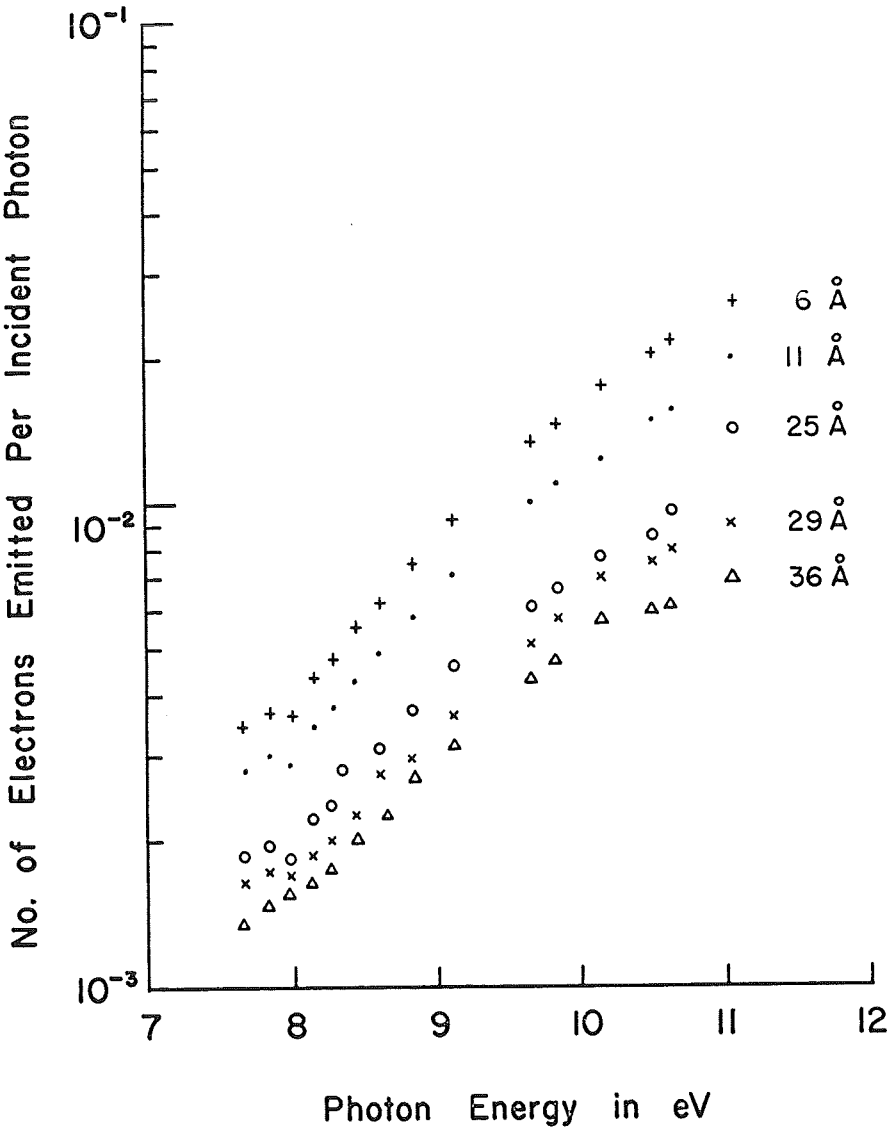

Fig. 14 Photoemission from nickel films under "back" illumination. The films were evaporated on LiF substrates.

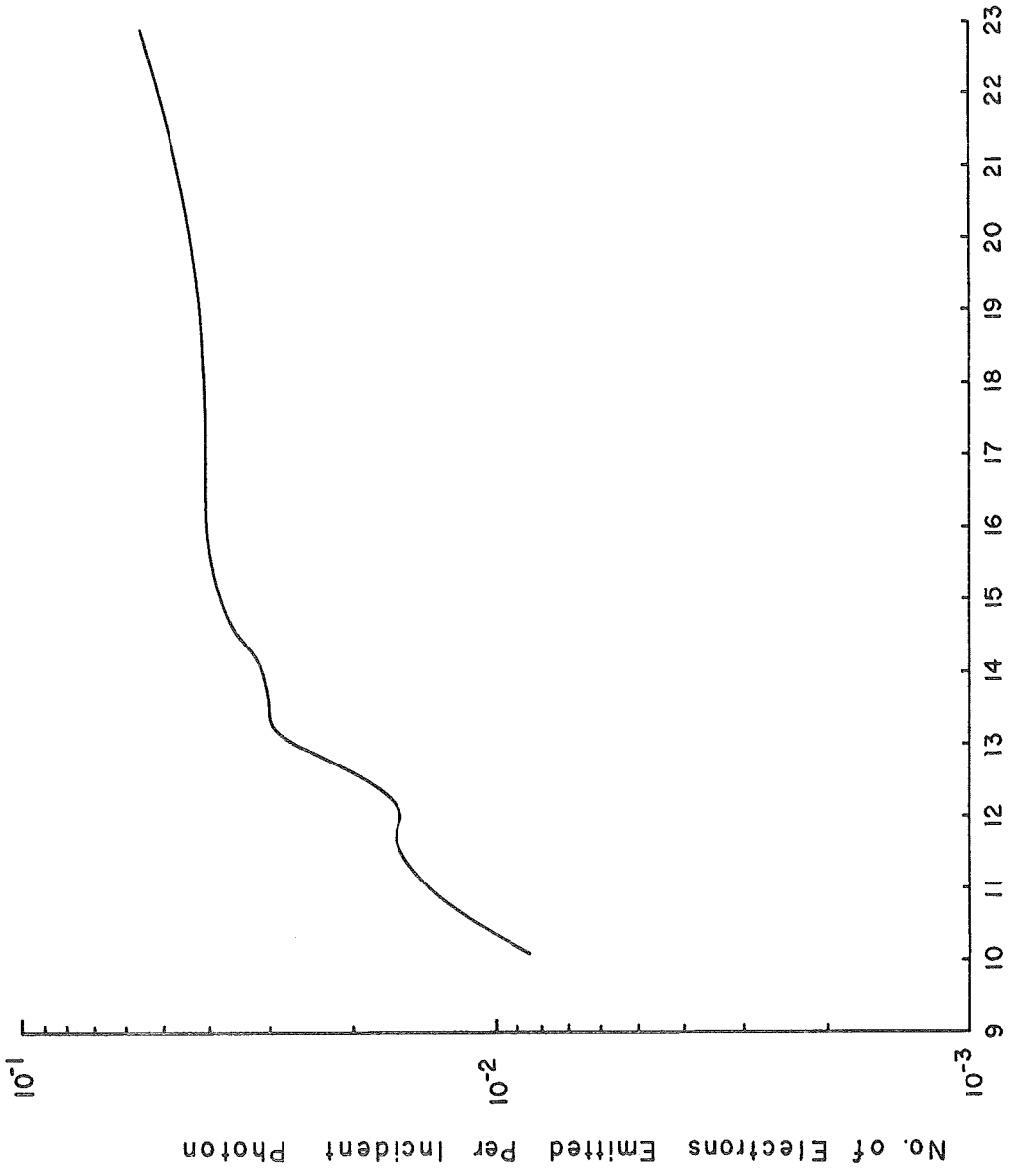

Fig. 15 Spectral quantum yield of evaporated Ni film under "front" illumination.

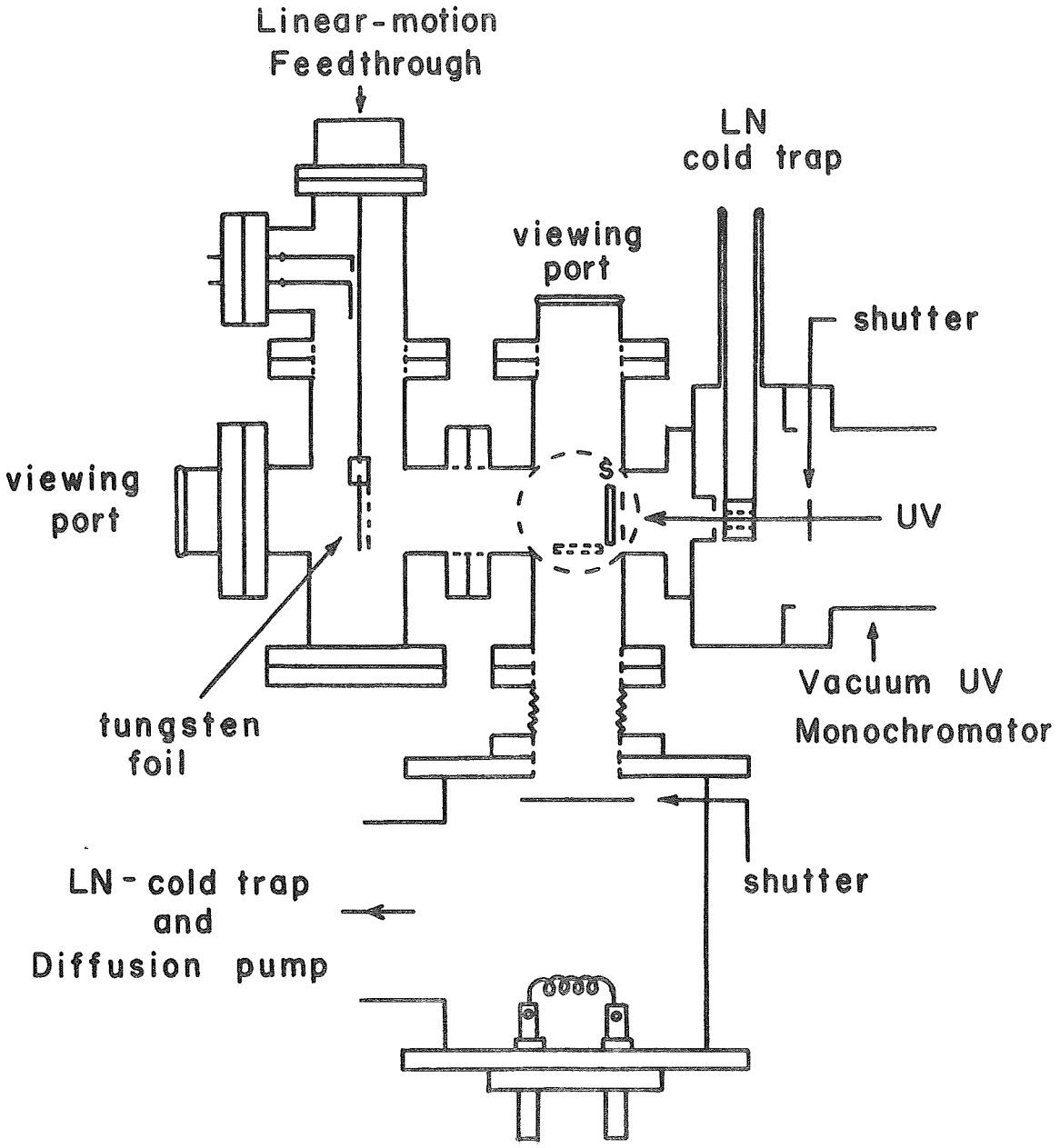

Fig.16 Equipment for Photoemission Measurements at Photon Energies between 10 and 23 eV.

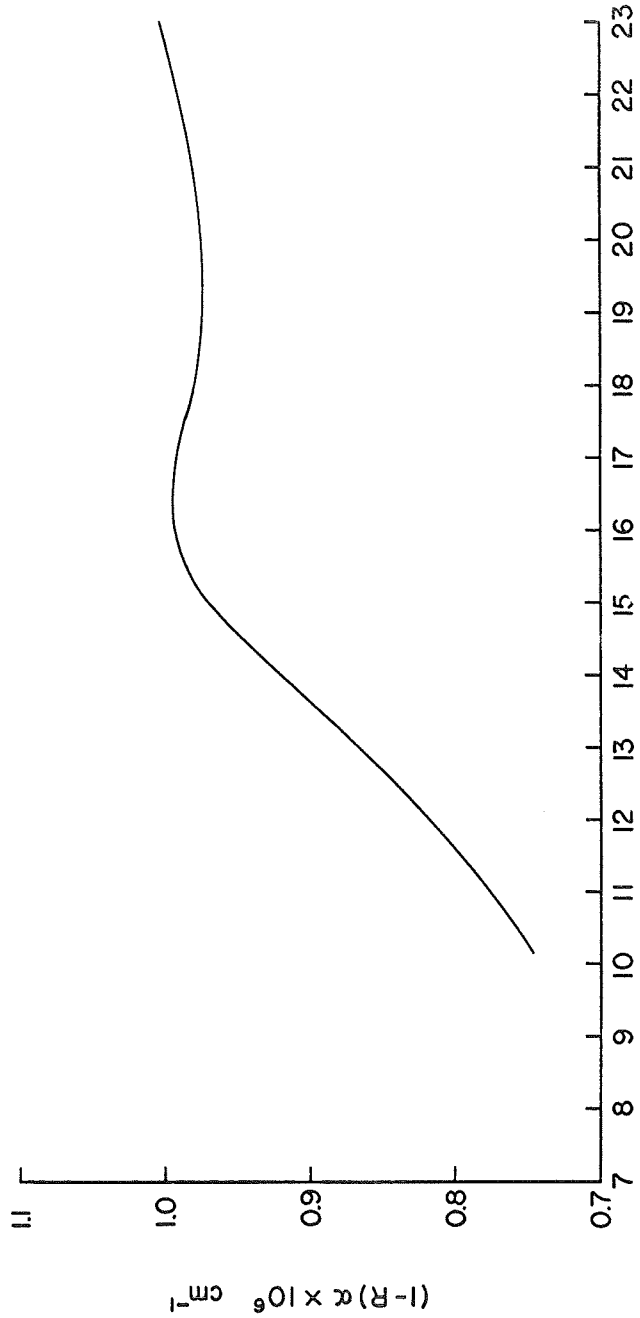

Fig. 17 $(1-R)\alpha$ vs Photon energy for Nickel .

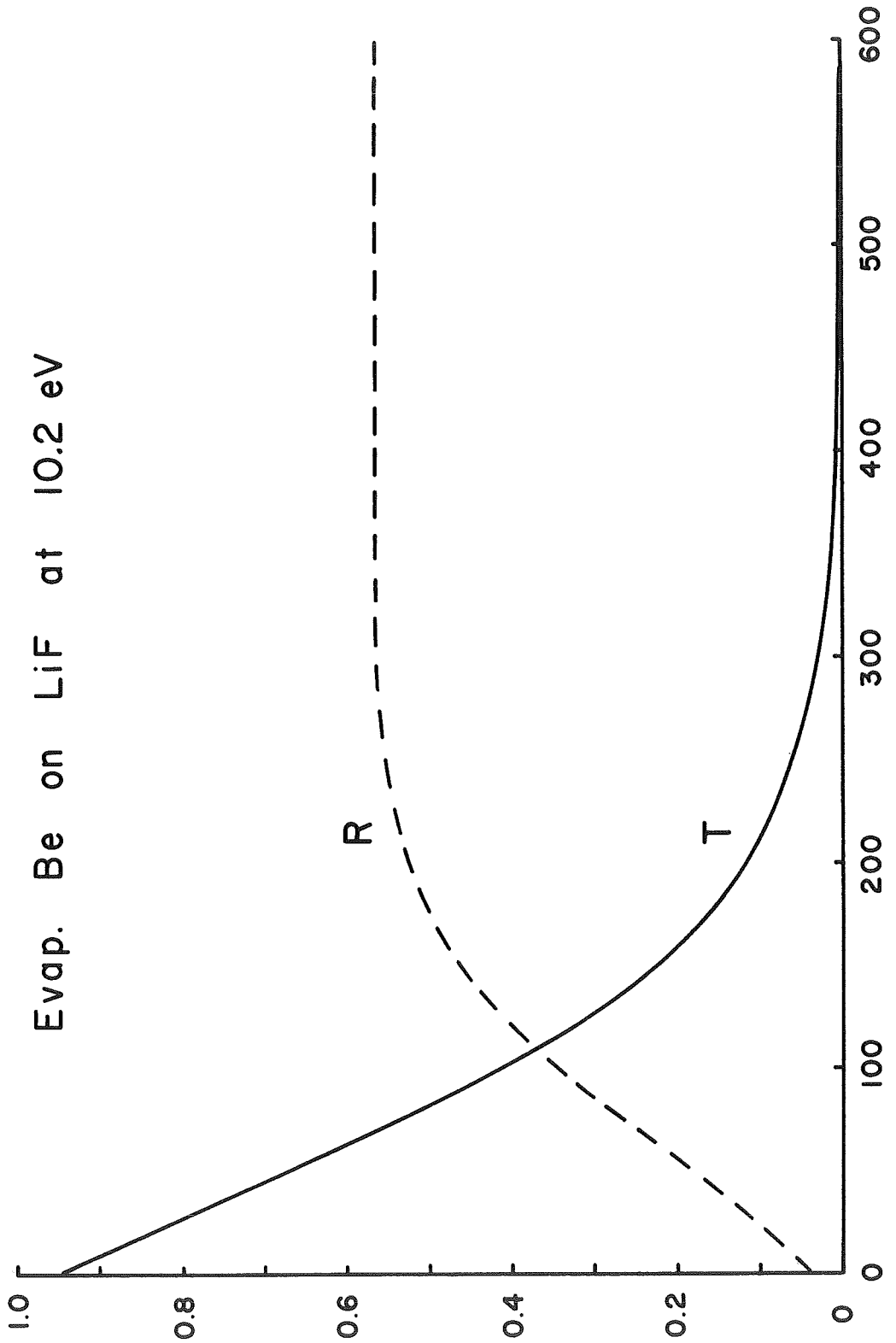

Fig. 18 Transmittance and Reflectance vs film thickness.

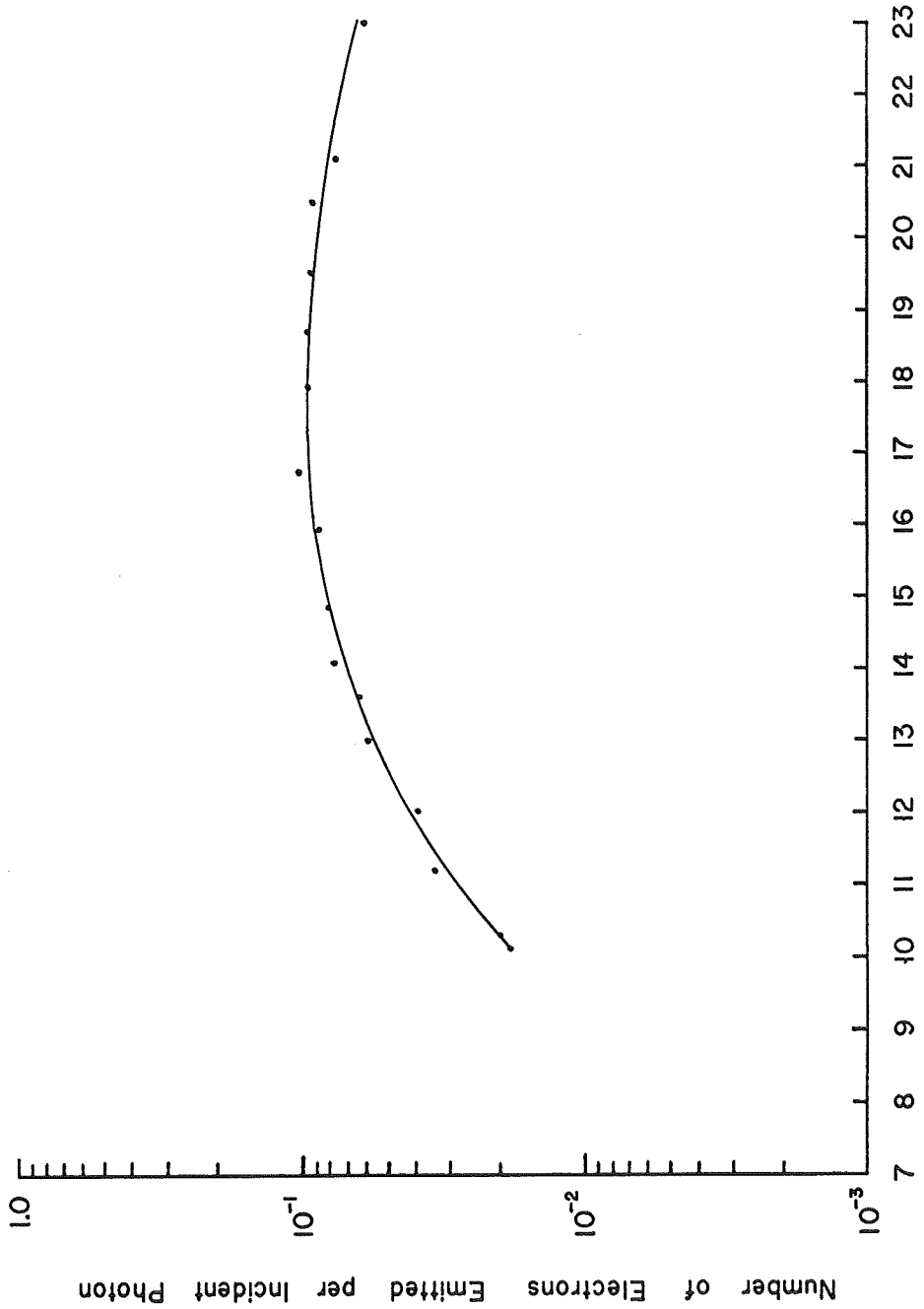

Fig. 19 Spectral quantum yield of Be film .

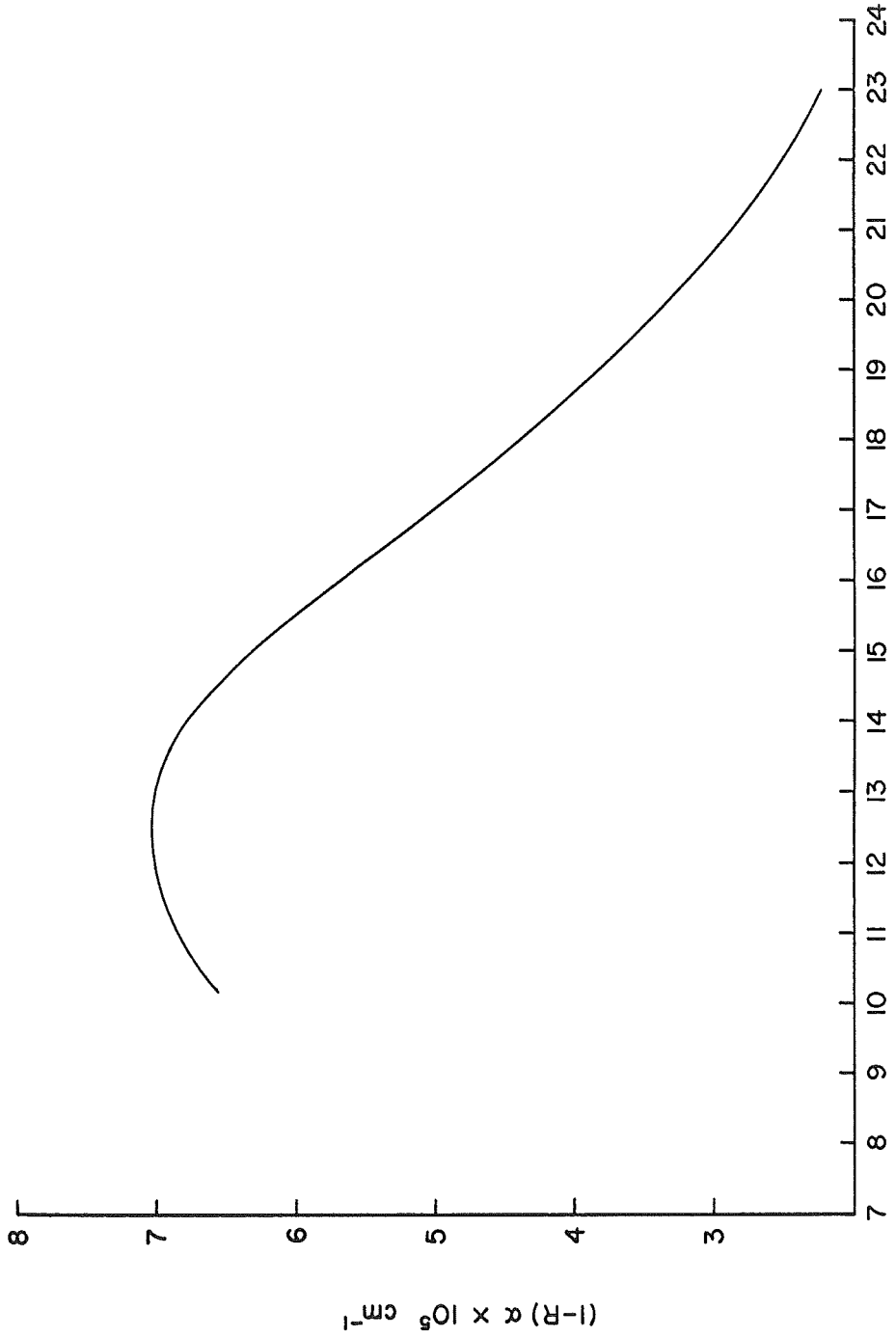

Fig. 20 $(1-R)\alpha$ vs photon energy for Be .

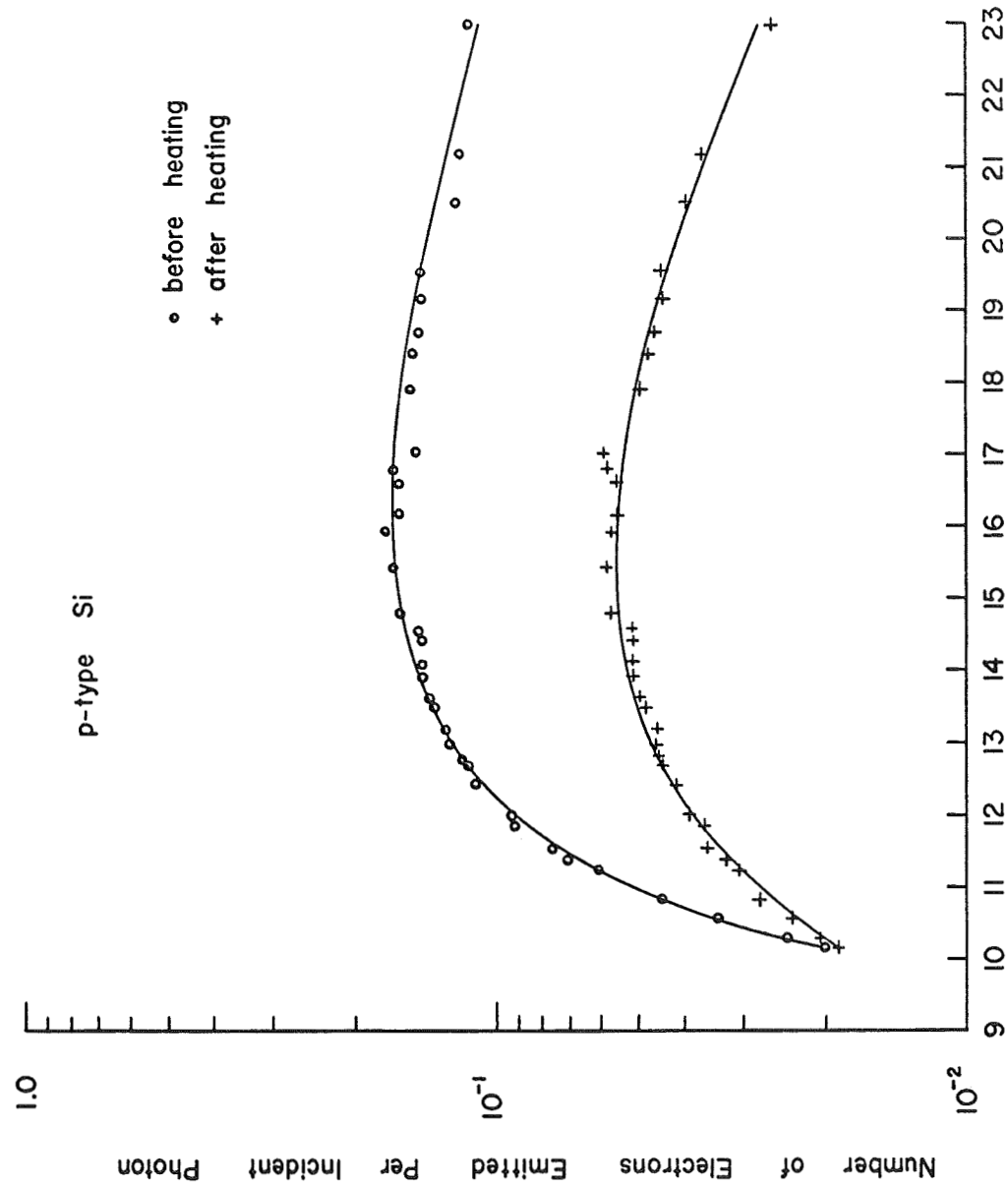

Fig. 21 Effect of heat-treatment on the quantum yield of Si crystal .

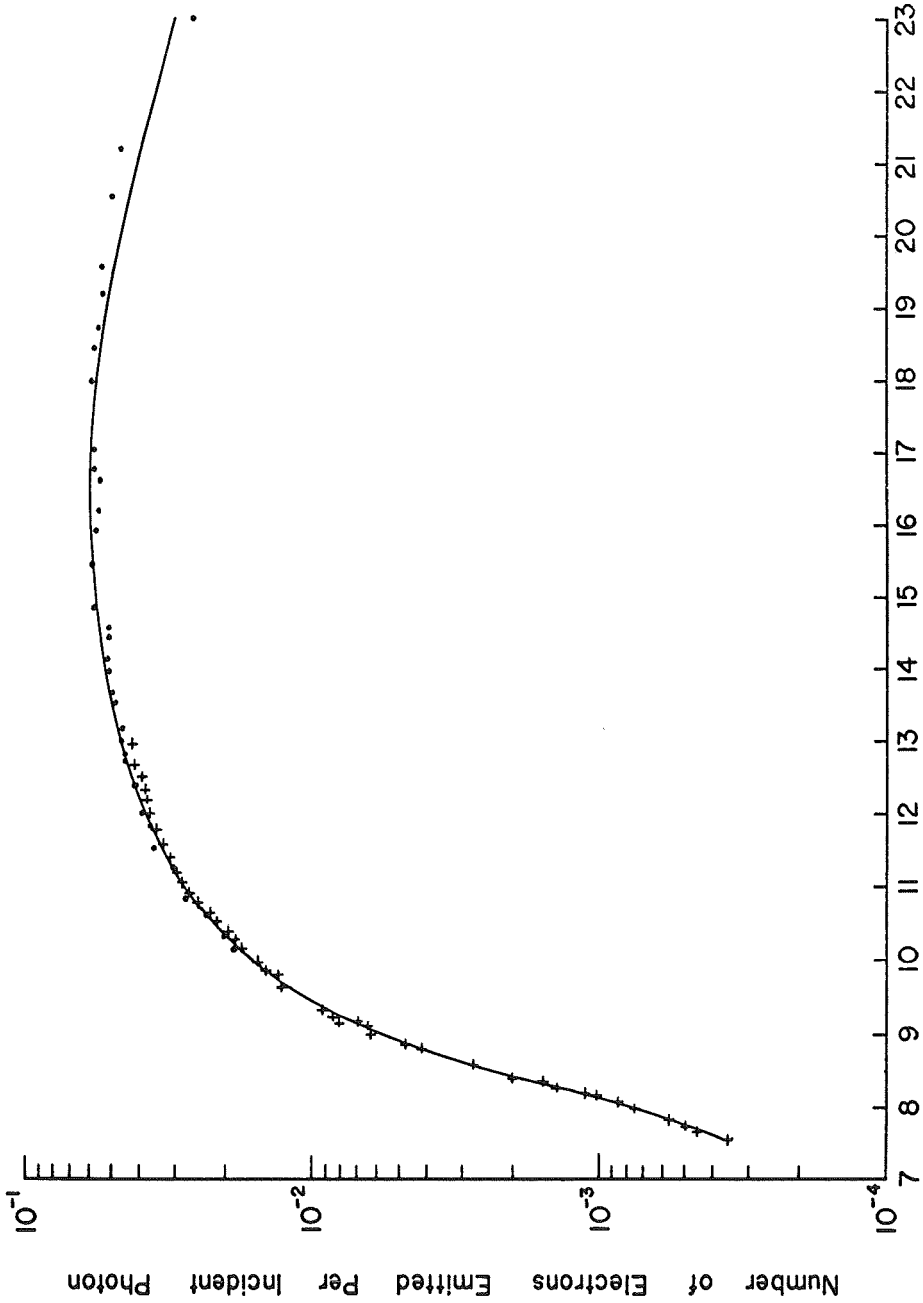

Fig. 22 Spectral quantum yield of heat-treated Si crystal.

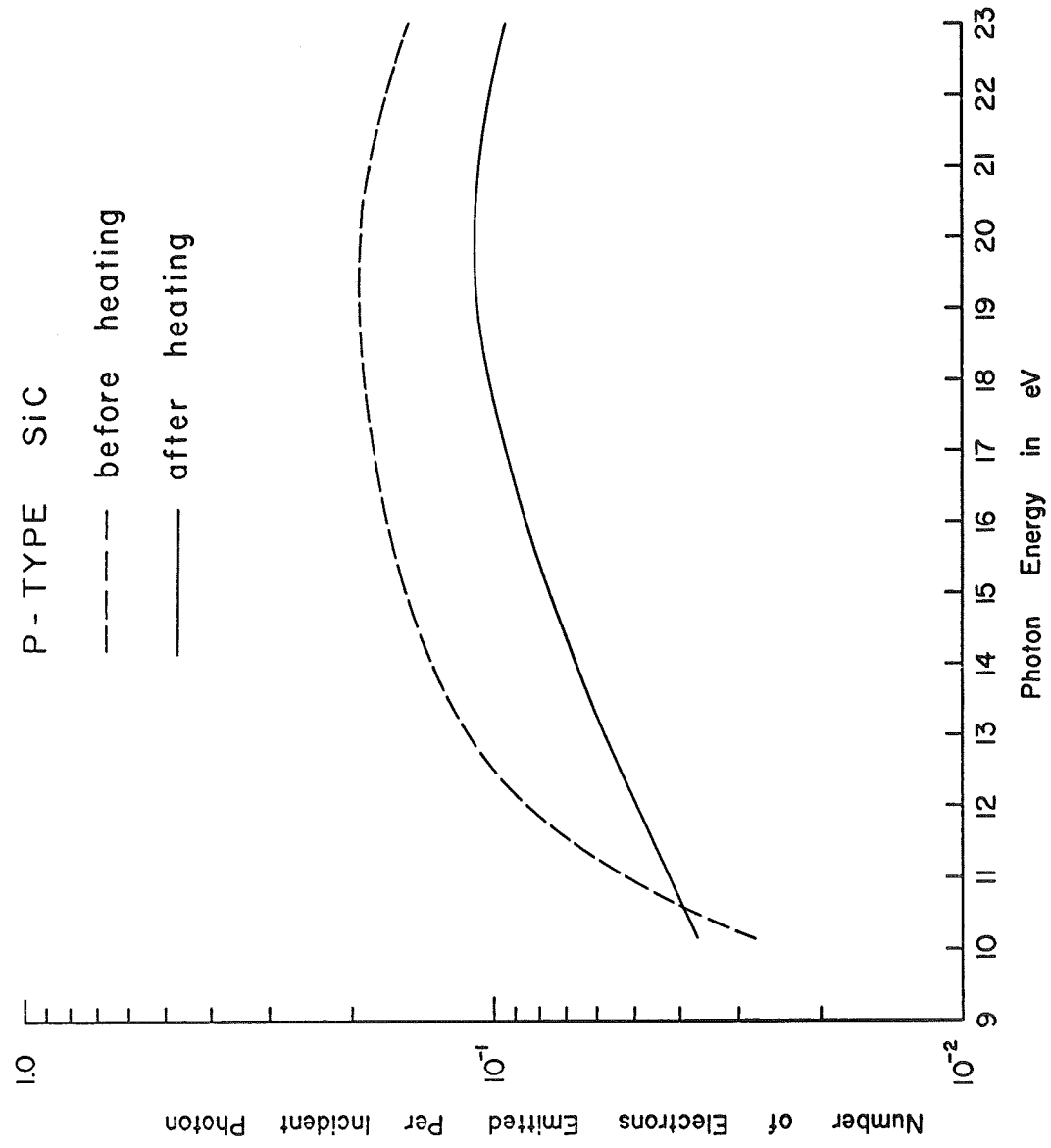

Fig. 23 Effect of heat-treatment on the yield of p-type SiC .

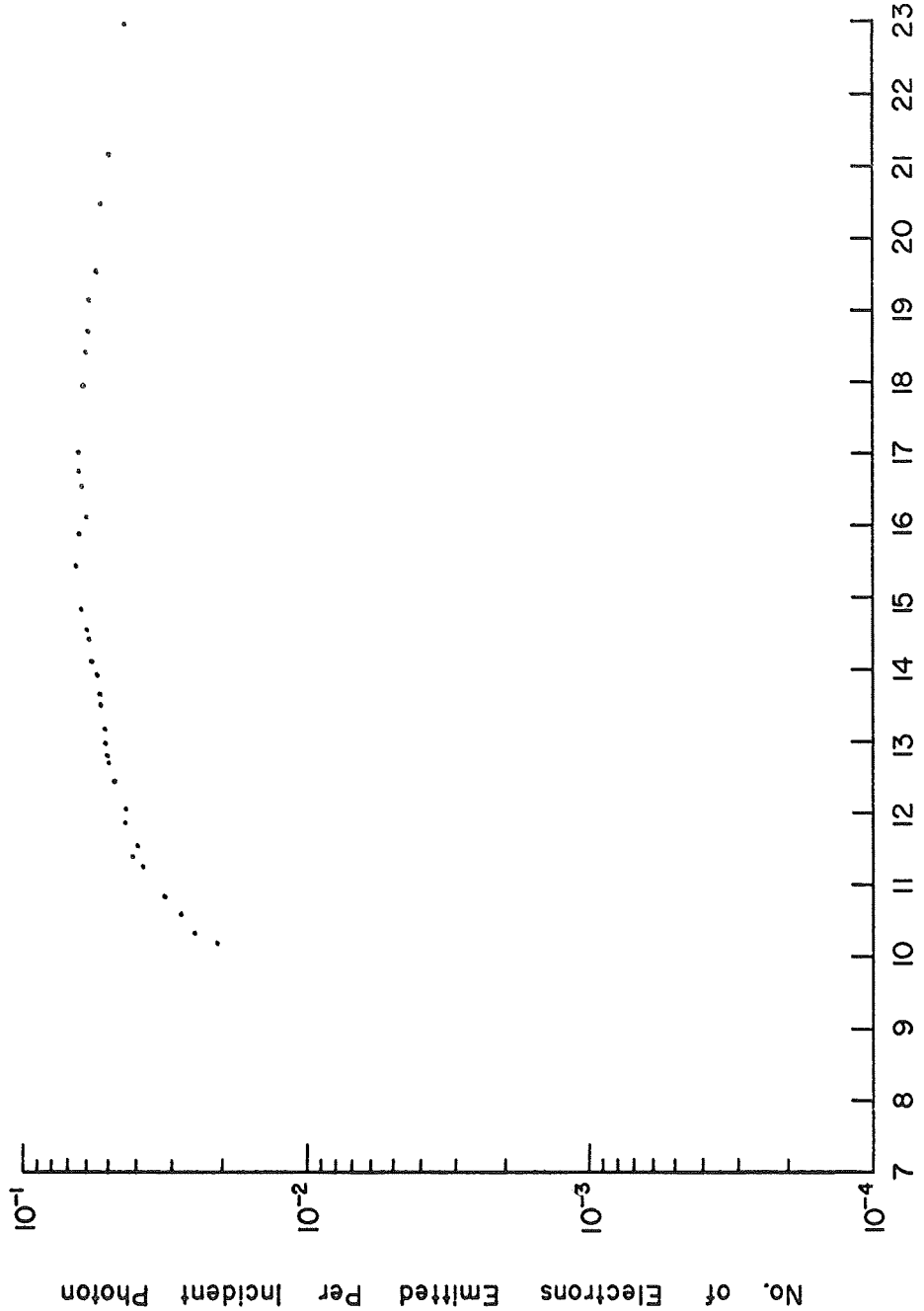

Fig. 24 Spectral quantum yield of amorphous Se. Film thickness: approx. 300 Å.

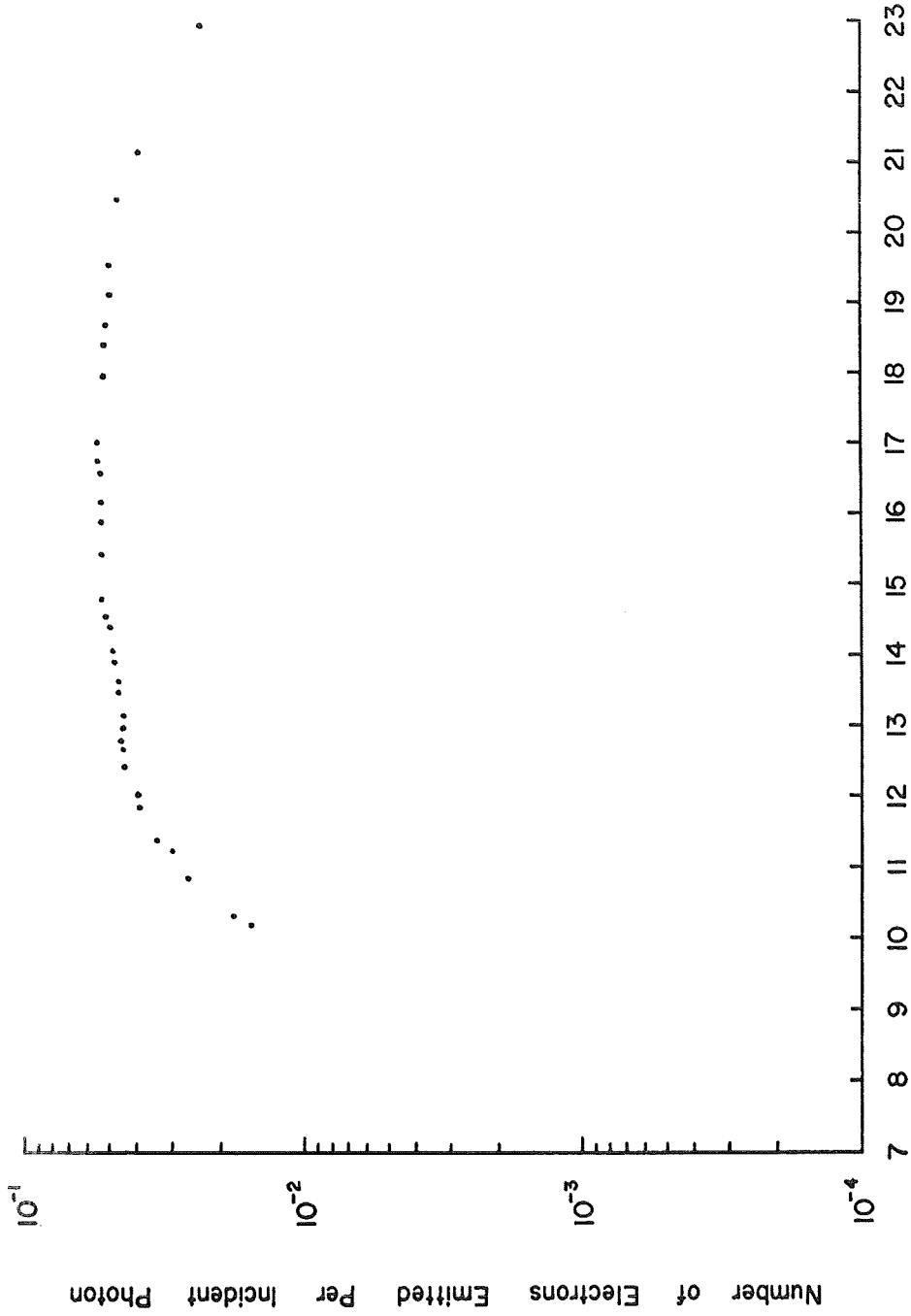

Fig. 25 Spectral quantum yield of Te film above 10 eV. Film thickness: approx. 180 Å.

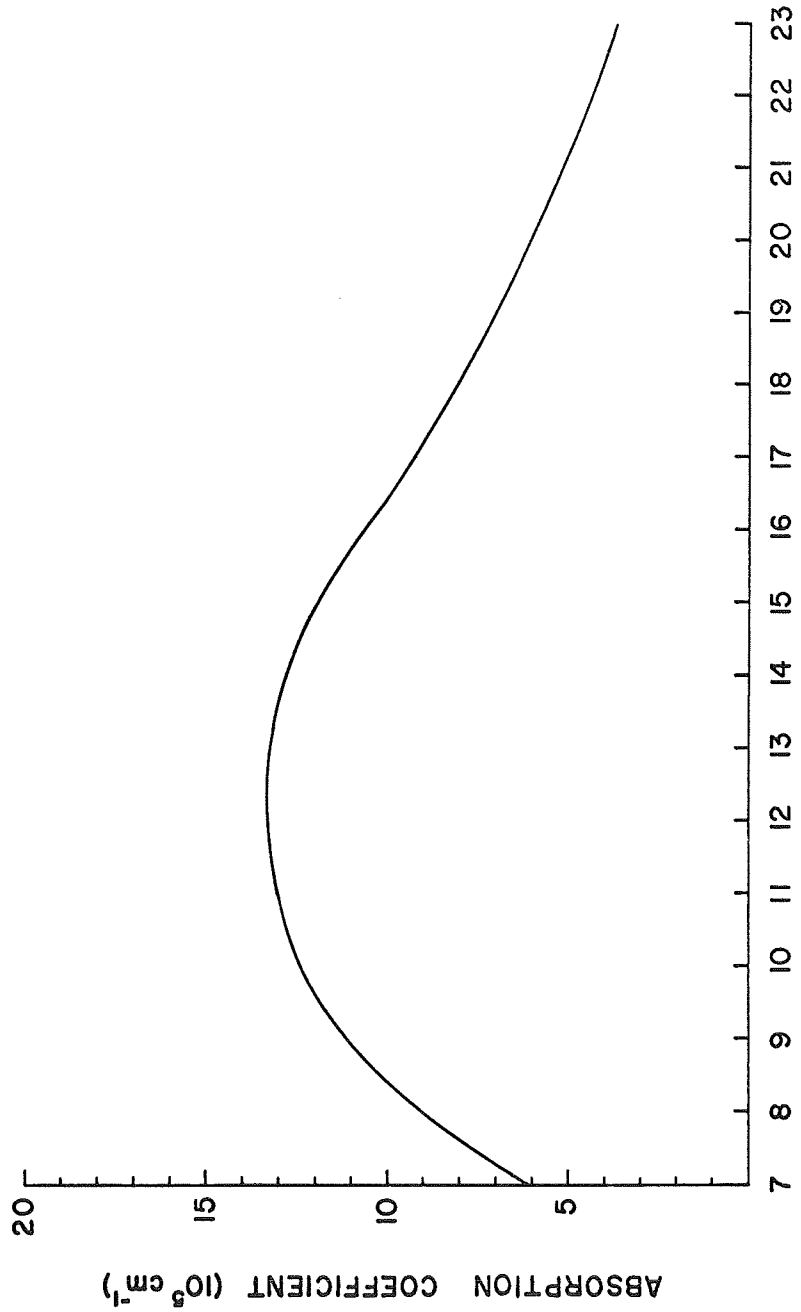

Fig. 26 Spectral absorption of amorphous selenium.

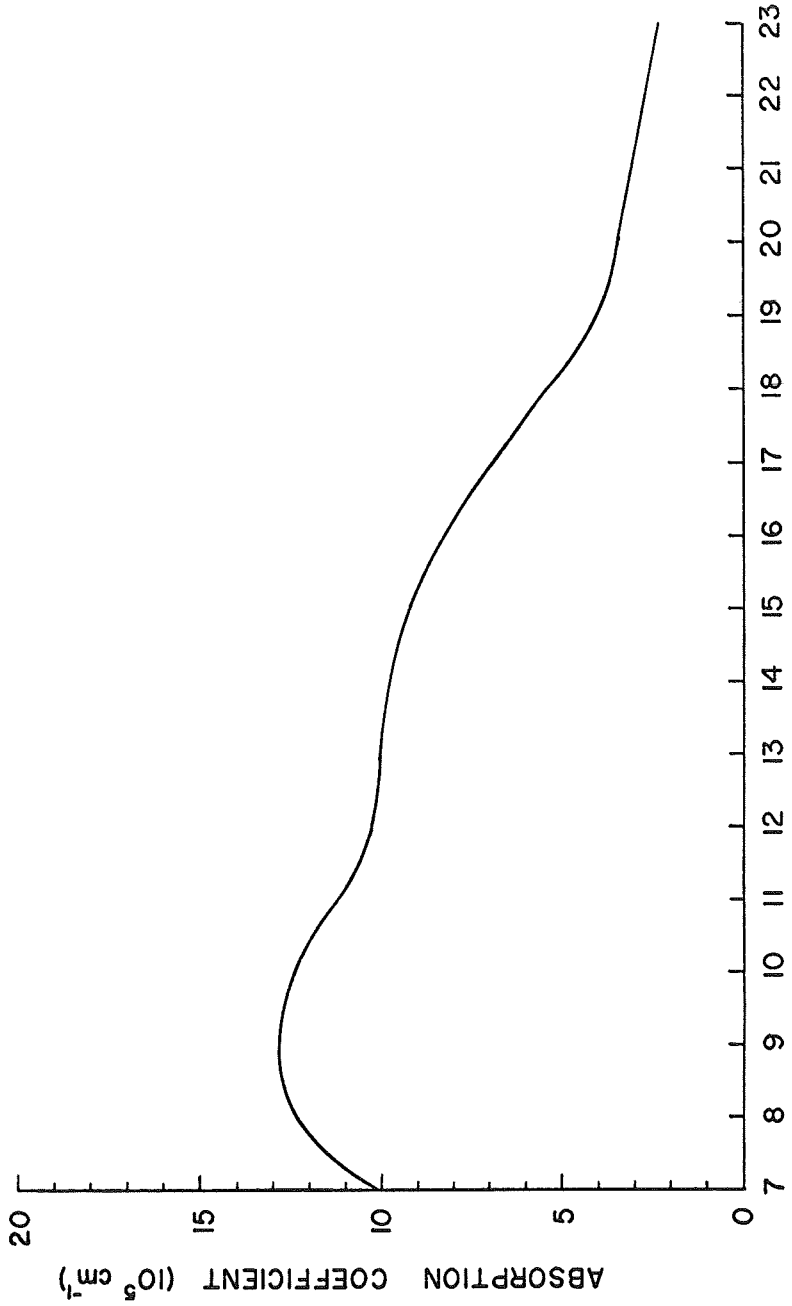

Fig. 27 Spectral absorption of tellurium film .

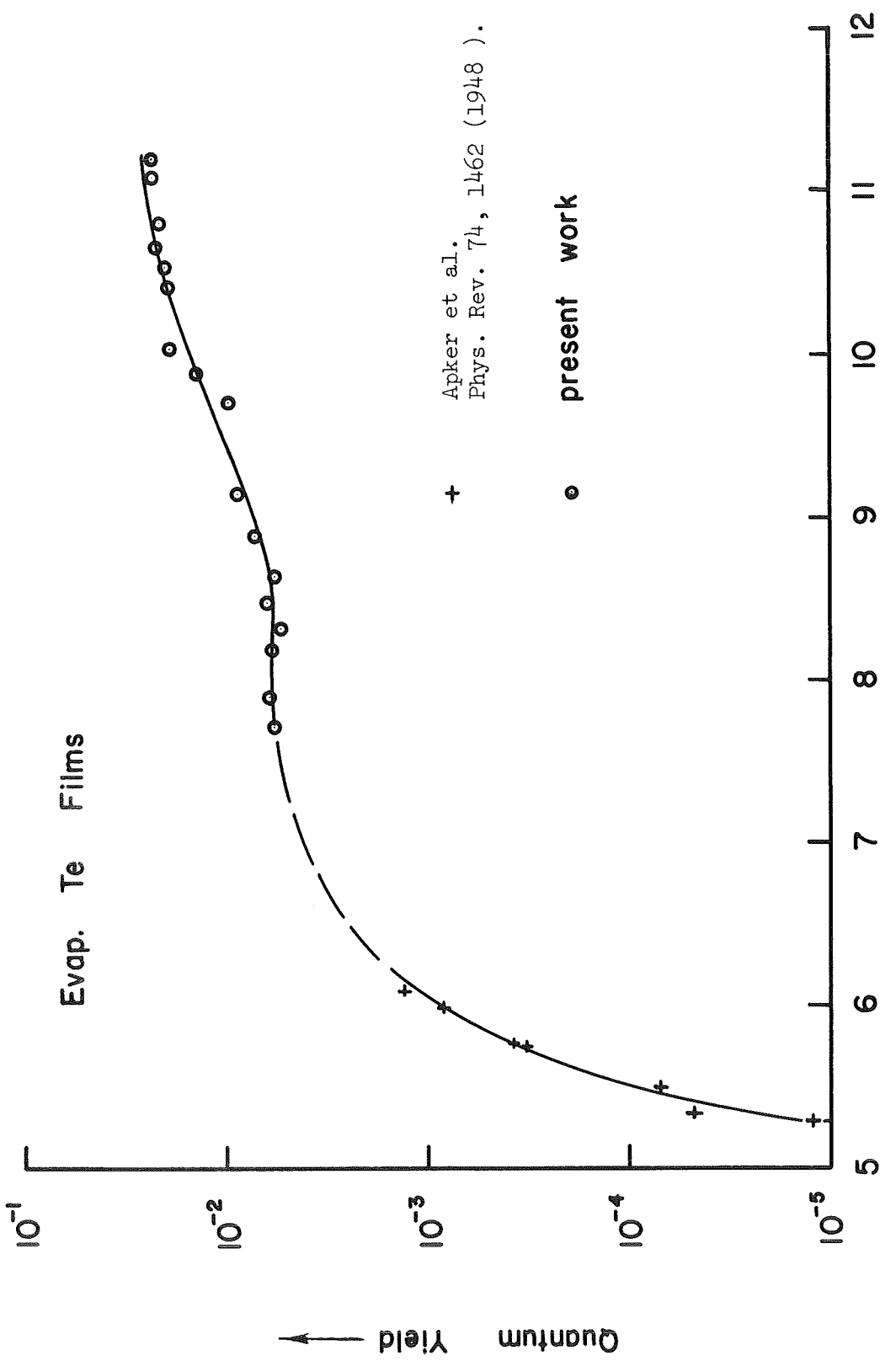

Fig. 28 Spectral yield of Te below 11 eV . o represents yield in number of electrons emitted per incident photon. Film thickness: approx. 400 A.

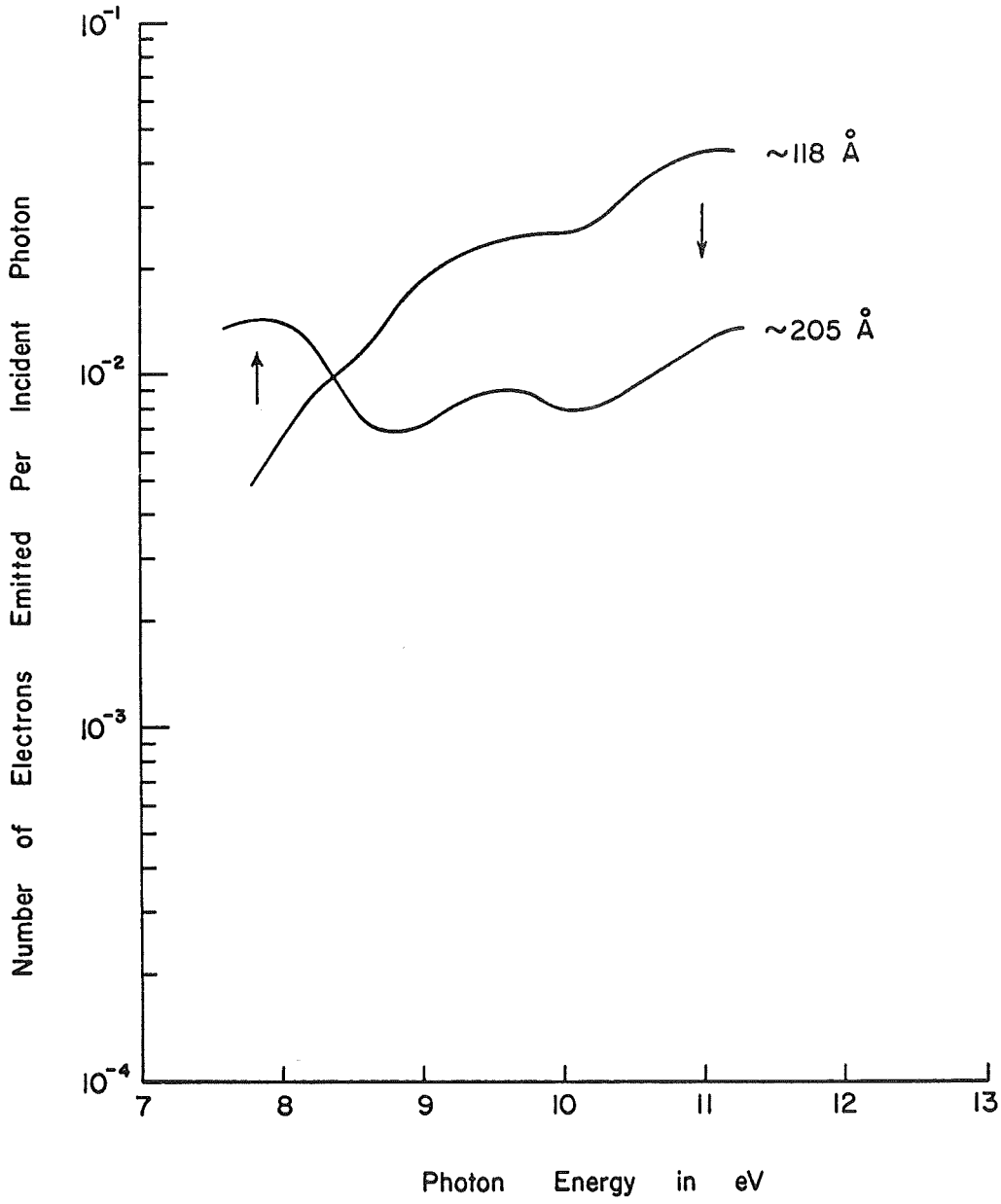

Fig. 29 Spectral yield of CuBr under "back" illumination.

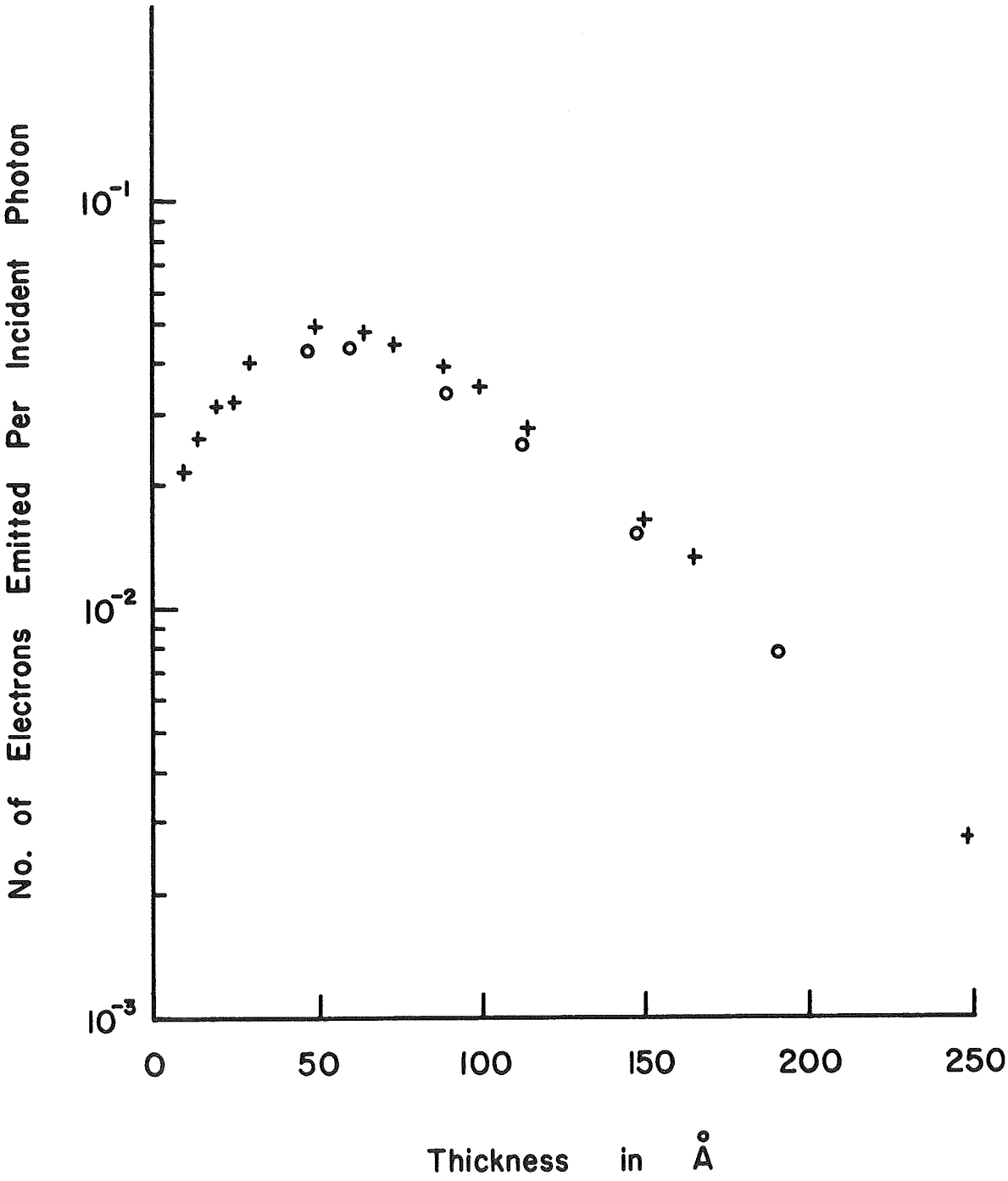

Fig. 30 Yield of evaporated CuI under "back" illumination at 10.2 eV.

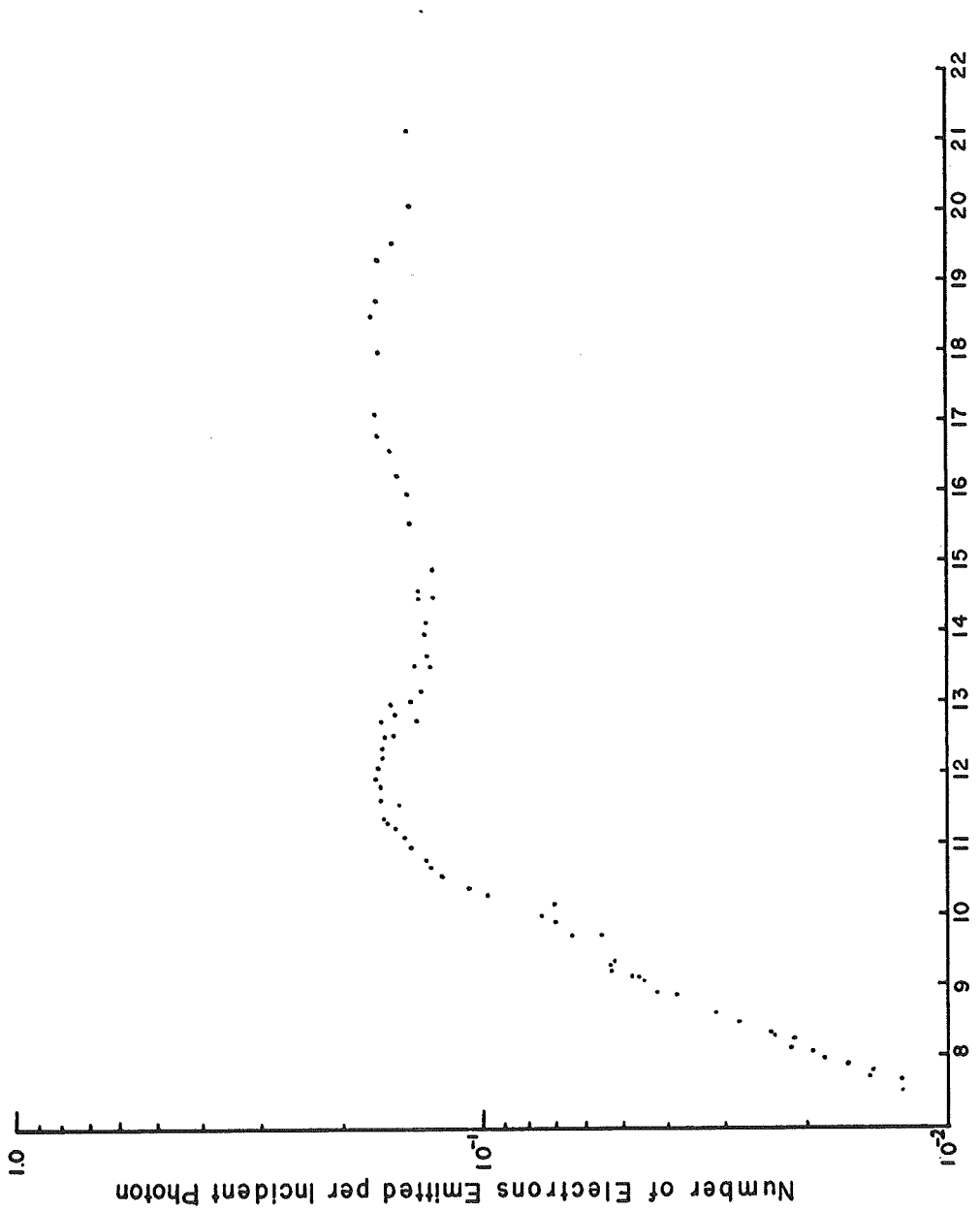

Fig. 31 Spectral quantum yield of evaporated CuI film. Film thickness: approx. 380 Å.

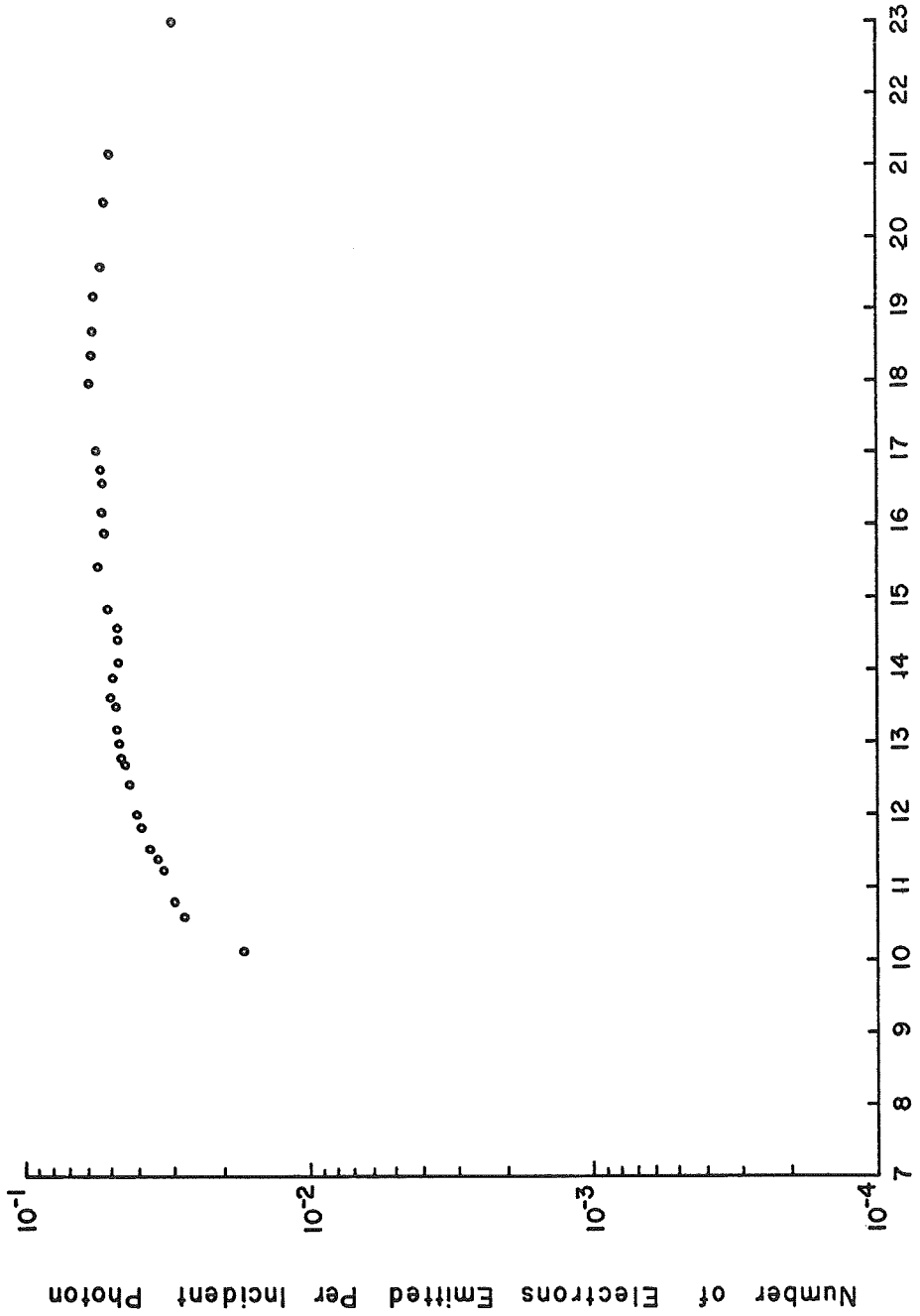

Fig. 32 Spectral quantum yield of CdTe film .

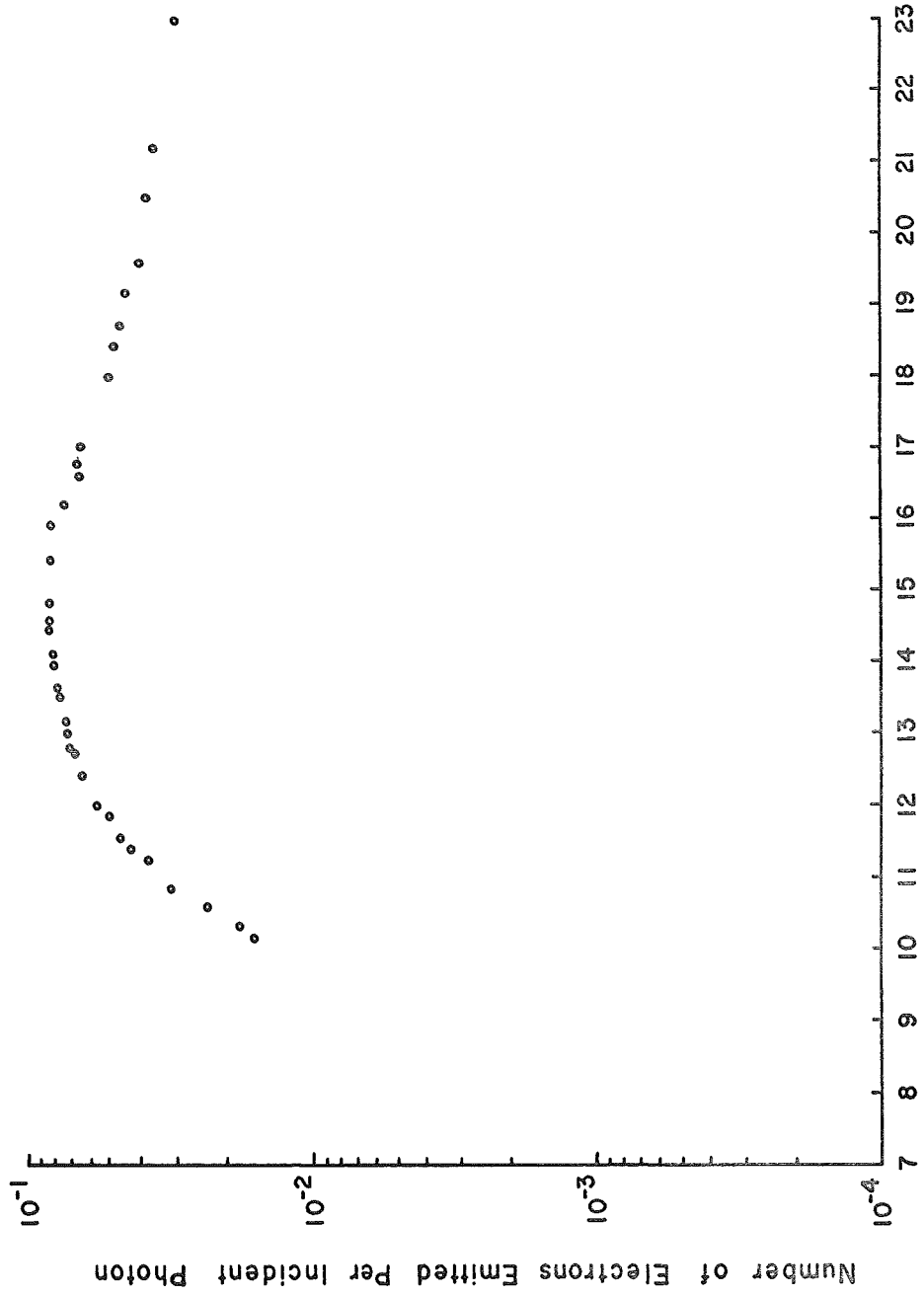

Fig. 33 Spectral yield of GaAs film on Ge crystal .

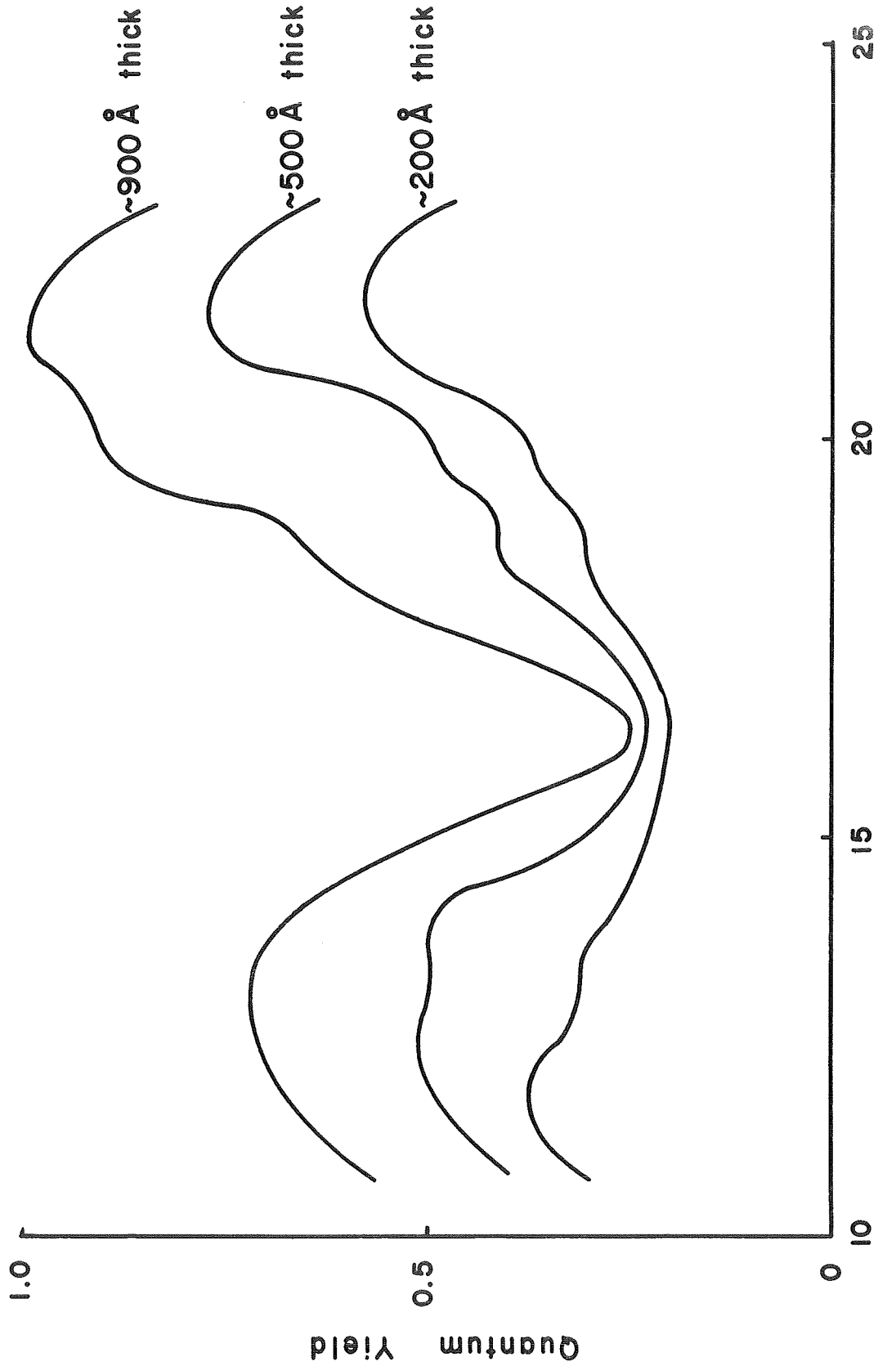

Fig. 34 Spectral quantum yield of evaporated KBr films .

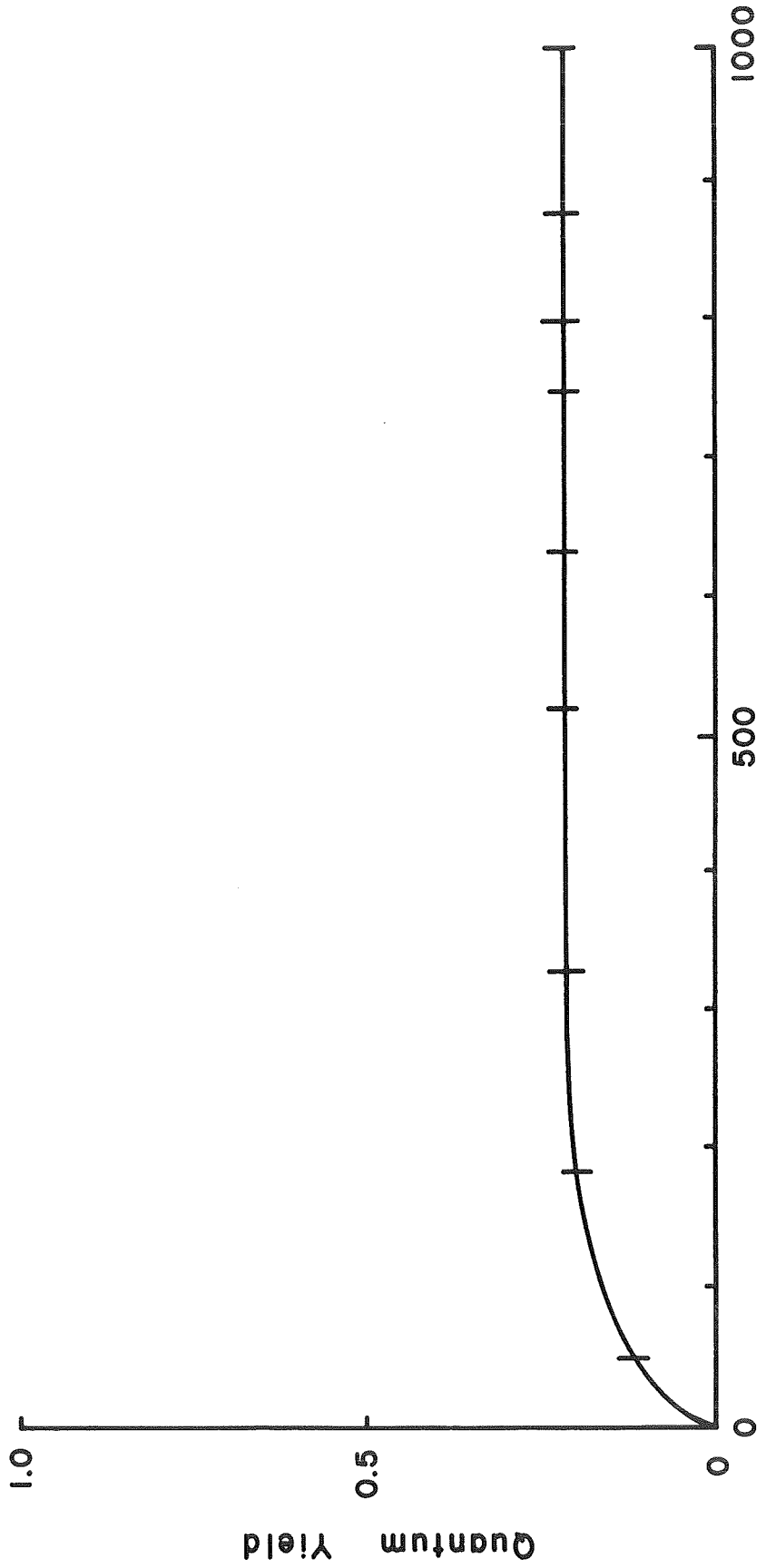

Fig. 35 Yield vs film thickness of KBr at 16.6 eV.

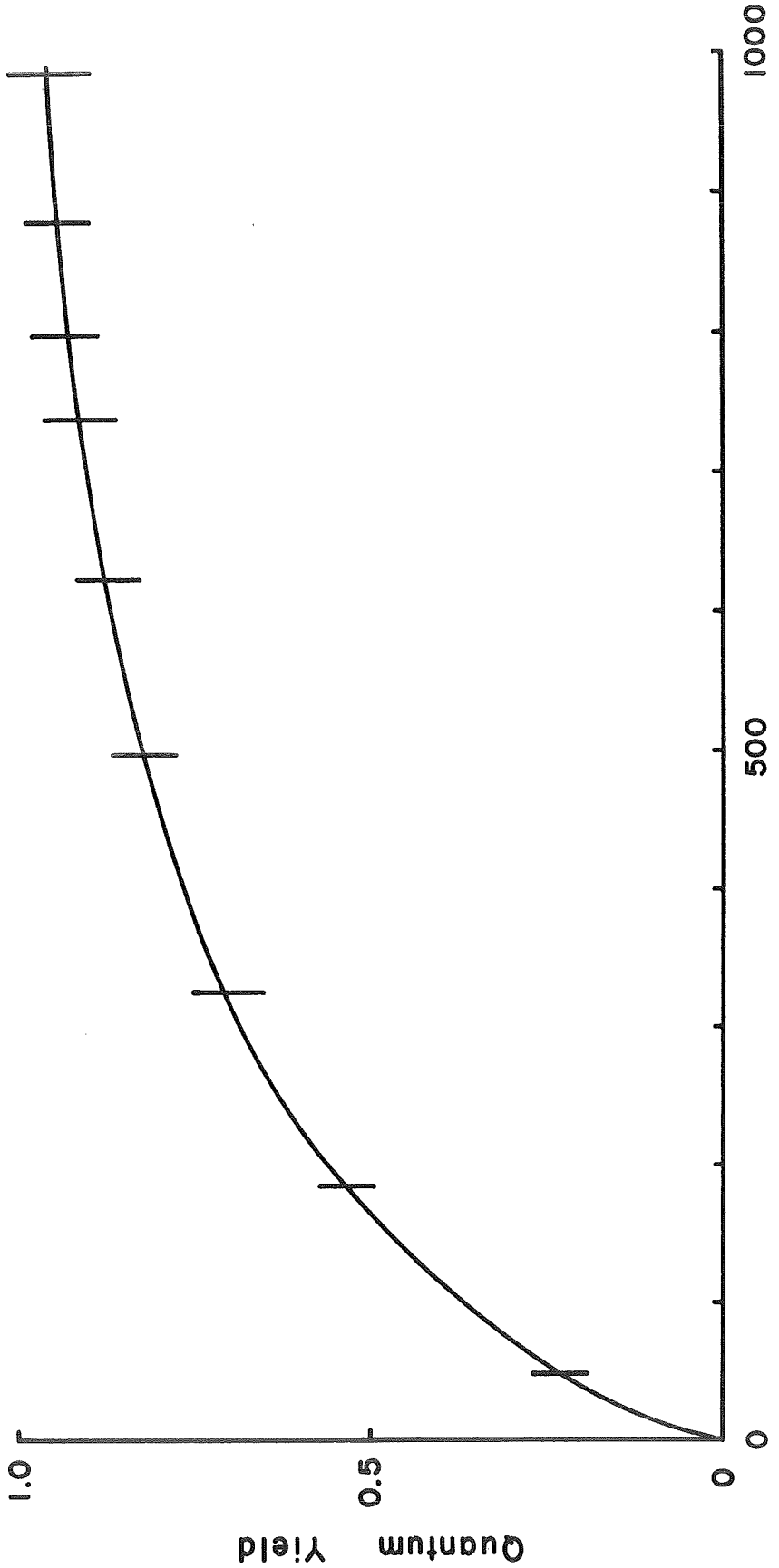

Fig. 36 Yield vs film thickness of KBr at 21.2 eV.

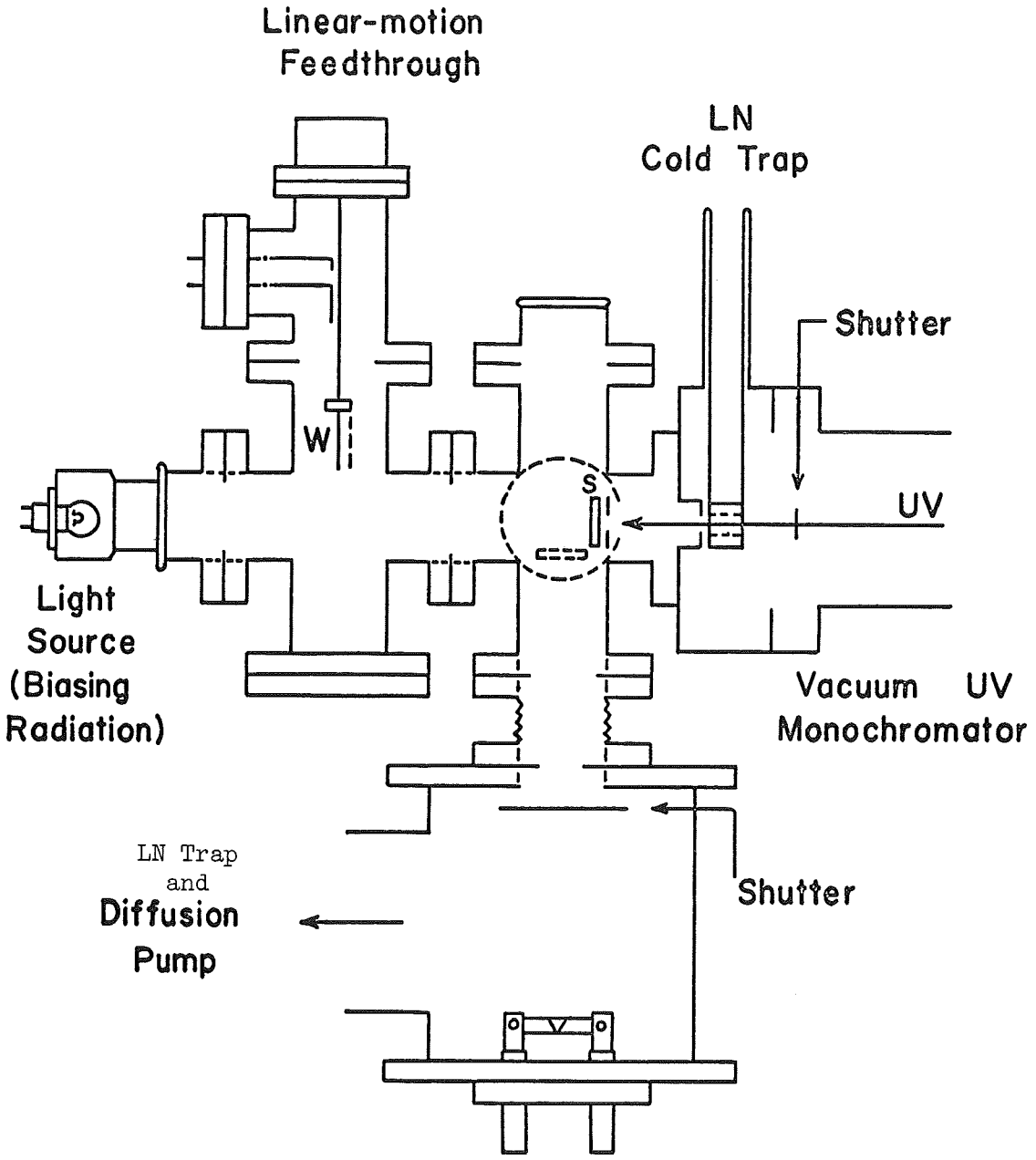

Fig. 37 Exciton-induced photoemission experiment.

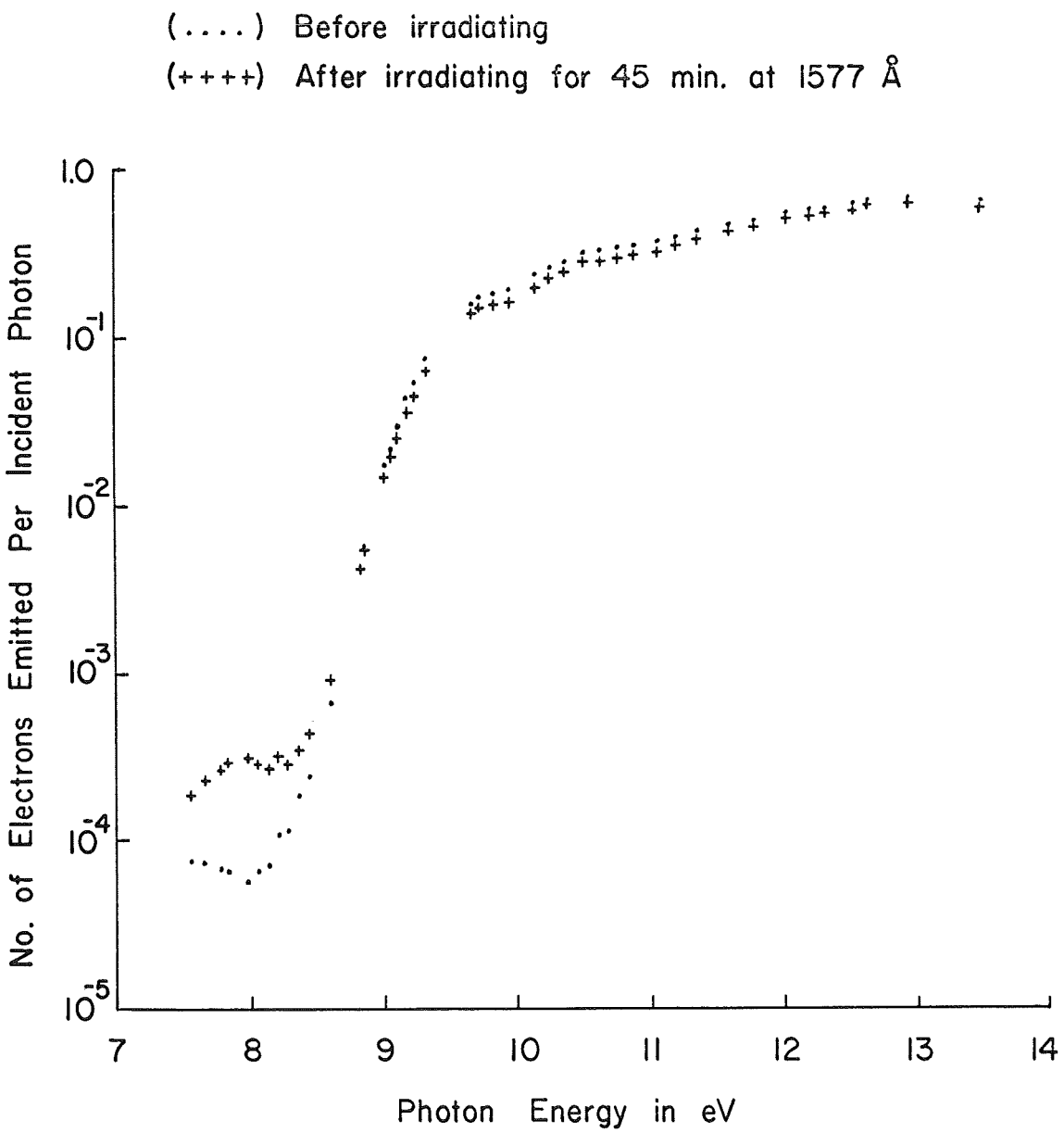

Fig. 38 Spectral quantum yield of KCl film.

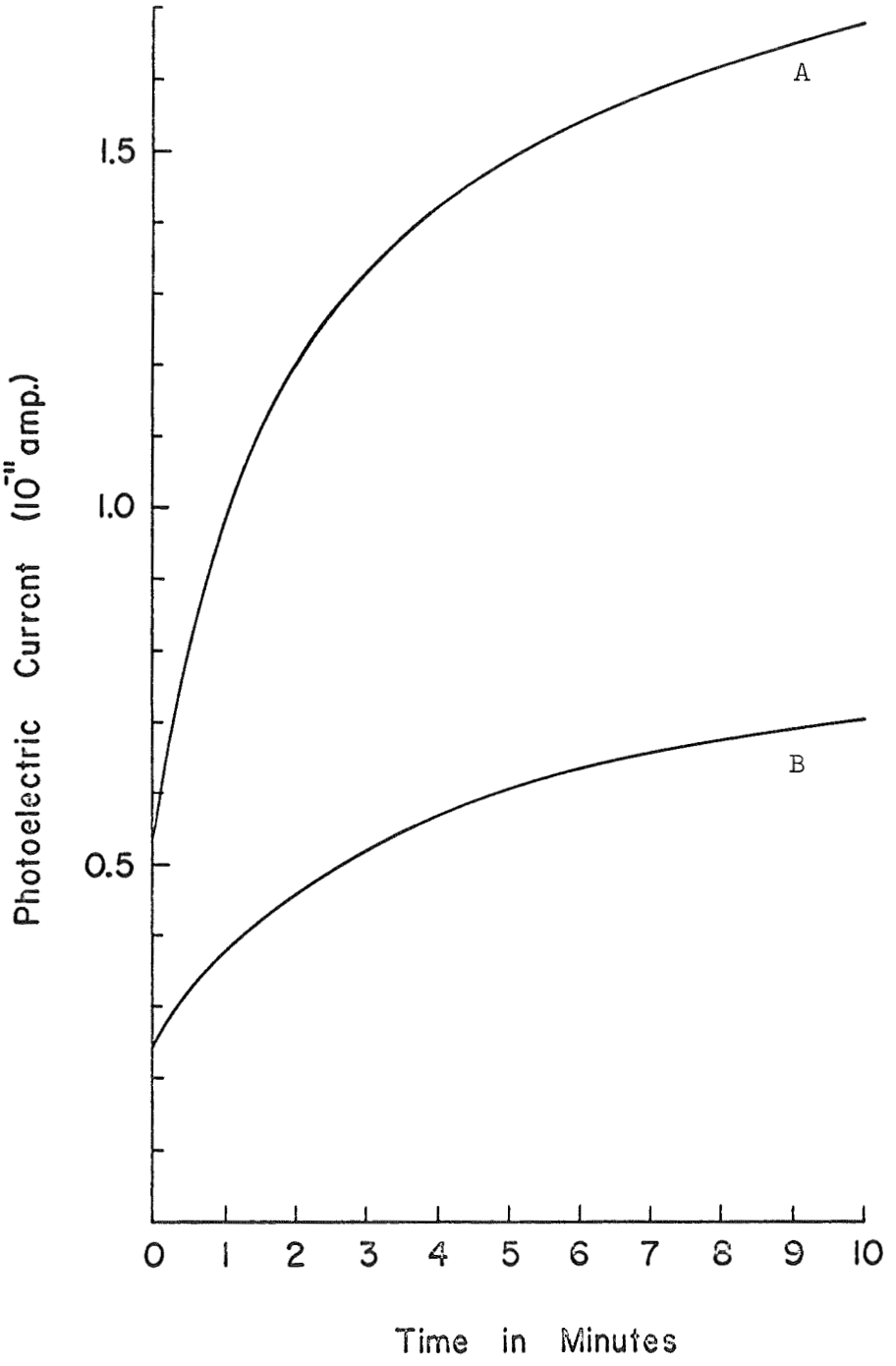

Fig. 39 Exciton-induced photoemission from KCl film at 1577 Å. Excitation intensity (1577 Å) of A was approximately twice that of B .

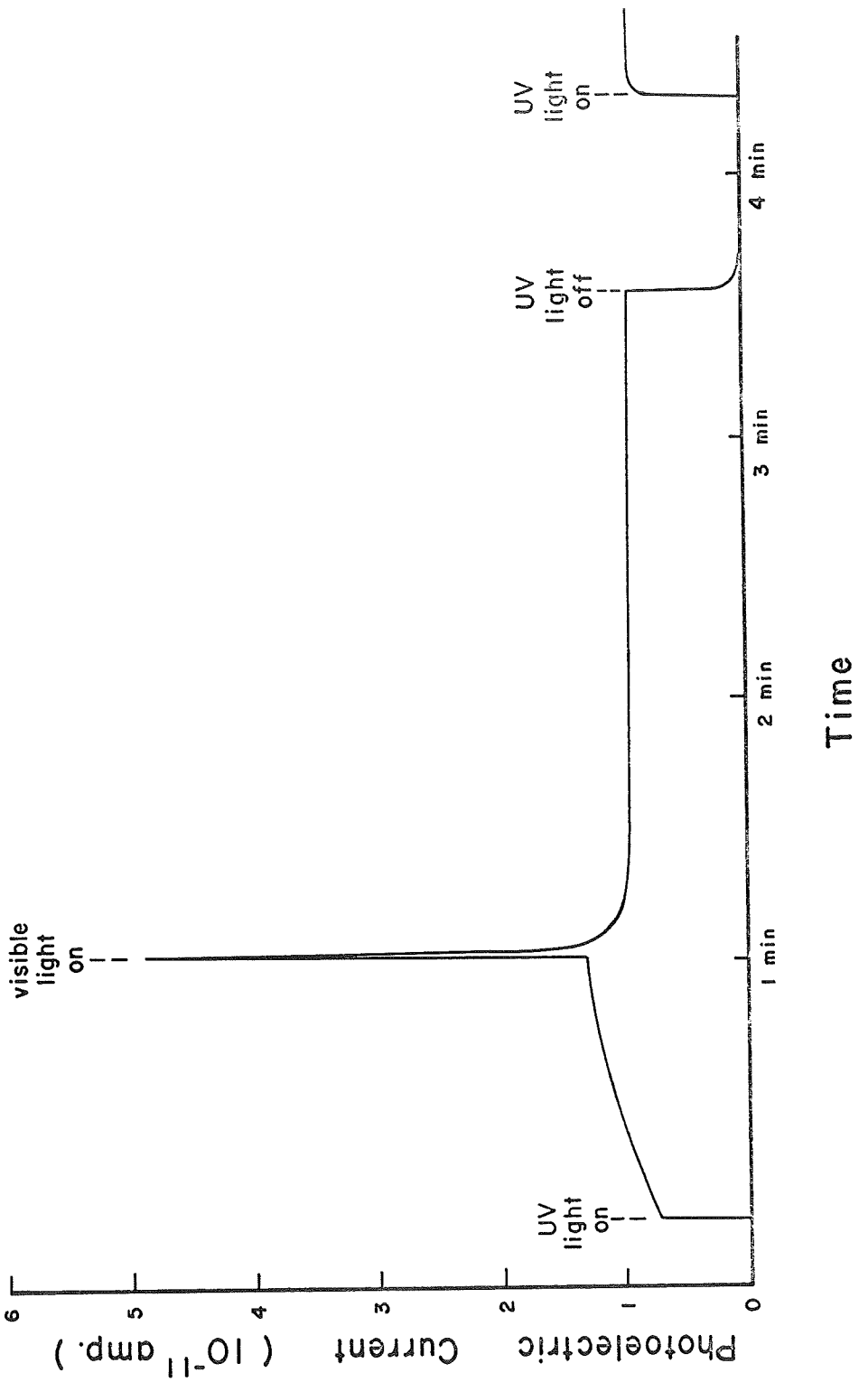

Fig. 40 Effect of biasing radiation (visible light) on exciton-induced photoemission.

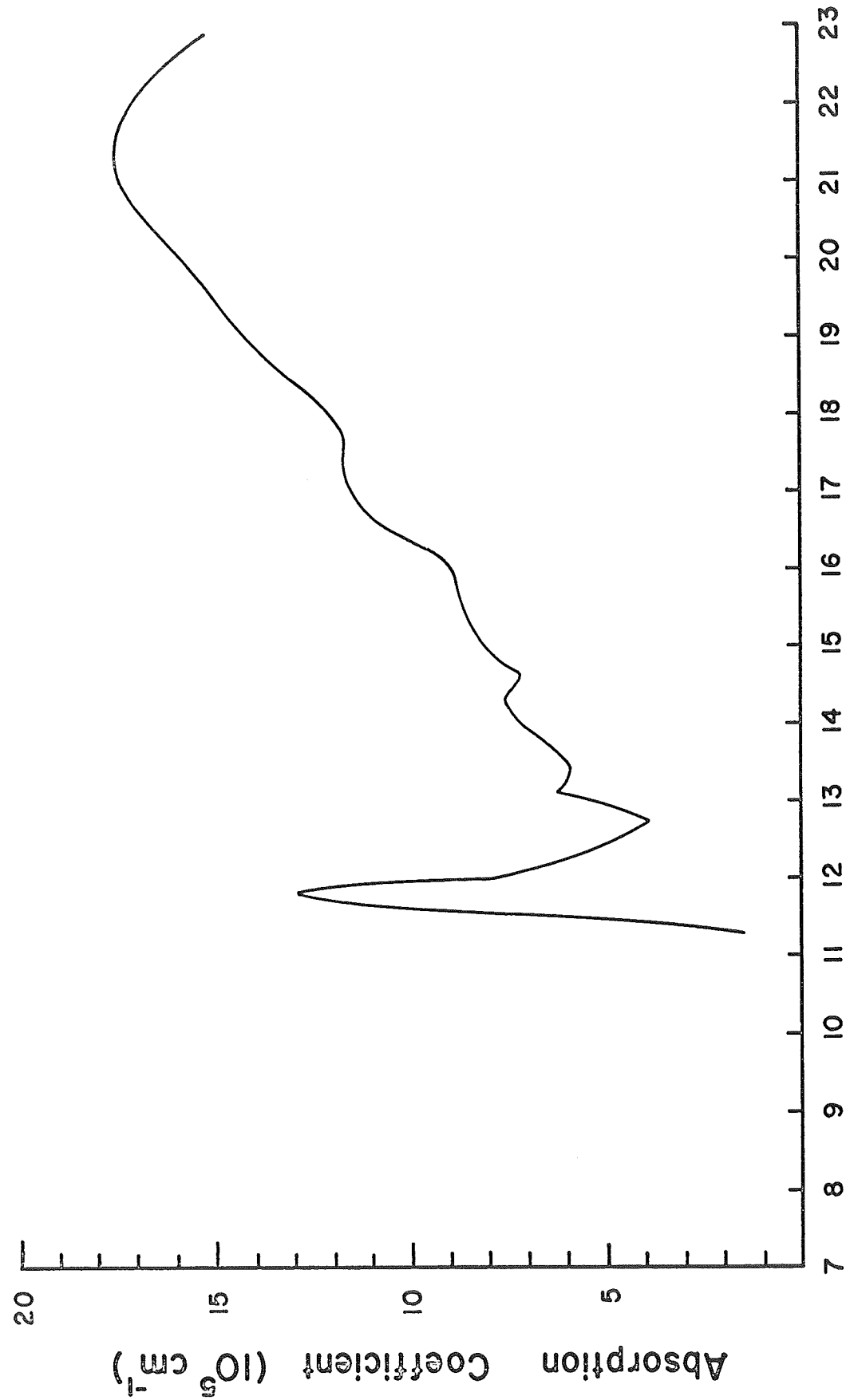

Fig. 41 Spectral absorption of MgF_2 Film

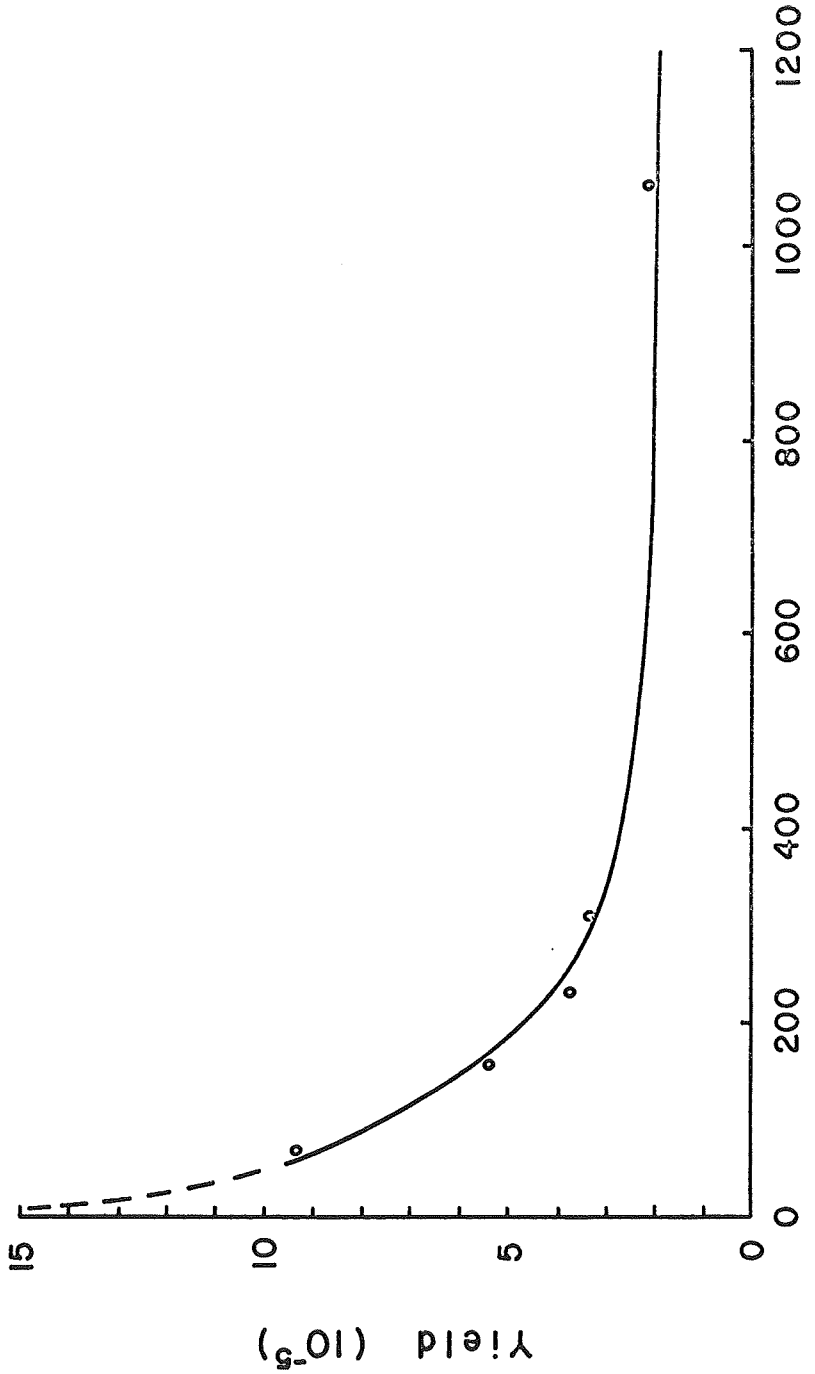

Fig. 42 Photoemission from MgF_2 films on nickel film substrates. The wavelength of the incident radiation was 1608 Å.

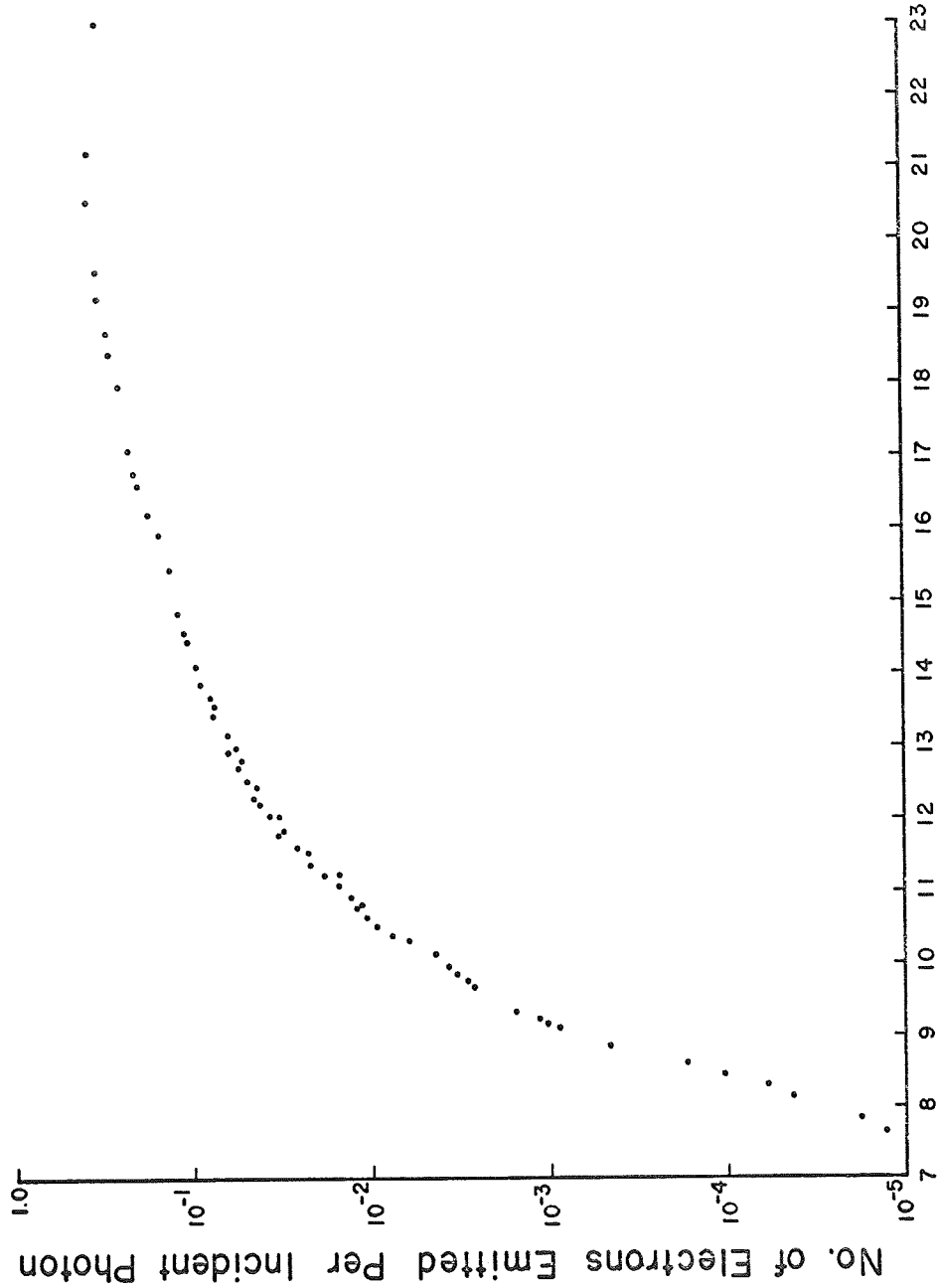

Fig. 43 Spectral quantum yield of MgF_2 film. Film thickness: approx. 2700 Å.

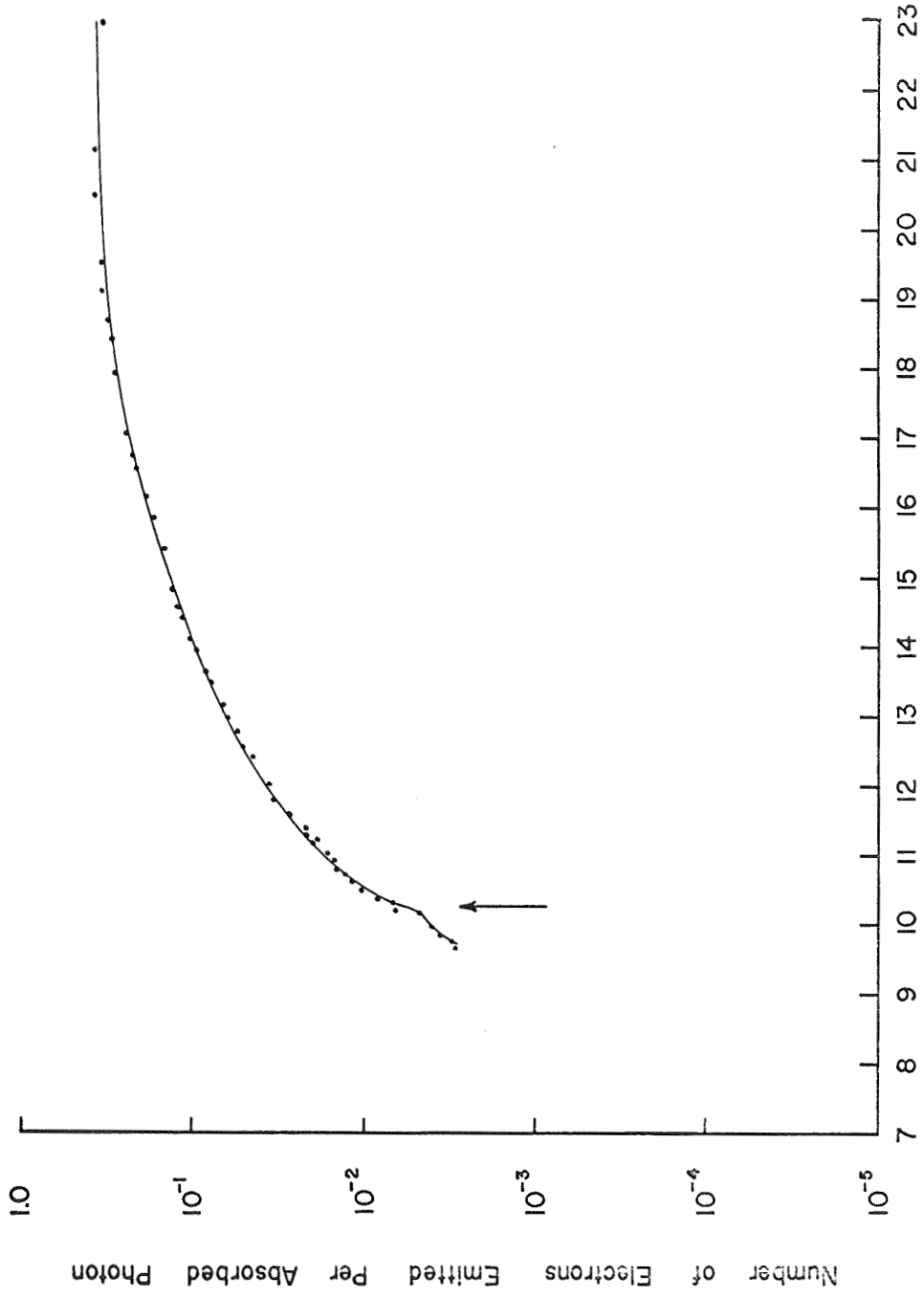

Fig. 44 Spectral yield of MgF_2 film: corrected for reflectivity. The yield is expressed in number of electrons per absorbed photon.

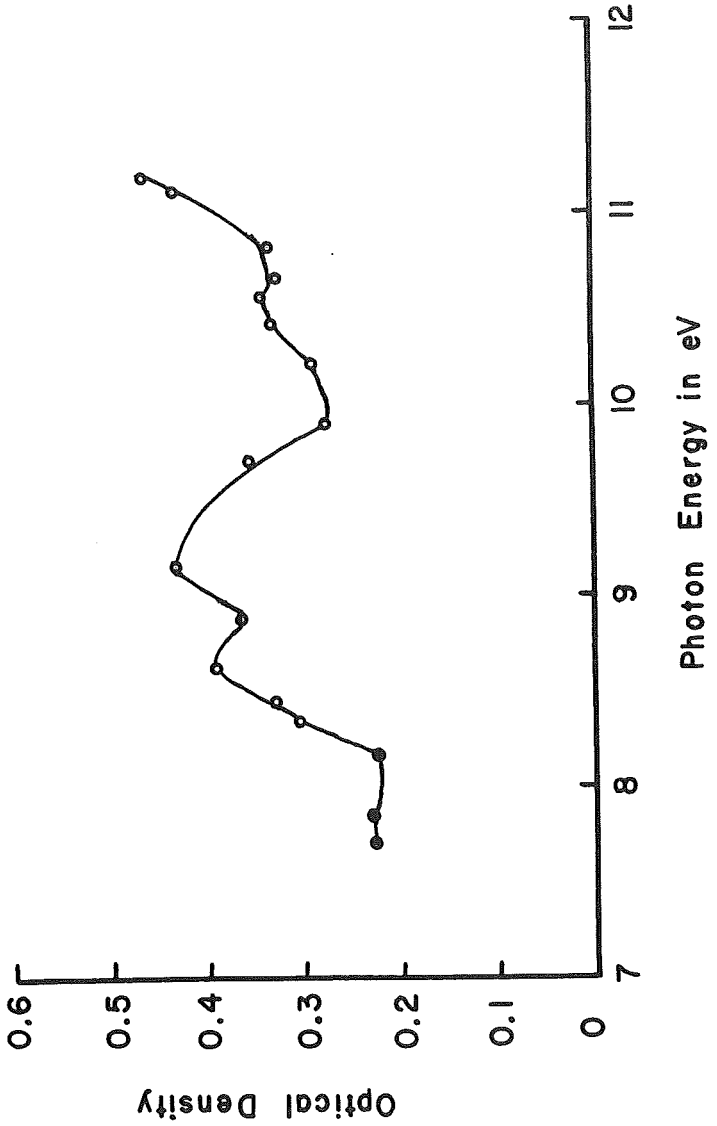

Fig. 45 Optical density of 50-50% KBr-KCl film.

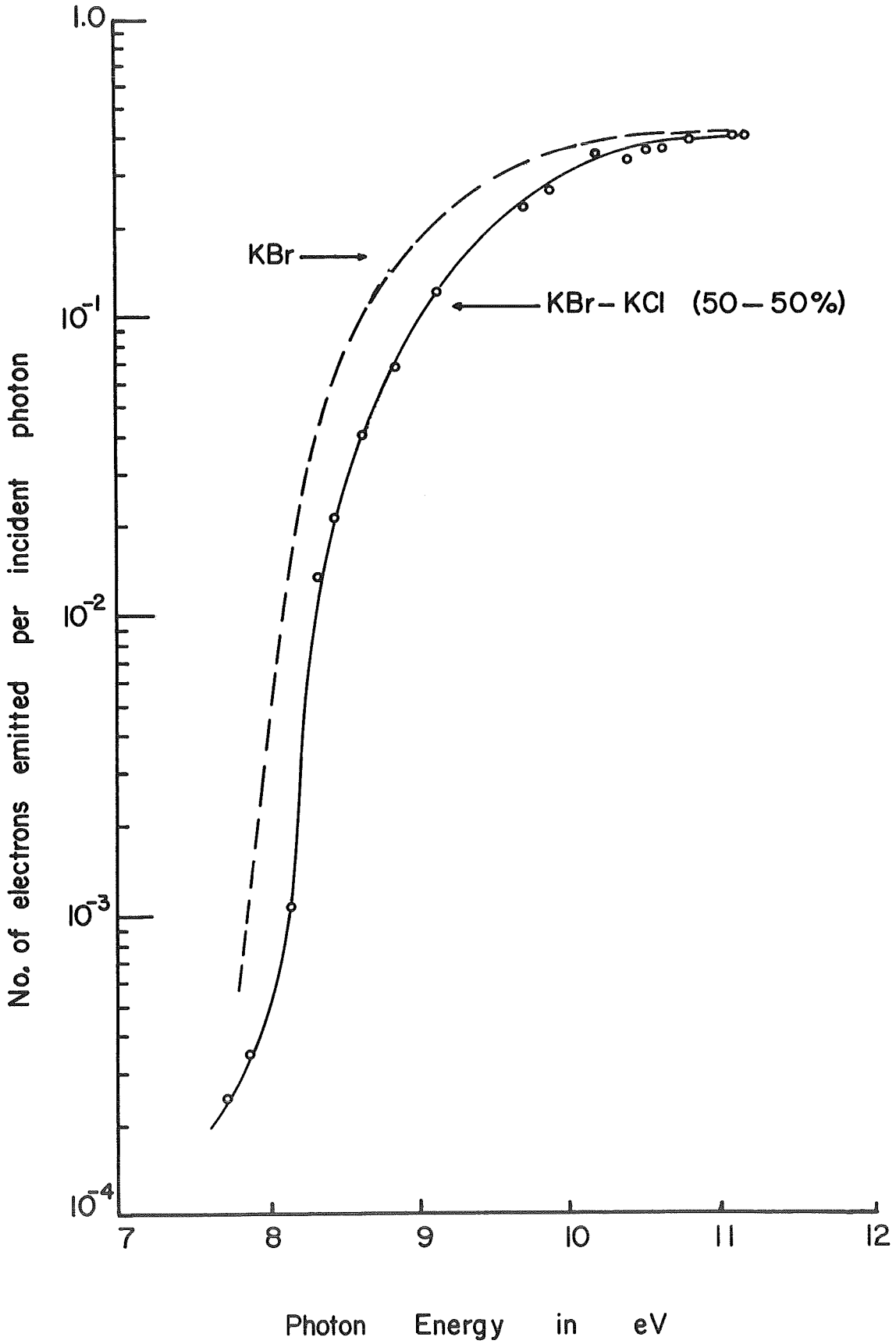

Fig. 46 Spectral yield of 50-50% KBr-KCl film.

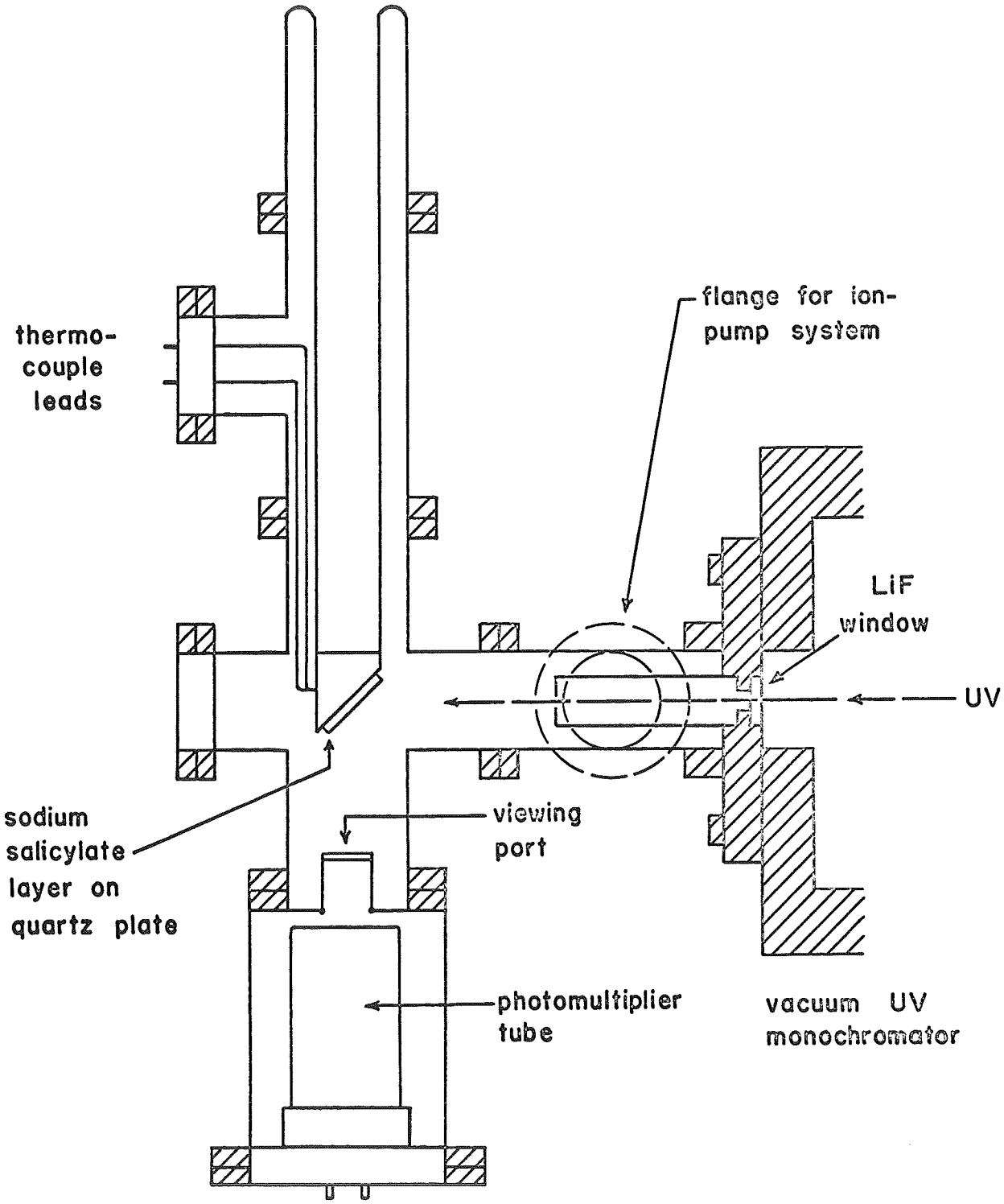

Fig. 47 Equipment for measuring the fluorescence of sodium salicylate.

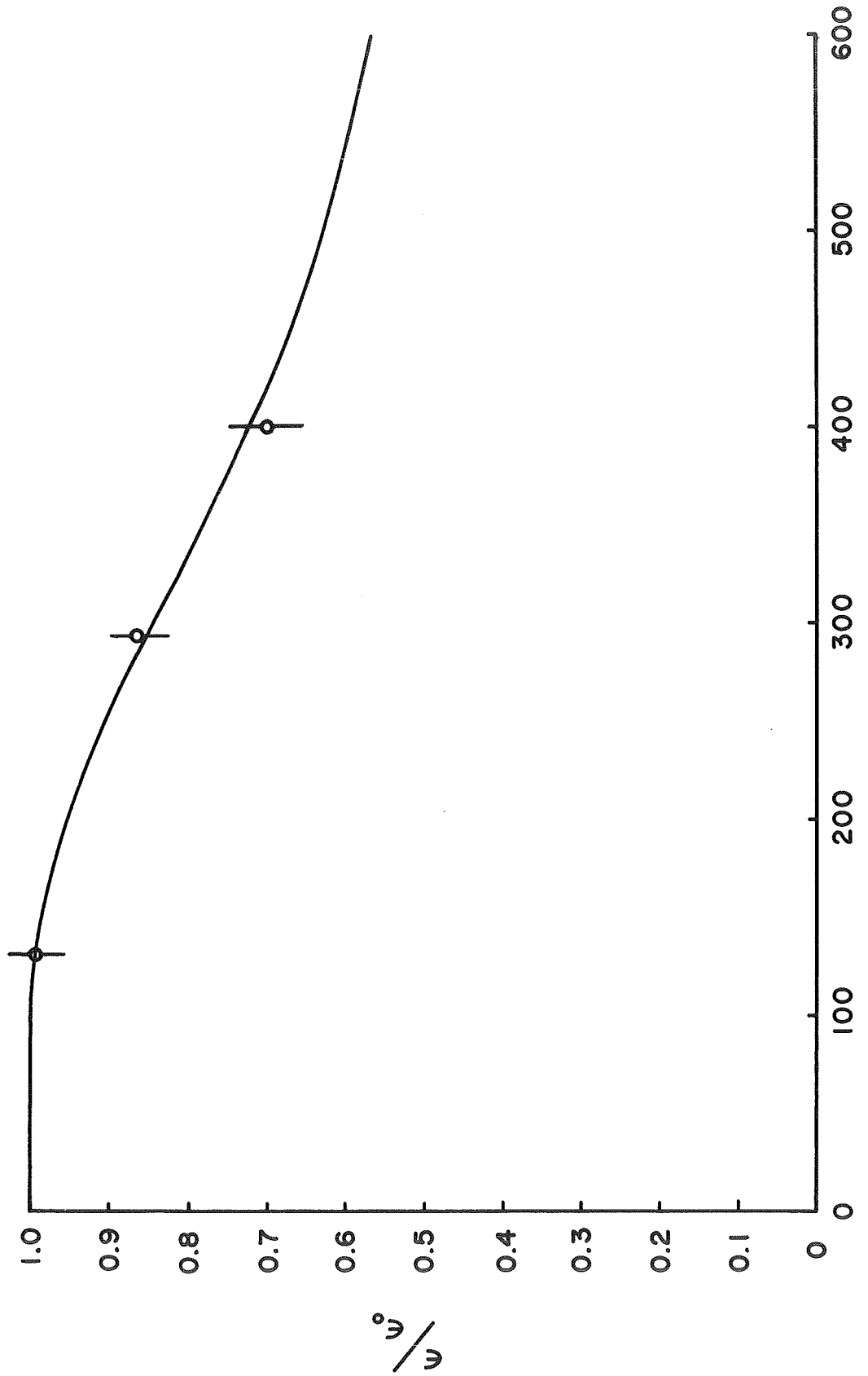

Fig. 48 Temperature dependence of photoluminescence of sodium salicylate.

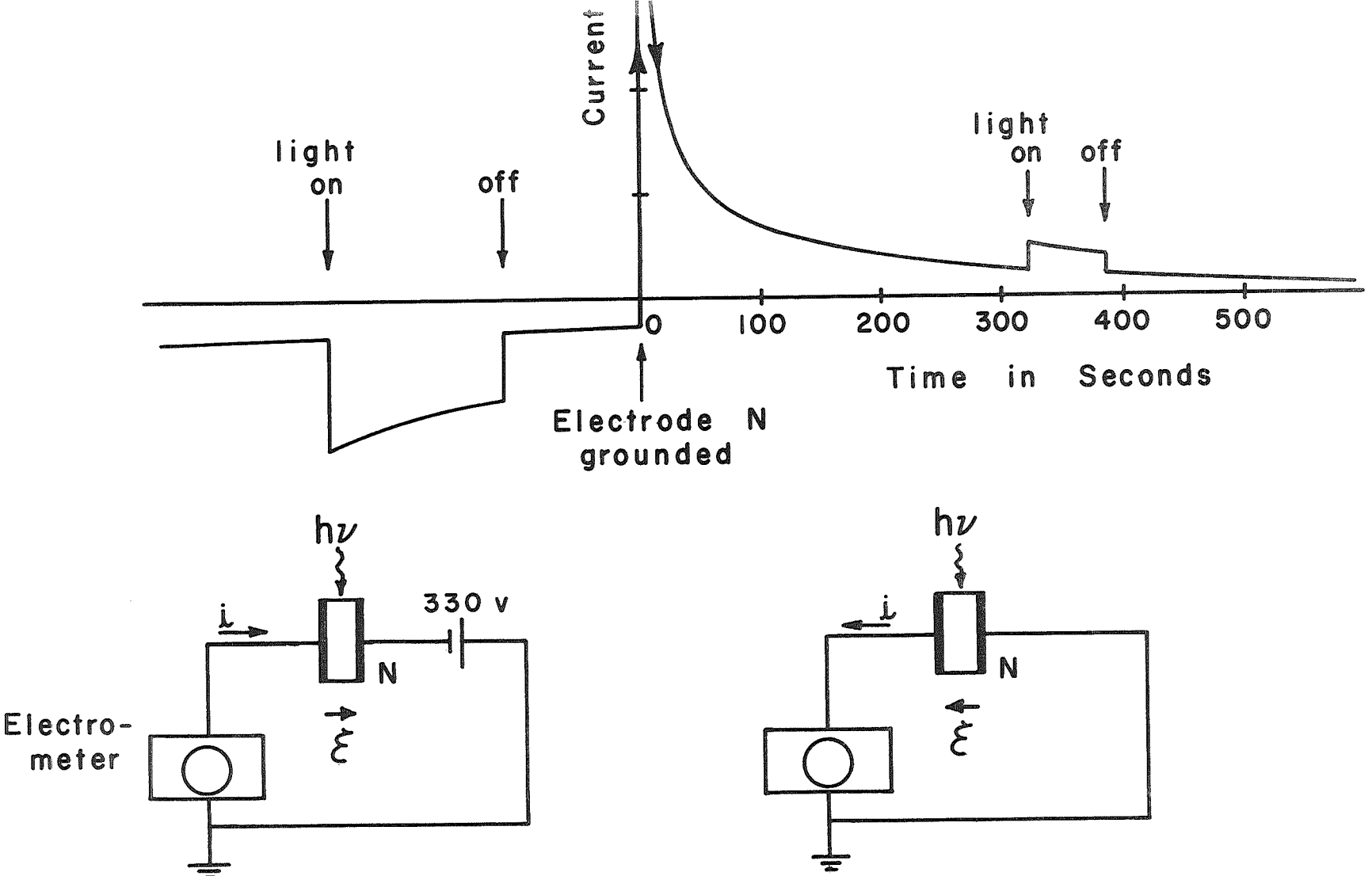

Fig. 49

Photoconductive response of KBr crystal.

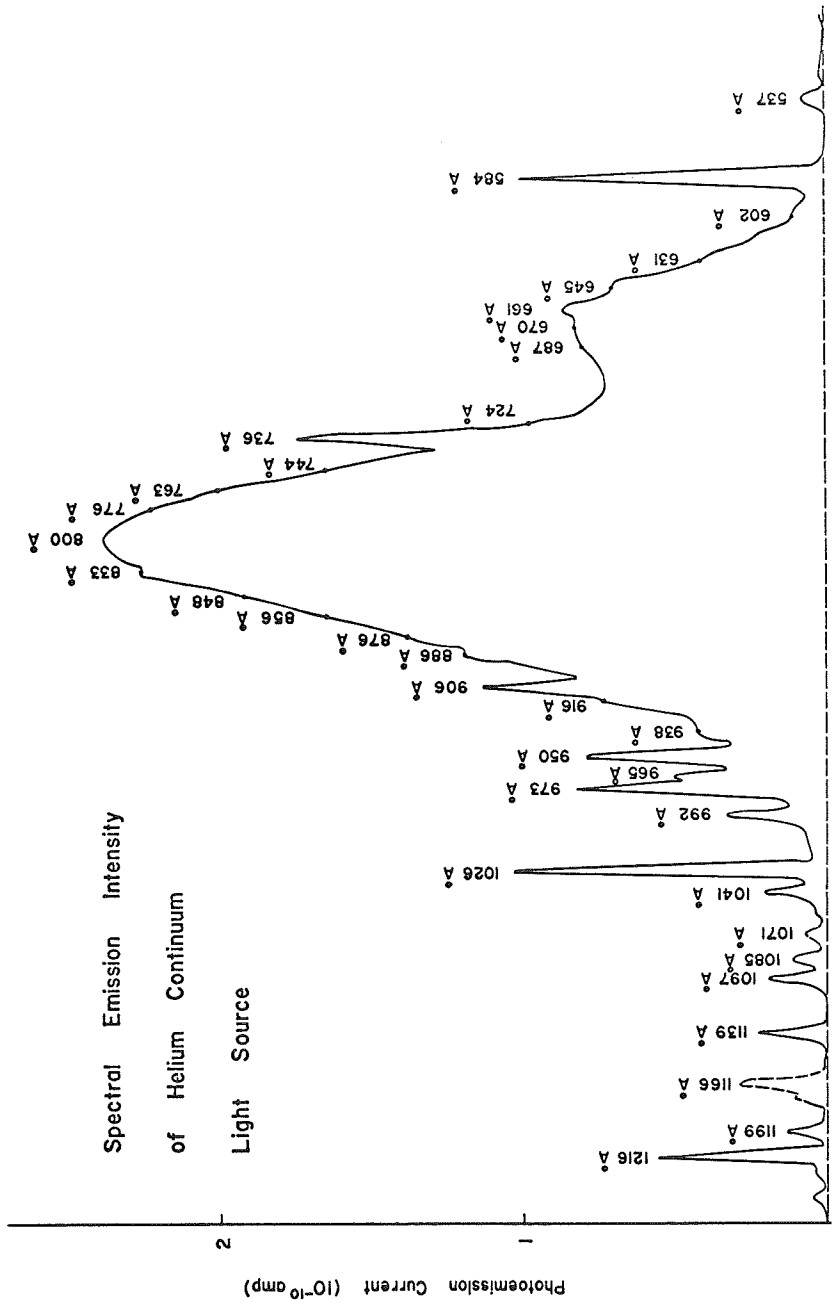

Fig. 50 Spectral intensity of helium-continuum source. Photocathode: tungsten foil.

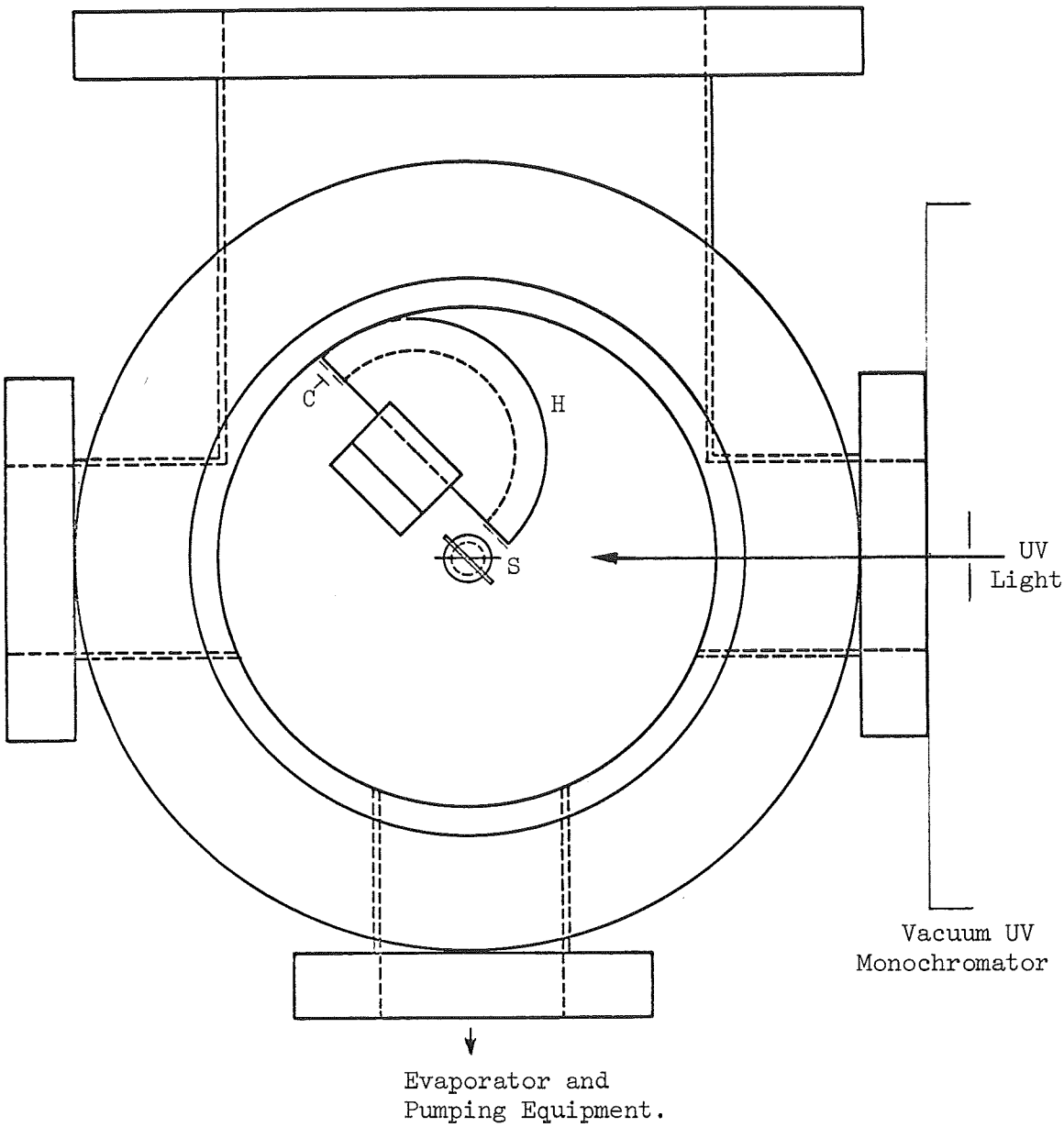

Fig. 51 Hemispherical analyzer for electron energy distribution measurements. S is the LiF substrate for the film; H, hemispherical analyzer; C, electron collector.

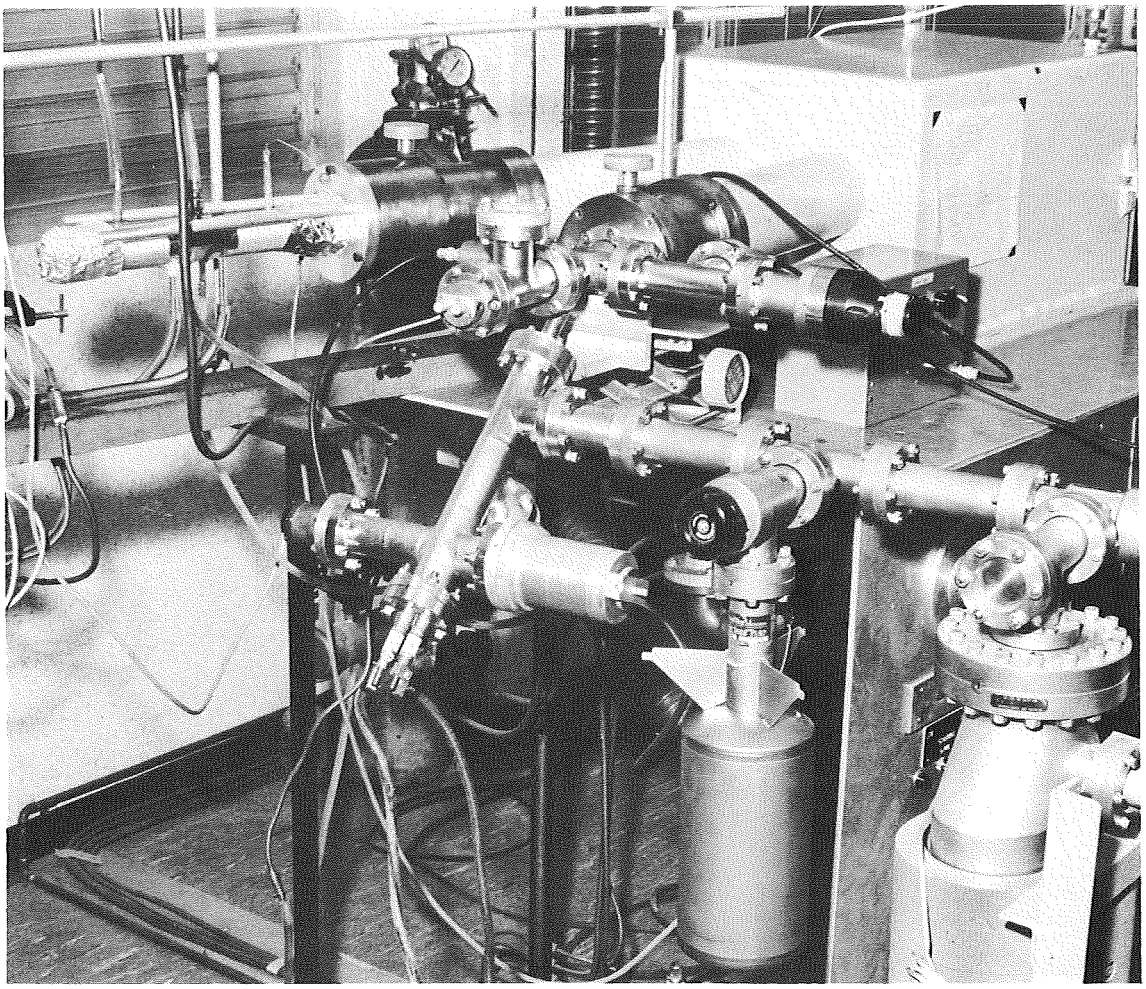

EQUIPMENT for PHOTOEMISSION EXPERIMENTS INVOLVING "BACK" ILLUMINATION ABOVE 1100 Å.

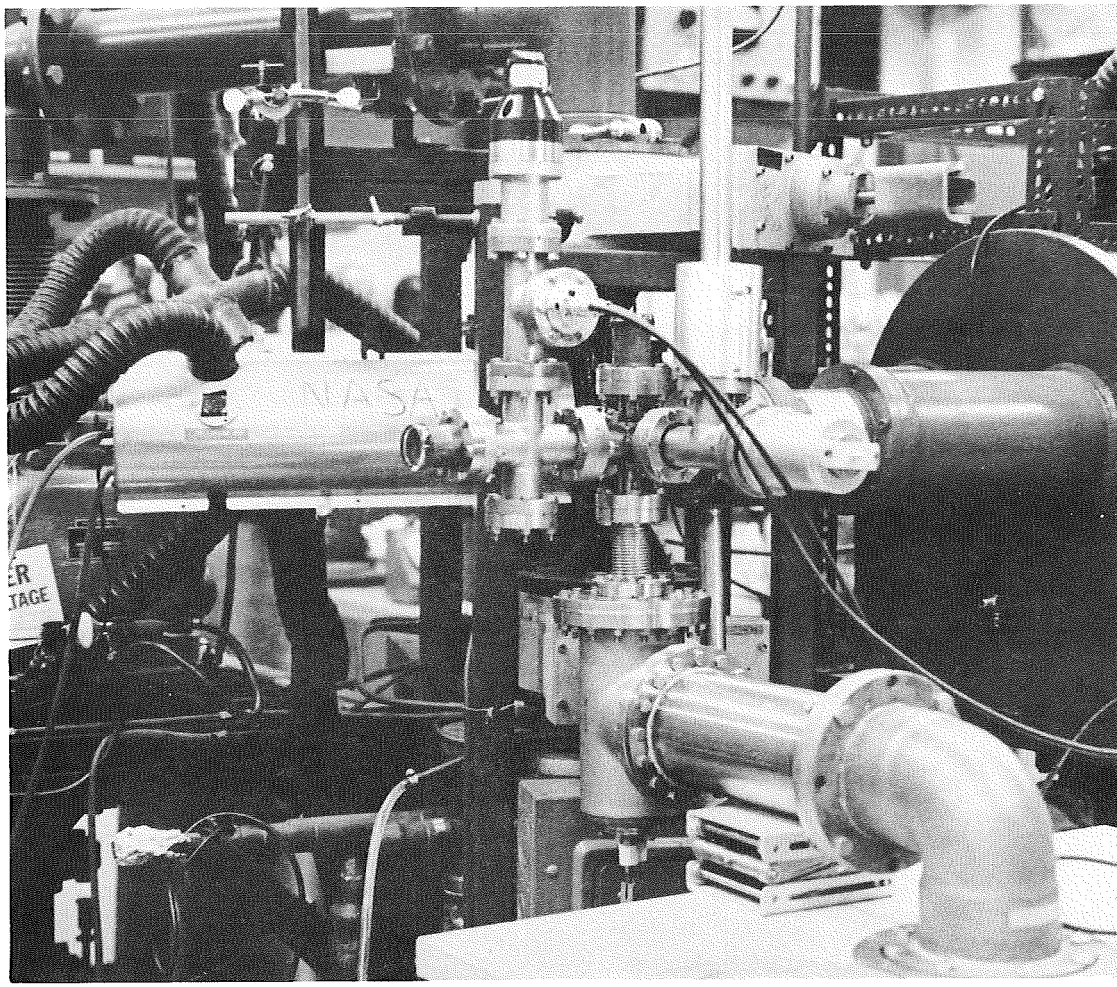

EQUIPMENT for PHOTOEMISSION EXPERIMENTS in the SPECTRAL REGION 10 to 23 eV.

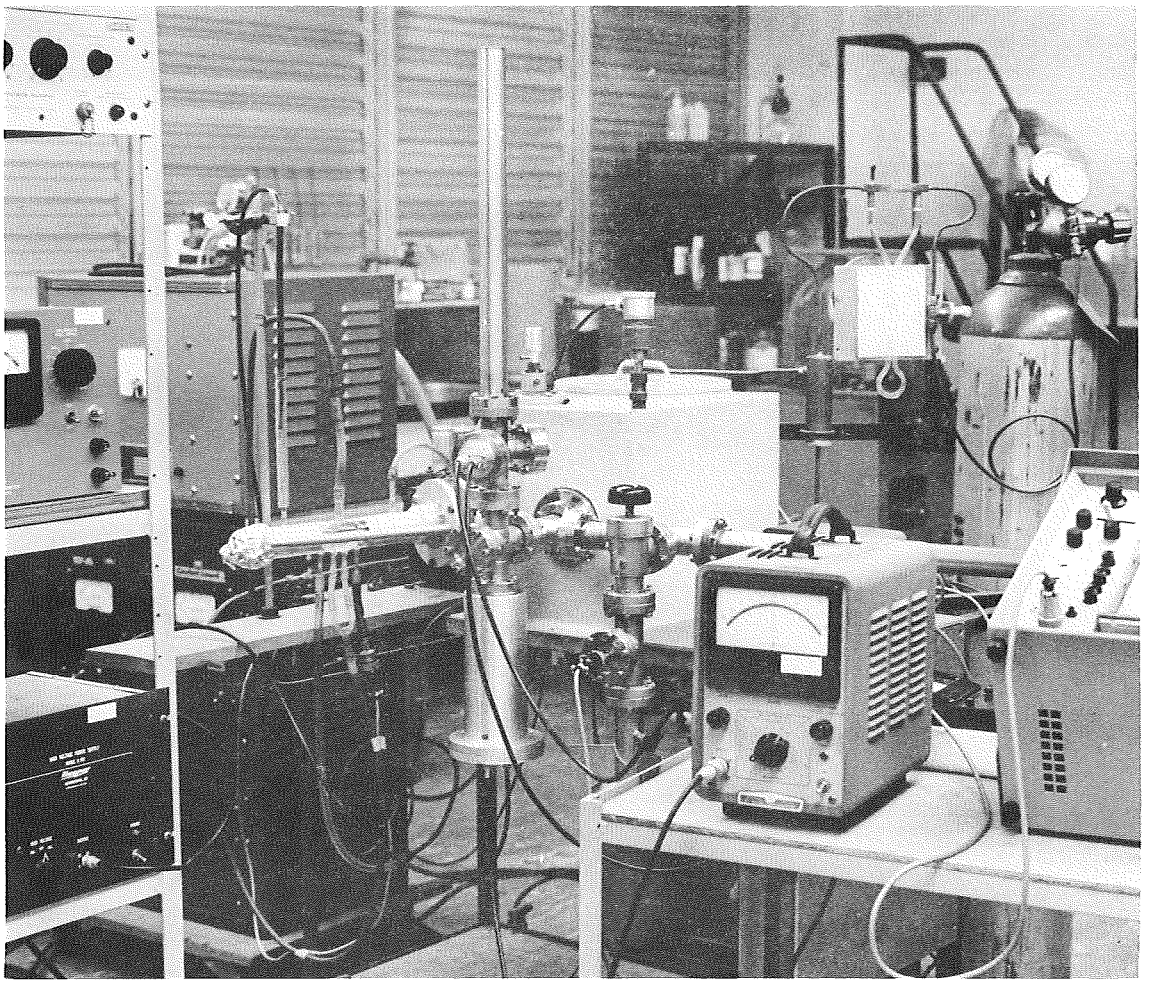

EQUIPMENT for PHOTOLUMINESCENCE STUDY of SODIUM SALICYLATE at DIFFERENT TEMPERATURES.